Synthesis and Characterization of Chitosan-Glutaraldehyde Sorbent Materials For the Removal of Arsenate

A Thesis Submitted to the College of

Graduate Studies and Research

In Partial Fulfilment of the Requirements

For the Master's Degree in the Department of Chemistry

University of Saskatchewan

Saskatoon

By

Shaguftah Younus

Permission to Use

In presenting this thesis in partial fulfilment of the requirements for a Postgraduate degree from the University of Saskatchewan, I agree that the Libraries of this University may make it freely available for inspection. I further agree that permission for copying of this thesis in any manner, in whole or in part, for scholarly purpose may be granted by the professor or professors who supervised my thesis work or in their absence, by the Head of the Department or the Dean of the College in which my thesis work was done. It is understood that any copying or publication or use of this thesis or part thereof for financial gain shall not be allowed without my written permission. It is also understood that due recognition shall be given to me and to the University of Saskatchewan in any scholarly use which may be made of any material in my thesis.

Requirements for permission to copy or to make use of material in this thesis in whole or part should be addressed to:

Head of Department of Chemistry

University of Saskatchewan

Saskatoon, SK (S7N5C9)

Canada

Abstract

Chitosan-based copolymers (CH-GL1:6, CH-GL1:1, CH-GL1:0.5, and CH-GL1:0.25) were prepared at variable weight ratios of chitosan (CH) to glutaraldehyde (GL). Physiochemical properties of cross-linked copolymers were characterized using FTIR (Fourier Transform Infrared) spectroscopy, PXRD (Powder X-ray Diffraction), CHN analysis, and thermogravimetric analysis (TGA). The swelling behaviour of the polymers along with chitosan was investigated. The sorption properties of copolymers with arsenate oxoanions were investigated at various pH using 10 mM phosphate buffer systems and also in aqueous solution without buffer. The Sips sorption model describes the best fit parameters for adsorption. The relative monolayer sorption capacities Q_m (mg/g) of the adsorbents are given in parentheses in the following order: CH-GL1:1(14.4) > CH-GL1:0.5(12.0) > CH-GL1:0.25(10.3) > CH-GL1:6(2.24). In general, the sorption capacities are listed in descending order as follow: un-buffered > buffered (pH 5.0) > buffered (pH 8.5). The removal efficiencies for 20 mg of polymers over a variable concentration range (1-200 mg/L) of arsenate in aqueous solution without buffer are as follow: CH-GL-1:1(20-95%), CH-GL1:0.5(14-97%), CH-GL1:0.25(10-98%), CH-GL1:6(2.0-56%), and CH (0.007-3.9%). The sorption properties of the adsorbents were also determined in bicarbonate buffer to evaluate the competitive effect of phosphate buffer on adsorption of arsenate oxoanions. X-ray absorption spectroscopy (XAS) of chitosan and CH-GL1:1 was performed after adsorption at different pH conditions using two buffer systems to evaluate the chemical environment around the arsenate species. In addition, sorptive properties of phenolic adsorbate (i.e. PNP) were estimated with CH-GL copolymers at various pH conditions. The estimated sorptive capacities ($Q_{m;}$ mmol/g) for PNP are in the range 0.07-0.21(mmol/g) while removal efficiencies for PNP are greater at lower pH conditions.

Acknowledgments

All praise for **The Almighty Allah** Who is the entire source of all knowledge & Wisdom to mankind and created the human to discover the hidden mysteries in the Universe; He had furnished us with a vision to make the difference and granted us the wealth of knowledge and the opportunity to share with our fellows.

I would like to thank Dr. Lee D. Wilson Associate professor, Department of Chemistry, University of the Saskatchewan, for being an exceptional research advisor. He had provided immense support, scholarly guidance, encouraging attitude, and constructive criticism throughout this research project. Furthermore, he has allowed me to reach new heights of research that I may have deemed unimaginable. I would like to thank my co-supervisor Dr. Professor, Ingrid J. Pickering Professor and Canada Research Chair in Molecular Environment Science, Department of Geological Sciences, University of Saskatchewan for her helpful advice. I am grateful for her keen observations, encouragement, precious suggestions, sympathetic attitude and moral support to complete this research work objectively and comprehensively.

I am thankful to the Department of Chemistry at the University of Saskatchewan for provision of an opportunity of teaching assistantship in the department. It has been the great learning experience to teach North American students. I would like to thank CIHR THRUST (CIHR Training grant in Health Research Using Synchrotron Techniques) for providing funding to me. Use of the Stanford Synchrotron Light Radiation, SLAC National Accelerator Laboratory, is supported by the U.S Department of Energy, Office of Science, Office of Basic Energy Sciences under contact No DE-AC02-76FS00515. The SSRL Structural Science Molecular Biology

Program is supported by the DOE Office of Biological and Environment Research, and by the National Institutes of Health, National Institute of General Medical Science (Including P41GM103393). The contents of this thesis are solely the responsibility of the authors and do not necessarily represent the official views of NIGMS or NIH.

I owe a great deal to my group members and friends for always being with me and helping me throughout my project. I would like to thank Dr. Mohamed Hamid Mohamed for data fitting and plotting of adsorption isotherms. I would like to thank to Dr. Graham N. George and members of Pickering and George research group for their assistance and advice with XAS data collection and analysis.

I express my great gratitude to my parents and siblings for never-ending love, affection, support, and prayers; which had been a constant source of encouragement for me to complete this work. I am under the debt of love and matchless support of my sister, Aysha Perveen and brother, Javaid Younus, whose dreams and wishes are my destination.

I have tried to safeguard the interest of the participants of this project, but if any deviance, I apologize.

Shaguftah Younus

Dedication

I would like dedicate this Thesis to

My Brother

Rana Muhammad Naqash Ali Rizvi

(Deceased 08, June 2012)

He was one and only reason for me being here to experience very different edge of life. My all endurance and persistence was because of his adoration. May ALLAH (S.W.T) bless him with Jannah. (Amen)

Table of Contents

List of Abbreviations

As	Arsenate
AC	Activated Carbon
Buff	Buffer solution
CH	Chitosan
DRIFT	Diffuse Reflectance Infrared Fourier Transform
DW	Distilled water
EXAFS	Extended X-ray Absorption Fine Structure
GAC	Granular Activated Carbon
GL	Glutaraldehyde
ICP-OES	Inductively Coupled Plasma-Optical Emission Spectroscopy
pKa	Acid Dissociation Constant
PNP	*Para* nitrophenol
PNP^-	Anion form of PNP
ppb	Parts per billion
ppm	Parts per million
PXRD	Powder X-ray diffraction
RF	Radiofrequency
ROX	Roxarsone
rpm	Revolution per minute
TGA	Thermalgravimetric Analysis
XAS	X-ray Absorption Spectroscopy
XRD	X-ray Diffraction
β-CD	β-Cyclodextrin
ε_R %	Removal efficiency

List of Figures

List of Schemes

List of Tables

Chapter 1 INTRODUCTION

1. Aims and Objectives

Water is one of the major resources essential for sustaining and developing life on this planet. In addition, water is a basic component for personal survival and continuation of life since good quality and safe drinking water is essential for good human health and biodiversity. The purity of water has been questioned owing to contamination by pollutants because the quality of water has been affected by various industrial, agricultural and domestic activities of humans. Numerous toxic inorganic or organic pollutants are accumulated in various forms such as dyes, solvents, detergents, insecticides, pesticides, and other wastes.

Relative mobility, carcinogenic properties, and increase concentration of these contaminants from certain specific levels cause drastic effects on ecosystems, human health, and animal life. Thus, it is essential to remove the pollutants from water as identified by the United Nations Environment Program (UNEP) who posits the importance of safe clean drinking water for improving the quality of life and economic development, among one of the eight millennium goals [1].

A number of methods for pollution control are available but sometimes the cost and practical feasibility are major obstacles for their implementation. Thus, there is an imperative need to search for strategies to remove pollutants from wastewater and development of cost-effective and efficient technology for reuse of adsorbent materials.

Chitosan is an amino polysaccharide biomaterial comprised of randomly distributed D-glucosamine and N-acetyl-D-glucosamine monomers linked with β-(1-4) glycosidic bond to be discussed later in this Chapter. Chitosan has been recognized as "*nature's most versatile*

biomaterial" [2]. Chitosan displays high chemical reactivity and possesses a relatively large number of functional groups (i.e. hydroxyl, amine, acetyl) which contribute to its utility as an adsorbent material of heavy metals and some anions, especially arsenic [3, 4-8-11]. Chitosan possesses very good properties such as high cationic charge density and long flexible polymer chains, which allow for bridging of aggregates and precipitation which enable efficient coagulant and flocculant behaviour for the removal of dissolved contaminants from aqueous solutions [12].

There are limited studies that report on the mechanism of the cross-linking of chitosan and glutaraldehyde [13, 14]. Also, the most reported studies use crossed-linked chitosan adsorbents for the adsorption studies under specific conditions to analyze, isolate, and collect metal ions at ppm levels but never studied the adsorption at ppb or sub ppb levels. Further, there are limited studies on the effect of other anions on the sorption of arsenate species by chitosan based sorbents.

It is also known that surface area of the adsorbent affect the adsorption properties of the material since high surface area often correlates with high adsorption [4]. Based on this hypothesis, the synthesis of chitosan based copolymers have been reported elsewhere [4]. However, it was not clear the extent of the cross-linking and what were the effects of pH on sorption properties (singly or doubly charged arsenate anions), including the effect of other anions like sulphate, carbonate, and phosphate were not studied. These knowledge gaps can be addressed by studying adsorption at low concentration levels and the presence of other ions to see the effect of the counter ions on adsorption properties.

The aim of this project was to synthesize chitosan-glutaraldehyde copolymers at controlled cross-linking ratios to get evaluate such structural factors on the sorption properties of such synthetic copolymers. The Schiff base reaction mechanism of glutaraldehyde with chitosan

allows to develop an understanding of the sorption process according to the structure of the cross-linked materials [13]. The synthesis of chitosan-glutaraldehyde cross-linked copolymers is based on the assumption that two monomers of chitosan react with one monomer of glutaraldehyde to form a cross-linked product (Modified scheme 3.1 for reaction is shown in Chapter 3).

A greater understanding of arsenate sorption in aqueous solution with chitosan-based copolymers (with controlled cross-linking ratios) is the overall aim of this study. To fulfill these objectives, some conventional synthesis is done since the reaction displays sol-gel behavior [13, 139,150]. The reagents are added rapidly to overcome mass transfer limitations prior to gel formation [13, 14, 17]. The copolymers were characterized using spectroscopic and other material characterization techniques.

The equilibrium sorption capacity or properties of polymers are investigated through analyses of the unbound adsorbate species (inorganic arsenate) and isotherms for mono and di-anions are obtained with chitosan and four different copolymers at pH 5.0 and 8.5 in the absence of buffer. The sorptive process and spectroscopic characterization of sorbent/arsenate complex are carried out using multi-instrumental methods.

The chemical environment of both sorbents and arsenic species in the solution can be studied using synchrotron-based X-ray absorption spectroscopy methods with the beamlines available at Stanford Synchrotron Radiations Lightsource (SSRL). Detailed structural information of copolymers were determined from the extended X-ray absorption fine structure (EXAFS) which enabled an assessment of the local coordination environment of the arsenate bound to the copolymer in the presence of two types of buffer systems (phosphate and bicarbonate).

This chapter describes the need for the development of suitable adsorbents for removal of various pollutants from aqueous solutions specifically arsenic oxoanions. Chapter 2 will focus on the experiment aspects of synthesis of (low, medium, and highly cross-linked) copolymers with the variable amount of glutaraldehyde and their physiochemical characterization, including their adsorption properties in aqueous solution. Subsequent chapters will describe the sorption properties of arsenate anions and *p*-nitrophenol in buffered and un-buffered solutions and also the use of synchrotron techniques and other spectroscopic techniques (i.e. IR, Raman) for characterization of the sorbents before and after sorption.

1.1 Arsenic

1.1.1 Physical Characterization of Arsenic

The word, "Arsenic" is derived from Greek name "arsenikon" meaning yellow pigment or orpiment [18-20]. The ancient Egyptians, Greek, and Chinese were familiar with arsenic in the form of minerals and some gilding metals or art crafts; during 1200 A.D, arsenic was first isolated by Albertus Magnus. Arsenic is the 20^{th} most abundant naturally occurring element and is widely distributed in the earth's crust (2 mg/Kg) [18-20]. Arsenic belongs to the Group VA, also referred to as the Nitrogen group of the Periodic Table. The elemental form of arsenic has atomic number 33 with an electronic configuration [Ar] $3d^{10}$ $4s^2$ $4p^3$ and relative atomic mass 74.92 amu. Pure elemental arsenic has three allotropic forms: white, black and gray and it sublimes at 613°C and has a low vapor pressure of 1 mmHg at 373° C and specific gravity 5.73. The naturally occurring forms of elemental arsenic (sometimes referred to as metallic arsenic) is a silver-gray, brittle, crystalline metalloid solid with no apparent smell or special taste[18-22].

1.1.2 Arsenic Compounds and their Occurrence

Arsenic is an elusive element which can be found in many chemical forms. Occasionally, arsenic is associated with various sedimentary rocks especially as sulfides in complex minerals and other ores containing copper, lead, iron, nickel, cobalt, and other metals. Elemental arsenic does not evaporate but when materials containing arsenic are burned, it can make an entry into environmental cycle as an oxide since many arsenic oxides are soluble in water. This element is also present in compounds with other elements like oxygen, hydrogen, carbon, chlorine, and sulfur. These compounds can frequently be found in rocks, soil, water, air, in plants, and animal tissues [18-22]. On thermal decomposition, many arsenic compounds emit toxic fumes [18-22]. Some arsenic compounds occur in crystalline, powder, and amorphous or vitreous forms [18-22]. Elemental arsenic is insoluble while some other forms such as calcium arsenate and arsenite are readily soluble. Various calcium, potassium, lead, sodium arsenate, and arsenite salts along with other arsenicals are also soluble in ethanol and various acids.

1.1.3 Applications of Arsenic Compounds

The Renaissance period pioneered the use of arsenic compounds in medicine [23-25]. During 1975, worldwide annual productivity of arsenic or arsenic compounds was "approx.60, 000 tons/year" [26-29]. Organic arsenic is one component of antibiotics for the treatment of spirochetal and protozoal diseases [25]. Inorganic arsenic compounds have applications in the treatment of leukaemia, psoriasis, and chronic bronchial asthma [25]. During the period 1800 to 1900, many arsenic compounds were used as herbicides, insecticides, cotton desiccants, defoliants, soil sterilants, pesticides, dyes, and paints. Some had applications in wood preservation, fertilizers, and production of glass. Metallic arsenic was used in the manufacture of

metallic alloys of lead and copper [24, 30, 31]. Sometimes, gallium arsenide or arsine is used in semiconducting devices, light-emitting diodes, high power microwave [24, 31, 32].

1.1.4 Arsenic in the Environment

Arsenic becomes mobile after changing its chemical form and by reacting with other molecules present in the air, water, and soil or by various bacteria. Upon dissolving in rain or snow, arsenic also get into lakes, rivers, and underground water. About "one-third of the estimated atmospheric arsenic flux is of natural origin" [18-22]. Volcanic eruption followed by low-temperature volatilization or erosion results in the release of the arsenic in the environment [18-22]. Various human activities like coal-fired power generation, gasoline production, and also incineration processes release arsenic to the environment [18-22].

In general, reduction of arsenic trioxide with charcoal produces elemental arsenic while, arsenic trioxide is a by-product of metal smelting operations. Arsenic is associated with many metallic ores, such as copper or lead, may enters the environment during natural weathering. Mining and smelting of non-ferrous metals and burning of fossil fuels also contribute to the arsenic contamination of the environment. Small amounts of the arsenic may be released during manufacturing of many chemicals like pesticides, herbicides, crop desiccant or wood preservatives. Large areas of agricultural land have been contaminated because of the use of arsenic contaminated pesticides [18-22]. Arsenic compounds also undergo biotransformation and bioaccumulation during redox reduction or biosynthesis of various organic arsenic compounds [33, 34]. Most of the arsenic compounds are notorious poisons [26-30]. The oxidation state of arsenic effects its toxicity; arsenite is (approximately 60 to 100 times) more toxic than its oxidised form (arsenate) and related organoarsenical compounds [29]. Similarly, lead and calcium arsenate containing insecticides are highly toxic [27-30].

In remote and rural areas, the total arsenic concentration in air ranges from 0.02-4 ng/m^3. On the other hand, in urban areas the total arsenic concentration ranges from 3 to 200 ng/m^3.The concentration of arsenic in ocean seawater is 1-2 µg/L and typical arsenic concentrations in rivers and lakes are < 10 µg/L. Groundwater contains higher levels of arsenic than surface water, where arsenic concentration lies in range 1-10 µg/L [35]. Marine organisms contain residues of organic arsenic greater than 100 mg/Kg [35]. The maximum acceptable level of arsenic concentration in water established by the World Health Organisation (WHO) is 10 µg/L [35].

1.1.4.1 Environmental Arsenic Impacts on the Human Health

Human population can be effected by arsenic contamination through ingesting drinking water or crops which contain high levels of arsenic from natural or industrial sources. For example, a large population in Taiwan has been affected by the arsenic trivalent species present in well water [36] was evidenced by hyperpigmentation, keratosis, and cancer of lung, skin or prostrate in various patients [36]. In some parts of Vietnam potential risk to public health are greater because of the large concentration (3050 µg/L) of arsenic in groundwater supplies [37]. The uncontrolled release of arsenic in aquatic bodies engendered a serious threat to global water security as indicated by the "*cancer belt*" regions of China [38, 39], Bangladesh [40], and India [41]. Accordingly, the arsenic levels of some regions exceed the EPA guidelines at 100-900mg/L [38]. By comparison, several areas in Canada are identified as arsenic *"hotspots"* with elevated levels (>10 µg/L) of both arsenic species in ground and drinking water [1, 42, 43].

Human beings are exposed to arsenic by food, drinking water or air. It has also been documented that about 40%-60% ingested arsenic can be retained by human body after changing chemical form [44] while the remainder can be excreted by the human body through the renal system. In addition, it has been reported that pulmonary exposure for a smoker is ~10 µg per day

and is greater than a non-smoker. Food is a major contributor to daily intake of arsenic; the primary dietary sources of arsenic are meat, poultry, seafood, rice, cereal, and mushrooms which contain high levels of arsenic. Approximately, 25% of the arsenic in food exists as inorganic form and these levels depend on the nature of the food. Some fish or shellfish also accumulate arsenic in an organic form called *arsenobetaine* (known as fish arsenic).

Elevated levels of arsenic in water cause dermatitis, anaemia, nerve condition abnormalities, hyperpigmentation, keratosis, and possible circulatory disorder or complications [45]. Inorganic arsenic compounds are carcinogenic for skin and lungs. High risk of lung cancer in the population near emission sources of inorganic arsenic has been documented [30, 44, 45]. Vomiting, oesophageal and abdominal pain, diarrhea melanosis, leuco-melanosis, dorsum, warts, and gangrene of the skin, are the result of short-term chronic or/and drinking water exposure to arsenic. Long-term exposure via drinking water can also cause the cancer of the urinary bladder, muscular weakness, loss of appetite, kidney cancer, and other skin disorders such as hyperkeratosis [28].

Roxarsone (3-nitro-4-hydroxyphenylarsonic acid) is one of the organic arsenic compounds with an aromatic ring. Roxarsone (ROX) has been used extensively as a feed additive for broiler chicken. The potential use of this food additive is to control intestinal parasitic diseases, enhancing feed efficiency, and also to promote growth [46, 47]. It also helps in pigmentation, high egg production, and better feathering of chickens. After microbial biodegradation, roxarsone converts into inorganic forms which are mostly soluble in water and then cause transportation from application sites. 3-amino-4-hydroxyphenylarsonic acid, methylarsines, and AsO_4^{3-} are important biodegradation products of roxarsone under aerobic conditions and these are toxic species. Photodegradation of roxarsone is a slow process which is

pH dependent. Arsenic concentration levels in roxarsone fed poultry waste products ranged from 14 to 76 mg Kg^{-1} while surface soils contain arsenic levels between 12 to 15 mg Kg^{-1} [47].

Poultry feathers (a by-product of the poultry industry) are the major part of the raw material for the render industry for the production of feather meal. Residual arsenic present in "feather meal" may be harmful to human and animal health [48-51]. Characterization of arsenic species and concentration levels in poultry feather meal has been evaluated [48]. The adsorption of roxarsone on carbon nanotubes was studied and it was indicated that ionic strength and pH of the solution has the great effect on the adsorption properties [49]. In another study, manganese green sand (MGS) was used to remove organic arsenic (MMA and DMA) from water samples. Furthermore, iron oxide-coated sand resin was also used in the same study [50, 51].

1.1.4.2 WHO Guidelines for Arsenic

The WHO reported that more than 200 million people are drinking arsenic contaminated water. The WHO provided various norms or guidelines for drinking water quality. The main aim and goal of the WHO' Guidelines for Drinking Water Quality (GDWQ) is to provide clean, safe, and quality drinking water to address public health. During the year of 1958, the WHO documented specific standards for arsenic concentration in drinking-water. According to those norms, the allowable concentration for arsenic in drinking water is 0.20 mg/L [1, 18-22, 25, 33-35].

The international standards for drinking-water were reduced to 0.05 mg/L in 1963 and these standards became national targets for many countries as described in WHO's "Guideline Value" in 1984. In the last edition of GDWQ published in 1993, provisional guideline value for arsenic in drinking water was set at 0.01 mg/L. In the year 2000, a grant of 2.5 million was approved by United Nations Foundation to address this public problem [52, 53] in Bangladesh.

The goal of that project was to provide clean drinking water to various affected regions in Bangladesh [52-53]. Similarly, EPA has passed an ACT called, "Safe Drinking Water Act" in 1974 and revised during 2002. EPA set maximum contaminated level (MCL) at 0.010 mg/L or 10 ppb for arsenic [25, 33, 34, 38, 52, and 53].

1.1.4.3 Aqueous Speciation of Arsenic

Arsenic is present in two environmentally common primary forms; organic and inorganic such as arsenites, arsenates, methylarsenic acid (MMA), dimethylarsenic acid (DMA) [26, 554, and 5]. In general, the organic forms are less harmful than inorganic [18-22]. Inorganic arsenic can occur in several valence states; 0, -3, +3, +5 [35, 54, 55]. In general the trivalent form is much more toxic form than pentavalent and zero-valent arsenic [18-22]. Inorganic forms of arsenic, e.g., arsenite and arsenate preferentially exist in water supplies. Arsenates are present as H_3AsO_4, $H_2AsO_4^-$, $HAsO_4^{-2}$, and AsO_4^{-3}, depending upon the pH (Fig.1.1). Arsenite likewise can exist as H_3AsO_3, or As $(OH)_3$, $H_2AsO_3^-$, $HAsO_3^{-2}$, and AsO_3^{-3}. In natural waters, trivalent arsenic oxoanion exists as $As(OH)_3$ with pK_a ~9.2, which show very less adsorption on most mineral surfaces compared with negatively charged pentavalent arsenic oxoanions (pK_a ~ 2.22, 6.98, 11.53)[34].

Under strong reducing or waterlogged conditions, elemental arsenic and/or arsine are dominant species. Under oxygenated environments and aerated conditions, arsenate (V) is the more thermodynamically stable oxidation state. In general, the rate of conversion is dependent on the redox potential and pH, as well as on various physical, chemical, and biological factors [35].

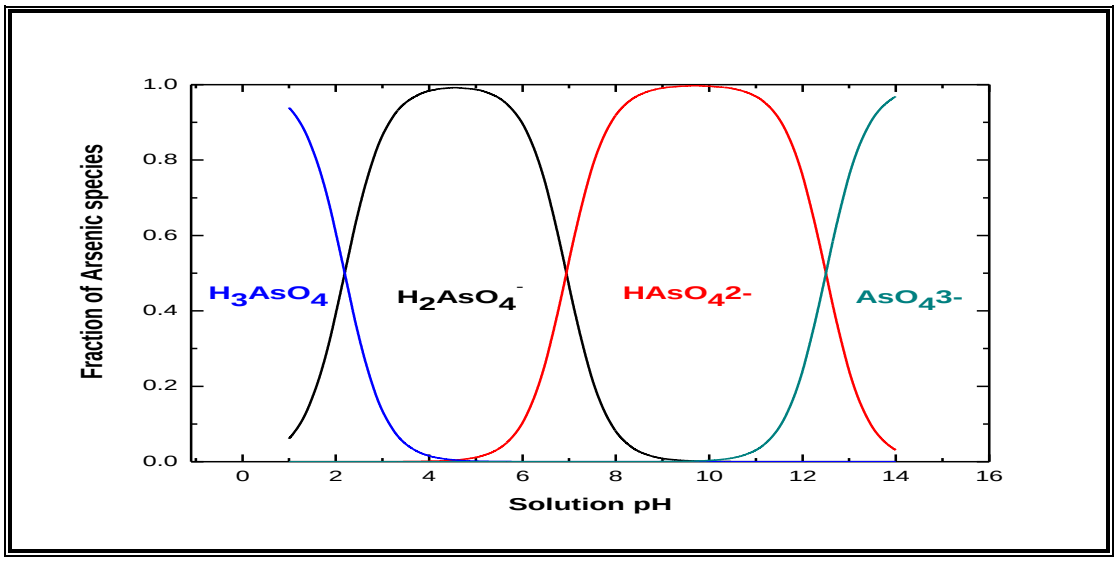

Figure 1.1: Arsenic speciation in aqueous solution at various pH [Modified from refs 35 and 56].

According to the speciation diagram in Fig. 1.1, the predominant of arsenic species [35] in an aqueous system under reducing condition or at less than pH 9.2 are uncharged arsenite species H_3AsO_3. By comparison, while under oxidising conditions or at pH 6.9, $H_2AsO_4^-$ is the more stable species (Fig.1.1). At extreme acidic and alkaline conditions H_3AsO_4 and AsO_4^{3-} are dominant species respectively [35]. Environmental conditions play an important role for speciation, mobility, and transport of the arsenic in air, water, and soil. Also, the chemical form, valence state of arsenic, and the solubility of arsenic species are key factors for bioavailability and toxic assessment of the arsenic [35].

1.1.5 Phenolic Compounds (*Para-nitrophenol*)

Phenol, also called phenic acid, was first isolated from coal tar by German chemist Runge in 1834. He gave it a name of "Carbolic acid" or coal oil acid. In general, phenols are aromatic compounds containing a hydroxyl group (-OH) substituent on the benzene ring. Owing to the hydroxyl group they can undergo hydrogen bonding, which results in variable solubility of

phenols in water. Sometimes, intramolecular hydrogen bonding is prominent which make phenols more insoluble in water; solubility of *o*-nitrophenol is 0.2g/100ml of water and *p*-nitrophenol is 1.69/100ml of water. Phenols are polar and acidic in nature. 4-nitro-phenol also known as *p*-nitrophenol (PNP) is an important member of nitrophenols family [57,58].

This nitroaromatic compound is chromogenic and is very stable. *Para*-nitrophenol is a synthetic compound, colorless to light yellow crystalline solid with light odor, and moderately soluble in cold water. PNP is a relatively small molecule and polar in nature and a weak acid with a pK_a value of 7.14 at 25° C and can exist as neutral or anionic form (Fig.1.2 and Fig.1.3) [57]. In the presence of metals, PNP can be easily reduced by $NaHB_4$ [57, 58].

This nitroaromatic dye shows strong absorption at 400 nm and molar absorptivity in range of 18-20 $\times 10^3$ $Lmol^{-1}cm^{-1}$ [59-61]. Para and *ortho*-nitrophenols are a "high-production-volume chemicals" of the nitrophenol family [59-61] and products of the same reaction in variable proportions.

Ortho substituted phenol has stronger intramolecular hydrogen bonding which is responsible for less solubility (0.2 g/100 ml water) and high volatility as compare to *p*-nitrophenol. They have similarities in physical characteristics, chemical reactivity, and applications [59-61].

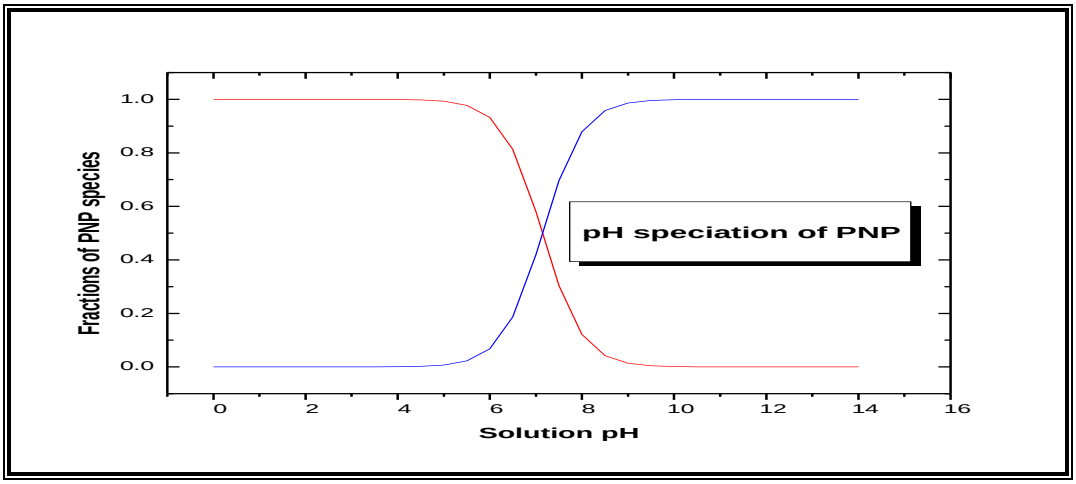

Figure 1.2: PNP speciation in aqueous solution at various pH conditions, red color indicates protonated (non-ionized) form while blue indicates deprotonated (anionic) form.

1.1.5.1 Applications of Phenolic Compounds

Phenolic compounds have many applications in the synthesis of various synthetic compounds such as paints, lubricants, plastics and resins [59-61]. Because of the presence of phenolic functional group in the structure, phenols have relatively low bond dissociation enthalpy; they can be used as antioxidants to reduce the rate of oxidative degradation in living organisms and many synthetic organic materials [62]. They have applications as food additives in food technology, petrochemicals, and textile manufacturing [59-61].

Many phenolic compounds are used to suppress lipid peroxidation or some are used as pesticides (e.g., parathion) and insecticides (e.g., fenitrothion). PNP is also a by-product during the synthesis of many insecticides, herbicides, and synthetic dyes. PNP is a major component of many drugs and is also used in manufacturing analgesics (e.g., acetaminophen). PNP has extensive uses in synthesis of fungicides, explosives, and dyes. Furthermore, it can be used by the leather industry to darken leather [57-62].

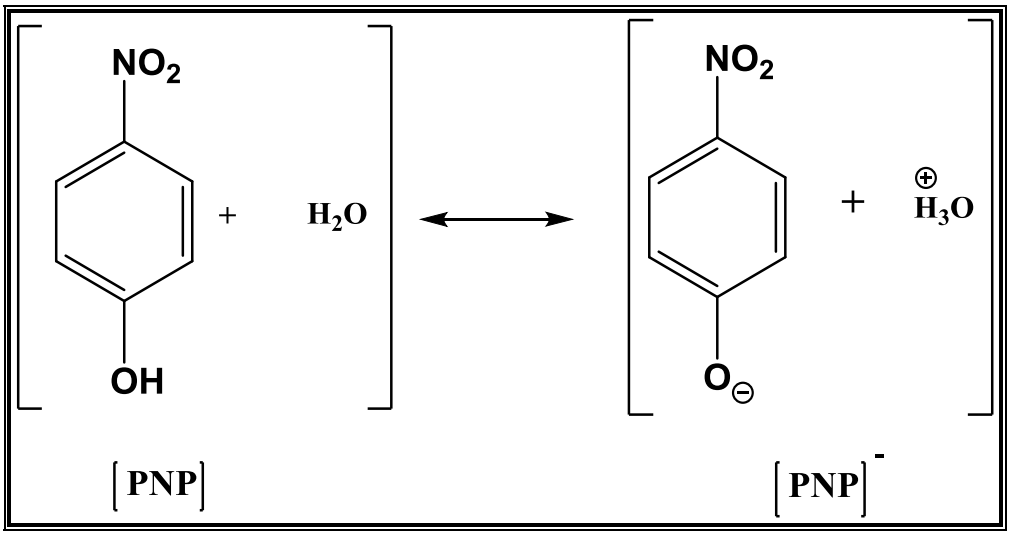

Figure 1.3: Acidic and basic form of PNP under different pH condition. Note here [PNP] is neutral form while $[PNP]^-$ is anionic form.

1.1.5.2 Phenolic Compounds, their occurrence, Source, and Impacts

When chromogenic dyes and pigment containing compounds are present in elevated concentration levels they are harmful and toxic. Nitrophenols are released by industries as effluent during manufacturing and production processes [57-61]. As phenolic compounds have a specific odor and color so, phenolic discharge has a carbolic smell and distinct color which impact toxic effects on aquatic life, plants, and animals [57-61]. PNP is known to cause skin and eye irritation after long exposure and it is also causes blood disorder, anaemia, liver and kidney failure. PNP enters into the aquatic and terrestrial environment from effluents of many industries such as petroleum refineries or insecticides or herbicides industries. It is a by-product of many toxic organophosphate pesticides [57-61]. By hydrolytic decomposition or bacterial biodegradability of PNP [63], it can enter the soil and surrounding waters (ground water, streams or rivers) because of its high solubility. PNP is carcinogenic, mutagenic, cytotoxic, and shows toxicity to mammalian embryos. The WHO has recommended the 0.001 mg/L of phenolic

concentration in waters [64]. According to Central Bureau of Water Pollution Control, the maximum concentration of phenolic compounds in industrial effluents is 1-5 mg/L [64].

1.2 Methods for the Removal of Waterborne Contaminants

A number of cost-effective and efficient methods have been developed for the removal of pollutants from water system; where the removal of waterborne contaminants such as PNP, arsenic, and various other organic compounds can be achieved through various physical and chemical processes.

1.21 General Removal Methods for PNP

The presence of this chromogenic dye (PNP) at low concentration is visible, undesirable and potentially a hazard for terrestrial ecology. Various common methods used for removal of PNP from industrial effluent are; catalytic wet air oxidation, ion exchange, biodegradation, solvent extraction, UV-oxidation, and adsorption [64-67]. Sometimes biological processes are also used to remove phenolic compounds from wastewater.

Coagulation or flocculation is also an efficient method to remove large concentration of phenolic compounds from waste water [68, 69]. Adsorbents containing β-cyclodextrin modified with magnetic chitosan nanoparticles have high surface area and show high reactivity for recovery of various phenols (1.75 mmol/g) from aqueous solutions [70-72]. Activated carbon [73] is one of the efficient adsorbent for removal of many dyes from water and it has the great role in dephenolation (removal of phenols from wastewater). Its use as an adsorbent is limited because of its high cost and preparation or regeneration problems [64-66].

During the history, activated carbon had been used for removal of many phenolic dyes from aqueous solutions [65,66]. Adsorption of phenolic compounds on activated carbon depends

on the physical nature, ash contents, and pKa of phenolic compounds, pH, solution concentration, and ionic strength. The various soils such as primary clay minerals or bentonites have potential use for removal of phenol from water solution [74]. Some other low cost adsorbent are saw dust, fly ash [75], and various kind of wood [76]. Recently, a number of unique adsorption methods have been developed to remove PNP from water. Ngah et al. evaluated the adsorption efficiency of chitosan glutaraldehyde cross-linked beads and chitosan flakes for *p*-nitrophenol [77]. Chitosan cross-linked beads had higher removal capacity (2.48 mg/g) as compare to chitosan flakes (0.63 mg/g) [77].

1.2.2 General Removal Methods for Arsenate

Coagulation is a traditional treatment process for the removal of various particles like insoluble metal hydroxide particles. Among various coagulants, alum, ferric chloride, calcium salts, and ferric sulfate are efficient coagulants for removal of arsenate species than arsenite [78, 79]. Some other organic and inorganic coagulant include aluminum sulphate, polyaluminium chloride, polyaluminosilicate sulphate, and many others polyelectrolytes [80]. However, the presence of other inorganic ions like sulphate and calcium can decrease or enhance the removal uptake accordingly [81]. The pH of the solution plays an important role on removal efficiency such as ferric sulfate can remove 40-60 percent of arsenite as compared to alum in the pH range of 5.0-8.5 [81]. In another study, the effect of solubility and stability of metal hydroxide on removal efficiency has also been studied [82].

Coagulation/Coprecipitation and electrocoagulation are low-cost and simple operational processes which are effective over a wide pH range [38, 82]. However, these methods have low removal efficiency and can produce some toxic sludge during operation [38]. Coagulation assisted with microfiltration is also a fairly efficient method for removing arsenic at very low

concentration levels [83]. Moreover, oxidation of iron or manganese is a useful method for removal of arsenic from groundwater [79]. In a different experiment 99% of the arsenic was removed using ferric chloride, hydrated lime, sodium sulfide, and alum [84].

Sometimes, water treatment residuals can be used for removal of arsenate and phosphate [38]. The iron based residual solids can show arsenic adsorption up to 2230 mg/Kg of solid mass. Furthermore, surfactant-modified zeolites are effective sorbents for the removal of pentavalent arsenic from aqueous solution [85]. Clinoptilolite is an easily most abundant natural zeolite which shows greater affinity towards positively charged exchangeable ions [86].

1.2.1 Analytical Techniques for determination of Arsenic

Identification and quantitative determination of arsenic species (organic and inorganic) at low concentration is not an easy task and there are very few developed methods for identification of arsenic in the environment. In a modified method As (V) in drinking water was determined by a rapid colorimetric method [60]. Arsenate (V) forms a complex with reduced molybdate, which show absorption in the infrared region while As (III) does not form any complex [87]. Similarly, hydride generation atomic absorption spectrometry (HGAAS) is a very accurate technique for determination of volatile hydride-forming elements such as selenium or arsenic at very low levels. Various arsenic species can be determined using atomic absorption spectrophotometry; however the use of HGAAS involves the conversion of the pentavalent forms of arsenic and antimony to the trivalent form with a reducing agent, e.g., potassium iodide or L-cysteine. Flow injection analysis coupled with inductively coupled plasma mass spectrometry (FI-ICP-MS) has been used to determine various metals along with arsenic in the steel containing solutions [88]. The analysis and speciation of various arsenic organic and inorganic compounds in environmental samples using selective-reduction-HG-AAs has been reported [89]. Similarly,

direct determination of the As (V) and As (III) was done using flow injection hydride generation atomic absorption spectrometry (FI-HG-AAS) [91], where analysis without pre-reduction of arsenate was reported by Coelho et al. [90]. During 2003, hydride generation atomic absorption spectrometry was used to determine the total arsenic contents of various food items from Spain [92]. In another study, high concentration levels of arsenic were determined in various seafood; using the standard addition method [90].

ICP-OES is the analytical technique used for the determination of trace elements in samples [93]. ICP/OES provides a high atomization temperature, inert environment and very low detection limits for determination of the elements present in a substance. Multi-element detection or identification and determination can be performed simultaneously in many biological or environmental samples [93]. ICP (Inductively Coupled Plasma) is an efficient and reproducible analytical atomic excitation (or emission) source, which vaporizes, desolvates, atomizes, excites, and ionises a wide range of elements in various samples [93].

X-ray Absorption Spectroscopy (XAS) is an elemental-specific synchrotron probe potentially used to investigate the local atomic geometric and electronic structure of the metal species in various samples. X-ray absorption spectroscopy measures the absorbance of X-rays as a function of the incident X-ray energy since the absorption spectra can be divided into two important regions. The near-edge spectrum measurements are used to determine the oxidation state and chemical speciation of various metal species. This spectrum is “fingerprint” of each chemical species, containing some feature sensitive to different chemical type present. This fingerprint can also be used to quantitatively measure the fraction of the element present as a chemical type in the mixture of species.

Extended X-ray absorption fine structure (EXAFS) is a quantitative structural tool which comprises the structure above the absorption edge in the region 50-1500 eV. The structural features of the EXAFS region indicate the promotion of core electrons to bound states. Therefore EXAFS spectra provide precise electronic structural information around the central absorbing atom and also provide bond length or interatomic distance of the neighbouring atoms of the X-ray absorber.

Various studies have been done on the determination of arsenic species in different environmental samples using XAS [94-96]. Farquhar et al. elucidated the mechanism how arsenic interacts with the surface of goethite, lepidocrocite, meckinawite, and pyrite [95]. Arsenic oxidation states in the xylem sap of cucumber was determined by doing XANES measurements coupled with Synchrotron Radiation induced Total reflection X-Ray Fluorescence (SR-TXRF) at the K-edge of the arsenic in fluorescence mode [96].

1.3 Adsorption

The accumulation of specific arsenic species from aqueous media using solid phase adsorbents of biological origins is the most recent development because of relative ease, availability, and eco-friendly nature of these materials. However, there is clear need to further develop synthetically modified materials which are cost effective and also display improved physicochemical properties.

In past, wood charcoal has been used as a good adsorbent for filtration of water [97]. The ancient Hindus used charcoal for the filtration of drinking water and Egyptians used carbonated wood as a medical adsorbent and purifying agent during 1500 B.C [97].

1.3.1 Adsorption Methods

Adsorption is a broad term that involves physical, biological, and chemical processes. Adsorption is a "surface phenomenon" resulting from intermolecular attractive forces on surfaces or phase boundaries and is employer in the treatment of wastewater, pollution control, and chemical processing" [98-100]. The adsorption process involves two main constituents; one is the adsorbent and other one is the adsorbate. The adsorbate species is adsorbed onto the surface of the adsorbent [98-100] via range of intermolecular forces such as van der Waal's, H-bonding, and dipolar interactions.

Adsorption is dependent on the nature of adsorbent or adsorbate, especially the surface area of adsorbent and various experimental conditions such as temperature, concentration or/and time in the case of nonequilibrium processes. Physical sorption or physisorption, involve van der Waals interaction (dispersion) and electrostatic interactions between the adsorbate and adsorbent since there is no covalent bond formation. Physisorption is a reversible process where the heat of condensation is in the range of 20-40 kJ mol^{-1}. The thermodynamics of physisorption depends upon temperature, pressure (or concentration) of adsorbate, and the nature of the adsorbent material [97-100].

In chemical sorption or chemisorption, the adsorbate forms a chemical bond with the surface of the adsorbent. Chemical specificity and the heat of desorption for chemisorption is higher (> 100 kJ/mol), compared with physisorption. Chemisorption may be slow as compare to physisorption with high heat of adsorption in range of 40-400 kJ mol^{-1}. Chemisorption indicates presence of activation energy. Chemisorption is often limited to the formation of a monolayer whereas physisorption can be monolayer or multilayer in nature. Both processes are temperature

dependent and chemisorption is favoured at high temperature while physisorption prevails at low temperature according to the thermodynamic parameters [97-100].

1.3.2 Adsorption Isotherm Models and Equations

Adsorption process consists of removal of the adsorbate from the gas phase or/and solution and its concentration on the surface of adsorbent varies until equilibrium is attained between the amounts of solute remaining in gas or solution phase with at the adsorbent surface. In case of solid-solution equilibria, Q_e (the amount of adsorbate per unit weight of adsorbent) is a function of concentration and can be measured by equation (1.1)

$$Q_e = \frac{(C_o - C_e) \times V}{m} \qquad (1.1)$$

Q_e (mmol/g) is the amount of adsorbate adsorbed at equilibrium, C_e (mmol/L) is the concentration of the unbound adsorbate remaining in the solution of volume V at equilibrium, C_o (mmol/L) is the initial concentration of the adsorbate, V is the volume of the solution (L) and m is the mass of the adsorbent (g) [98-104].

Adsorption isotherms are a graphical representation of the adsorption process that occurs at gaseous or liquid surfaces at constant temperature. Adsorption isotherms give important information about the adsorption equilibria and aide in the prediction of the level of adsorbate uptake by a solid phase adsorbent. Thermodynamic parameters such as equilibrium constants, enthalpic or entropic parameters provide an understanding of the adsorption process.

The Langmuir adsorption model developed by Irving Langmuir provides a simple equilibrium expression for the adsorption of a monolayer process. It was developed to describe gas-solid-phase adsorption onto activated carbon. Subsequent development provided a description of adsorption behavior of solutes in a solid-solution system [101-103]. The Langmuir

model describes the monolayer adsorption of an infinite number of localized identical and equivalent sites.

A graphical representation of the Langmuir isotherm is a hyperbolic function which has a characteristics plateau indicating the equilibrium saturation point, characteristics of adsorption of gas on homogeneous surface [101-103].

$$Q_e = Q_{max} \frac{K_s C_e}{(1+K_s C_e)} \qquad (1.2)$$

Q_{max} (mmol/g or mg/g) is the maximum monolayer adsorbate uptake by the adsorbent under the given conditions, K_s is the equilibrium constant of the adsorption process representing the binding affinity of the adsorbate towards adsorption sites, and C_e is the equilibrium concentration of adsorbate.

The Freundlich model explains the exponential relationship between the adsorbent and adsorbate in the low to intermediate concentration range while Langmuir isotherms show better fitting of data at higher concentration. This model also assumes monolayer coverage of adsorbate on adsorbent surface. The Freundlich model represents adsorption of adsorbate per unit mass of adsorbent under pressure.

$$Q_e = k_f \, C_e^{\left(\frac{1}{n}\right)} \qquad (1.3)$$

Where; K_f and n are Freundlich constants, since "n" represents surface heterogeneity and is dimensionless. The Brunauer-Emmett-Teller (BET) model represents an extended form of the Langmuir equation by accounting for multilayer surface coverage where, the van der Waals interaction on the surface of the adsorbent is more favorable [101-103].

The Sips model [105] is a modified Freundlich isotherm applicable for solution phase adsorption and also assumes monolayer coverage. However it can also predict heterogeneous adsorption as presented as equation 1.4.

$$Q_e = Q_{max} \frac{K_s C_e^n}{1+K_s C_e^n} \qquad (1.4)$$

Q_e is maximum sorption capacity of the adsorbent, C_e is concentration of adsorbate after equilibrium and K_s is equilibrium constant indicating the affinity of the adsorbate towards sites of adsorbent. The n parameter denotes the surface heterogeneity, where *n=1* represents a uniform surface, according to the Langmuir isotherm. The monolayer capacity (Q_m) is shown in equation 1.4, and this model converges to Freundlich model at dilute concentration conditions.

1.3.3 Types of Sorption Isotherms

There are several types of adsorption isotherms, which can be explained as Type I (reversible) adsorption isotherm which describes monolayer adsorption resulting from microporous structures at relatively low pressure (<0.1). This kind of limited uptake behaviour is observed by solids having relative limited surface area such as activated carbon, zeolite and porous oxides [97, 100-102]. The Type II isotherm describes adsorption behaviour of macroporous adsorbents representing monolayer to multilayer adsorption [*cf.* Fig 1.4].

Type III and V isotherms involve multilayer adsorption and heterogeneous interactions between the adsorbent and adsorbate. The Type III isotherm shows very strong adsorbate-adsorbate interactions. However Type V is an uncommon type of isotherm because of the weak interactions between the adsorbent and adsorbate. Type IV has a characteristic hysteresis loop evidenced by various mesoporous adsorbents since capillary condensation may also occur [*cf.* Fig.1.4].

However, Type II, IV, and VI isotherms describe the occurrence of stronger interactions adsorbate with adsorbent [97, 100-102] whereas; while in Type VI isotherm multilayer adsorption is dependent on the energy difference between the adsorption sites.

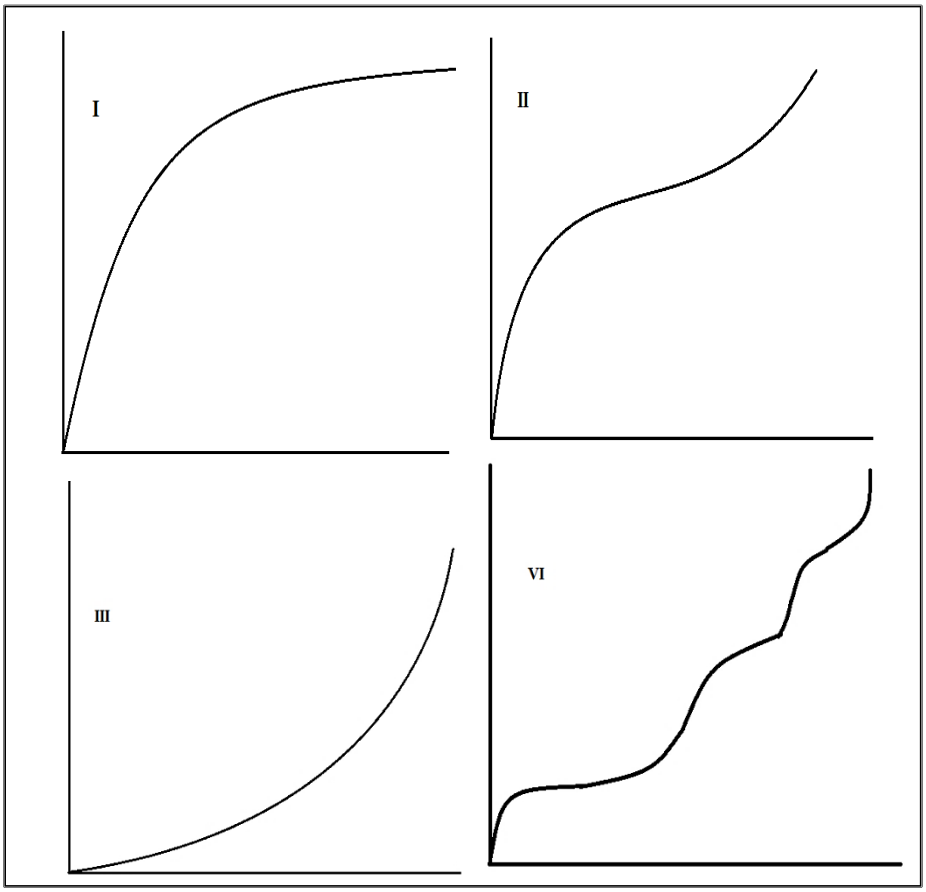

Figure 1.4: Various types of adsorption isotherms [refs.97,100-102].

1.3.4 Types of Adsorbent Materials

Nowadays adsorbents containing natural polymers or various waste products from agriculture biomass are widely used as adsorbents to potentially remove arsenic species or other heavy metals from aqueous environments.

Activated alumina (Al_2O_3, aluminum oxide), is an efficient mineral for the removal of arsenic from water. It has a large surface area with good distribution of macro and micropores but the level of removal depends upon the grade of alumina. For example, when using granular alumina the uptake capacity is usually lower than other kinds of alumina under the same conditions [106]. Moreover, activated alumina can remove As (III) and As (V) at optimal levels at pH 6.1 and 5.2, respectively. Regeneration of alumina is very difficult and tends to show low affinity towards As (III) [106].

Activated Carbon (AC) is one of the most extensively used adsorbent materials for the removal of many organic pollutants from water. It is an efficient sorbent for arsenic removal in drinking water. On the other hand, the slow sorption kinetics, effect of variation in pH during reaction, and regeneration methods decreases its affinity towards arsenic as confirmed by Gupta and co-workers [107]. Commercial activated carbon has a high sorption capacity (mg/g) [108] and it can be modified to increase the arsenic uptake using impregnation methods that employed metallic silver, copper, or iron to achieve high arsenic uptake [88]. Impregnated AC has limited adsorption capacity for As (III) as compared with As (V). It is an expensive adsorbent with limited availability and has little potential for As (III) [109]. Scattered research has been reported for a wide variety of natural sorbent materials for the treatment of contaminated wastewater. Such types of natural "sorbent materials" are relatively low cost and inexpensive to regenerate and various reviews have determined the sorption capacity and efficiency of such materials [109, 110]. Low-cost adsorbents include bark/tannin-rich materials, lignin, chitin/chitosan, dead biomass (e.g., hair), seaweed or algae, clay, zeolites, fly ash [111], iron-oxide coated sand [112], rice and modified wool [113], and/or cotton [114]. However the major problem with this kind of adsorbent (and some other industrial waste materials) is discoloration

which can be overcome by some chemical pretreatments, acids, bases, or acidified formaldehyde. Literature studies also show the use of red fire sawdust as an adsorbent for uptake of copper and hexavalent chromium. Dead biomass also has potential applications for the adsorption of various heavy metals [114]. Bark, has been used as an ion exchange adsorbent because of its high tannin content. Randall et al. reported that some tannin rich materials like bark can be used as cation exchange materials [115]. However, discoloration of the water from the soluble phenol has its limited potential use [115,116].

Other waste products such as sawdust and lignins are also reported as sorbents [117]. Clay and zeolites also show considerable adsorption capabilities but required some chemical and physical modifications to maintain high sorption affinity [118]. Large surface area of clay (up to 800 m^2/g) helps to attract and bond the heavy metallic species [119]. However, these sorbents have very low sorption capacity (~0.1-0.2 mmol/g) [120]. Cellulose-carbonated hydroxyapatite nanocomposites possess high surface area and functional groups which enable this adsorbent to remove As (V) with a good removal efficiency of 65-71% [121]. Another naturally abundant sorbent is chitin, found in the exoskeleton of crabs or other arthropods and along with waste by-products of various industries [121].

1.4 Chitosan

1.4.1 Origin of Chitosan

Chitosan can be produced by the partial deacetylation of chitin which is reported as "naturally abundant biopolymer". Chitin is found in nature in the cell walls of some fungi. Chitin and chitosan can be extracted from crustacean shells of prawn, squid, lobster, crab, shrimps, and

beetles [3]. Deacetylated derivatives of chitin such as chitosan display adsorption properties for removal of various kinds of pollutants from water [116, 121].

Chitosan is a relatively inexpensive adsorbent suitable for heavy metals. Chitosan and chitin have similar molecular structures with reactive hydroxyl and amino groups. Chitosan has greater crystallinity than chitin and also shows high solubility in many acids [2, 3,122].

1.4.2 Extraction and Production of Chitosan

Many aquatic organisms and supporting materials of various microorganisms are composed of chitosan and chitin [123]. On a commercial scale, chitin or chitosan can be isolated and produced from aquatic crustaceans. Chitin and chitosan can be extracted from the cuticle of insects and mushrooms by demineralization, deproteination, decolorization and deacetylation [124]. Isolation of chitosan from aquatic fungi Zygomycetes has significant and potential applications in industrial processing. However this extraction is temperature dependent since highly purified product can be obtained using various extraction strategies [125]. Extraction of chitosan from fungal mycelia was also reported [122].

1.4.3 Applications of Chitosan

Chitosan is a modified biomaterial and has potential commercial uses in biomedical engineering, dentistry, chemistry, food industry, sewage treatment, ophthalmology, biotechnology, cosmetics, and textile [13, 126]. Chitosan can be used as an insecticide or fungicide. It can be used as an adhesive or strength additives for paper and as preservative coating for many glass fibers. This versatile material also has potential applications in water and wastewater treatment as a flocculating agent and/or chelating agent [13, 126].

In waste water treatments, chitosan is suitable for absorbing harmful radioisotopes from industrial wastes and can be used to potentially recover uranium from sea water and fresh water [127]. Chitosan has many useful features like hydrophilicity, biocompatibility, and antibacterial properties. It has a potential use as a gene carrier since it possesses functional groups which can bind with nucleic acids and also shows nonallergenicity properties [128].

Chitosan has application in the manufacturer of many surgical and optical tools [129]. Chitosan is non-toxic material, non-corrosive, and biodegradable material [130]. Chitosan has no harmful effect on animals and plants and does not show any apparent negative effects on the environment [131].

1.4.4 Functional Characteristics

The main characteristics and properties of chitosan depend on its molecular weight (MW) and degree of deacetylation (DD) [3, 4]. Hong et al. performed a thermogravimetric analysis of chitosan to analyze the effect of heating rate on the degradation temperature of chitosan and they observed that the degradation of chitosan is a single-step process where the degradation temperature increases with heating rate [132]. The free primary amino groups (*cf*. Fig.1.5] of chitosan enable it to behave as a positively charged polycation in neutral or acidic solution as its pK_a is 6.2, where pH values below pH 6.0 result in protonation of the amine group ($–NH_2$ – NH_3^+) [133].

Chitosan is insoluble in pure water (pH~7) and other neutral aqueous media, whereas; ionized forms such as salts and complexes are generally more water soluble. Depending on the molecular weight distribution of a particular chitosan sample and its degree of deacetylation, chitosan can be dissolved to form viscous solutions and gels [134,135].

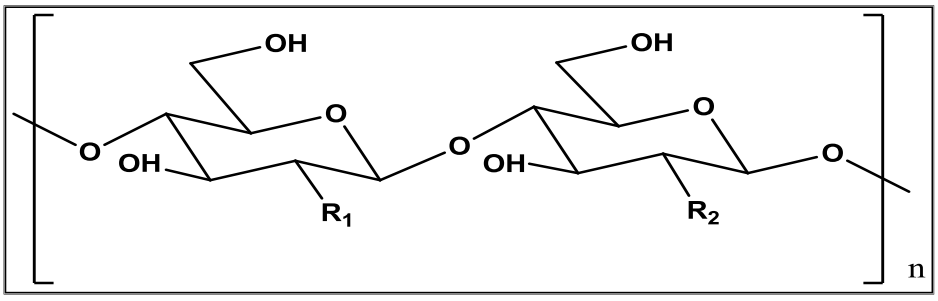

Figure 1.5: Structure of two chitosan monomers, where R_1 is indicating amine (NH_2 -) and R_2 is N-acetamide (CH_3CONH -) groups on the polymer chain depending on the degree of acetylation.

Chitosan, a linear polymer is an effective ion exchanger for heavy metals because of its free amino groups [*cf.* Fig. 1.5] which are involved in intra- or inter-molecular H-bonding which contribute to its ability to make a complex with transition metal ions. Greater metal chelation occurs due to the presence of amino groups of chitosan relative to either chitin or cellulose (i.e. no amino group). Different morphologies of chitosan materials such as membranes, films, gels, beads, fibers, and microspheres have variable ratios of surface area/mass, resulting in variable adsorption capacity [3, 4-6]. Flakes and powders have fairly low surface area and limited porosity that are not considered suitable for sorption. Chitosan gels can be modified chemically to adsorb the selective ions at various pH conditions [136]. Mesoporous chitosan-based aerogels have also been studied as adsorbent materials [7].

1.4.5 Chitosan Based Materials: Synthesis and Applications

Chitosan can be used as the coagulant for negatively charged contaminants in its protonated state. For the treatment of mineral and organic suspension, chitosan can be used as a flocculent above the pK_a of ionizable macromolecules [12]. The research conducted in 1984 by Yang and Zal, summarized that chitosan chelates five to six times more metal than chitin due to the free amino groups exposed during deacetylation [137].

Improvements in the availability of internal sorption sites and enhanced diffusion mechanism can be achieved by conversion of chitosan flakes into gel or beads. Chitosan beads have poor chemical resistance and mechanical strength with some material limitations [138]. Experimental results by Masri et al. compared chitosan adsorption properties with bark, activated sludge, clay and other materials and revealed that chitosan possesses exceptional binding capacity (i.e. $\geq$ 1 mmol metal ion/g sorbent for most metal cations) [139]. Also the greater adsorption capabilities than polyaminostyrene (a relatively expensive form of the ionic zeolite resin) was reported for chitosan [139].

Chitosan (N-deacetylated product of chitin) can be chemically and physically modified into its derivatives to attain greater accessibility to active sites and sorption capacity for arsenate anions or other pollutants. Hsien and Rorrer determined that the surface area of *N*-acetylated chitosan beads is greater (223.6 m^2/g) than *N*-acetylated beads (192.4 m^2/g) without cross-linking vs. N-acetylated cross-linked beads (42.6 m^2/g) [140]. Sometimes chemical modifications are required to attain increased porosity and reduced crystallinity [141]. Some resins containing copper (II)-complexed with chitosan show high selective adsorption for trivalent metal ions over divalent zinc ion. Copper is used to protect adsorption sites from cross-linking agents during synthesis of such resin materials [142].

A common method for the modification or tailoring of the physical and chemical properties of chitosan is cross-linking [143]. Cross-linking enhances the desirable functionality such as the resistance of chitosan against acids and it increases the sorptive uptake properties of chitosan. Generally, cross-linking is surface modifies the surface of various materials such as nucleic acids, protein and various drugs. Cross-linking is sometime used to determine the surface relationship between the ligands and surface receptors of various proteins and peptides. Chemical specificity and reactivity of particular functional groups are characteristic of the type of cross-linker employed. It is worth mentioning that chemical modification of chitosan was extensively studied and many chemical reagents have been used for cross-linking. Koyama et al. used chloromethyloxyrane as a cross linking reagent [144].

Several bi or poly-functional cross-linking agents can be used such as glutaraldehyde (GL), ethylene glycol diglycidyl ether (EGDE), glyoxal, and epichlorohydrin (EPI) [145]. Oshita et al. observed that chitosan cross-linked with ethylene glycol diglycidyl ether has good efficiency for the removal of mercury and other metallic ions at ultra-trace amounts under acidic conditions [146]. Muzzarelli et al. reported the chelating properties of the chitosan for transition metal ions in aqueous solution (pH~7) [143]. However, as indicated above, chitosan is characterized by its solubility in aqueous acidic media (acetic acid, hydrochloric acid or nitric acid) which hinder its practical applications for removal of metallic ions at low pH [142, 145]. Glutaraldehyde is a low-cost, highly reactive cross-linker since this linear dialdehyde (Fig.1.6a) has the ability to react with amine groups of carbohydrates to generate more stable cross-links. Glutaraldehyde has applications as an enzyme immobilization reagent. This 5-carbon oily liquid has a complex reactivity and a controversial behavior in aqueous solution (Fig.1.6) [144, 147]. The glutaraldehyde is also referred to as a traditional cross-linker since the main reaction site for

an incoming carbonyl group of glutaraldehyde is the amine groups of chitosan [14, 15]. During cross-linking reaction, a Schiff base reaction occurs and there may be several types of reaction. One of the aldehyde groups of glutaraldehyde will be free along with the formation of one Schiff base or two monomers of chitosan will react with one glutaraldehyde to give a highly cross-linked product. Another possibility is the self-polymerization of glutaraldehyde resulting in highly crossed-linked homopolymer [13, 14]. Moreover, aqueous solutions of glutaraldehyde have been reported to contain at least 13 different forms of glutaraldehyde at equilibrium (*cf.* Fig.1.6) [13, 14]. There is also a clear evidence of spontaneous polymerization in aqueous solution at ambient temperature even in the absence of the catalyst. Various tetrameric, pentameric [Fig.1.6c] forms, ring structure with α, β-unsaturated aldehyde [13,14] and some hydrated forms [13,14] have been reported in aqueous solution.

Chitosan and glutaraldehyde cross-linked polymers are used for recovery of various metals, cadmium, molybdenum, vanadium, and also for palladium sorption [148-150]. Chitosan flakes show relatively high sorption capacity ~ 1.8-2.2 mmol/g for positively charged copper ions [151].

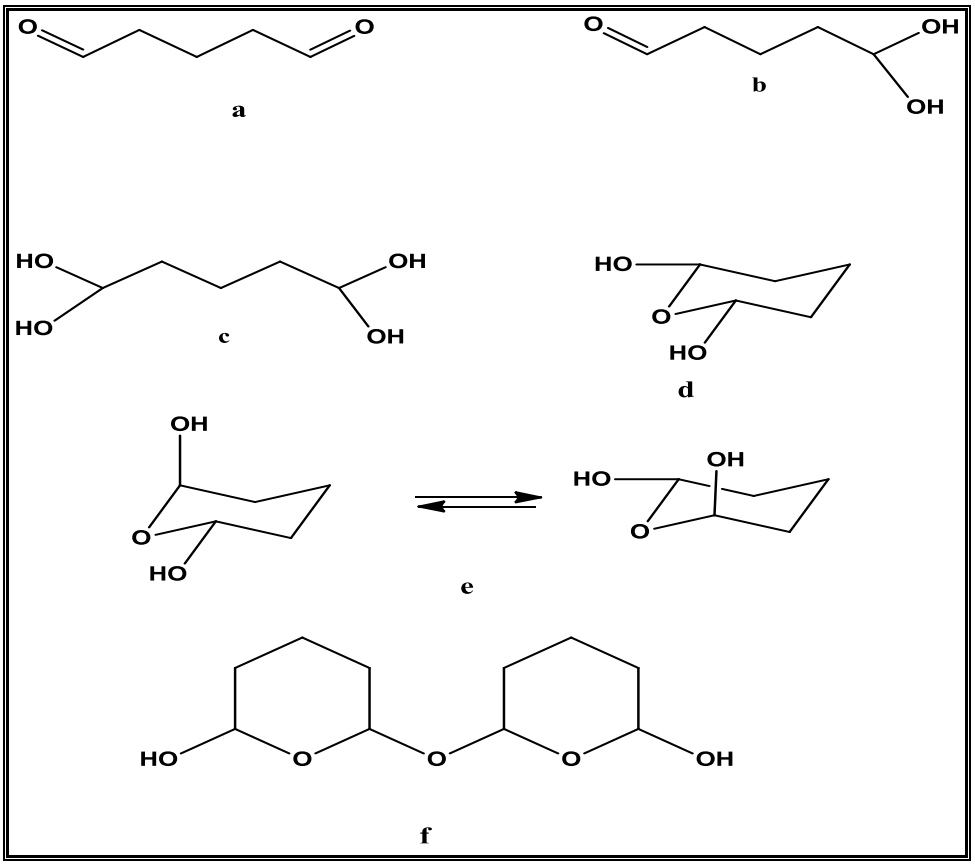

Figure 1.6: Various molecular forms of the glutaraldehyde in aqueous solution [14] where *a* linear form of glutaraldehyde, *b* and *c* are dehydrate, *d* and *e* are cyclic *cis* and *trans* isomers, and *f* one of the polymeric form.

1.4.6 Removal of Arsenic using Chitosan/Chitosan Based Materials

Raw chitosan shows limited arsenic uptake (ca. 0.052 mg/g) [11] whereas; modified chitosan materials are effectively used as sorbents to extract arsenic species from water. It is also reported in the literature that protonation of the primary amino group of chitosan enables it to behave as a cationic adsorbent for anionic dyes [152] and metal anions such as hexavalent chromium [153] species in acidic media, whereas; the role of the amino groups as a binding site for metal ions is also recognized [154]. In addition, chitosan/chitin mixtures have been used for

removal of various anions along with arsenate [154]. In general, cross-linking enhances adsorption capacity and stability under various pH conditions [146].

The efficiency of chitosan based semi-interpenetrating polymer network (semi-IPN) hydrogel composites were investigated for the uptake of anionic and cationic dyes [155]. Similarly, chitosan cross-linked with glutaraldehyde can be used to remove arsenic from water [4]. Chitosan impregnated with various metals like iron, molybdenum can be used selectively for arsenic removal in water systems [4]. Chen and Chung studied chitosan beads and the effect of pH and temperature on the adsorption of arsenic [6]. They observed that optimal pH for removal of As (V) and As (III) was 5.0 and there was little effect of other ions present at concentration lower than 50 mg/L [6].

Chapter 2 EXPERIMENTAL WORK

2.1 Material and Methods

2.1.1 Materials

Sodium hydroxide, potassium phosphate monobasic, *para*-nitrophenol (PNP), disodium hydrogen arsenate heptahydrate ($Na_2HAsO_4.7H_2O$) [Caution: Arsenic compounds are carcinogenic, highly toxic *via* inhalation, and skin contact], low molecular weight chitosan (85% deacetylated, molecular weight range: 50,000-190,000 kDa), glacial acetic acid and 50 wt.% glutaraldehyde in water were obtained from Sigma-Aldrich Canada Ltd and were of the best quality available. Various HPLC grade solvents such as acetone, methanol were product of Sigma-Aldrich Canada Ltd. The dried reagents were stored in a desiccator containing activated molecular sieves as the desiccant until required and all other reagents were used as received unless specified otherwise. All stocks solutions were freshly prepared using 18 MΩ-cm Millipore water and pH of the various solutions was adjusted with 0.01 M NaOH. Unless otherwise mentioned, all experiments were carried out at room temperature 22±1°C.

2.2 Spectroscopic Techniques

2.2.1 Ultraviolet-Visible (UV-Vis) Spectroscopy

UV-Vis spectroscopy and with the Beer-Lambert law were used to quantitatively determine the concentration of the absorbing species in the given solution. All sorption analysis for PNP were obtained on a Cary 100 scan UV-Vis spectrometer at pH 8.5 and 5.0 at room temperature (295 K). Absorbance values of PNP using a quartz cuvette, were recorded at λ= 400 nm for pH 8.5 nm to determine the unbound PNP concentration (C_e) of species of interest [156].

The molar absorptivity (ε) of PNP estimated using the Beer-Lambert law was 18,030 and 10,252 L mol^{-1} cm^{-1} at pH 8.5 and 5.0 in 10 mM potassium phosphate buffer respectively, in agreement with previous reports [35, 156].

2.2.2 Inductive Coupled Plasma-Optical Emission Spectroscopy (ICP-OES)

ICP-OES was used to measure the concentration of arsenic species in aqueous solution. During the analysis, sample is introduced into a radiofrequency (RF) induce argon plasma though a concentric nebulizer (Fig. 2.1) with an axial plasma configuration into a glass chamber (Fig. 2.2) where it is converted to aerosol. Because of high temperature at the core of inductively coupled plasma, this aerosol undergoes desolvation, evaporation, dissociation at high temperature. Analyte element undergoes the ionization by collision, excitations, and/or by aid of high energy. Upon relaxation these atomic or ionic state species emit photons of specific energy [158].

The wavelength of emitted photons is characteristics of a specific element and can help to identify the element while the intensity of photons emitted is directly proportion to the concentration of a specific element in the sample [93]. Then particular element is detected by atomic emission spectrometry detector. The concentration of unbound arsenate in the solution was estimated using ICP-OES (Fig. 2.1).

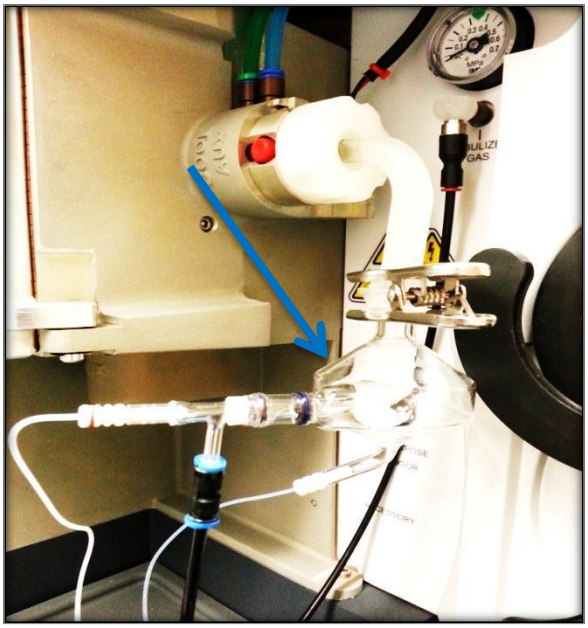

Figure 2.1: ICP-OES(Inductive coupled Plasma-Optical Emission Spectrometry) instrument showing glass spray chamber (refer to blue arrow).

The instrument was calibrated at concentration of the arsenate oxoanions, flush pump rate was 100 L/min and analysis pump rate was 40 L/min with 5 sec stabilization time. RF power used was 1150 W with auxiliary gas flow rate at 0.5 L/min and nebulizer gas flow was 0.50 L/min (Table.2.1).

Table 2. 1: Optimized parameters used for ICP-OES Analysis.

Element	Arsenic(As)
Wavelength	189 nm
Auxiliary gas flow	0.50 (L/min)
Nebulizer gas flow	0.50 (L/min)
Flush pump rate	100 (L/min)
Analysis stabilization time	5 sec
Analysis pump rate	40 (L/min)
RF power	1150 Watts
Calibration	Linear Calculated Intercept
Plasma View	Axial

2.3 Synthesis of Chitosan-Glutaraldehyde (CH-GL) Copolymer

Chitosan glutaraldehyde crossed-linked polymers (CH-GL) were synthesized with variable amounts of glutaraldehyde where the amount of chitosan was fixed chitosan mass as reported elsewhere [4, 165, 157]. The aqueous chitosan solution (2%) was prepared by dissolving 2 g of chitosan in 200 mL of 2% (v/v) acetic acid solution. The resulting viscous solution was stirred for ~12 h to complete dissolution at room temperature since the pH of the solution was 3.94. An aqueous solution of 0.01 M sodium hydroxide was added drop-wise to the acidic chitosan solution to raise the pH to 5.6. At pH 5.6 and room temperature, the desired amount of 50% glutaraldehyde was added to achieve various weight ratios of chitosan/glutaraldehyde polymers (CH-GL1:6, 1:1, 1:0.50, and 1:0.25, respectively). The degree of gelation and cross-linking depend on the relative mass ratio (CH-GL1:6, 1:1, 1:0.50, and 1:0.25).

The gel formed immediately while stirring and color of transparent gel became dark yellow over a one hour period. Then gel was left overnight to complete gelation. Thereafter, a 2 M aqueous solution of NaOH was allowed to react (~3-4 h) with gel network until a dark brown suspension was produced since final pH of the solution was ~7.0.

The precipitated products were vacuum filtered with Whatman filter paper and subsequently washed with several portions of Millipore water (500 mL) and cold HPLC grade acetone (50-100 mL). The material was then crushed after partial air-drying. Then product was allowed to dry in the oven~ 30-40° C, along with regular gentle grinding to get a darker brown homogeneous powdered material. The product was washed in a Soxhlet reflux extractor using HPLC grade methanol solvent for 48 h at 60° C followed by drying in the vacuum oven at 60° C under reduced pressure. The final product was ground in a mortar and pestle and then passed

through a 40-mesh sieve to ensure a maximum upper size limit on the particles. Thereafter, the products were stored in a desiccator until further use.

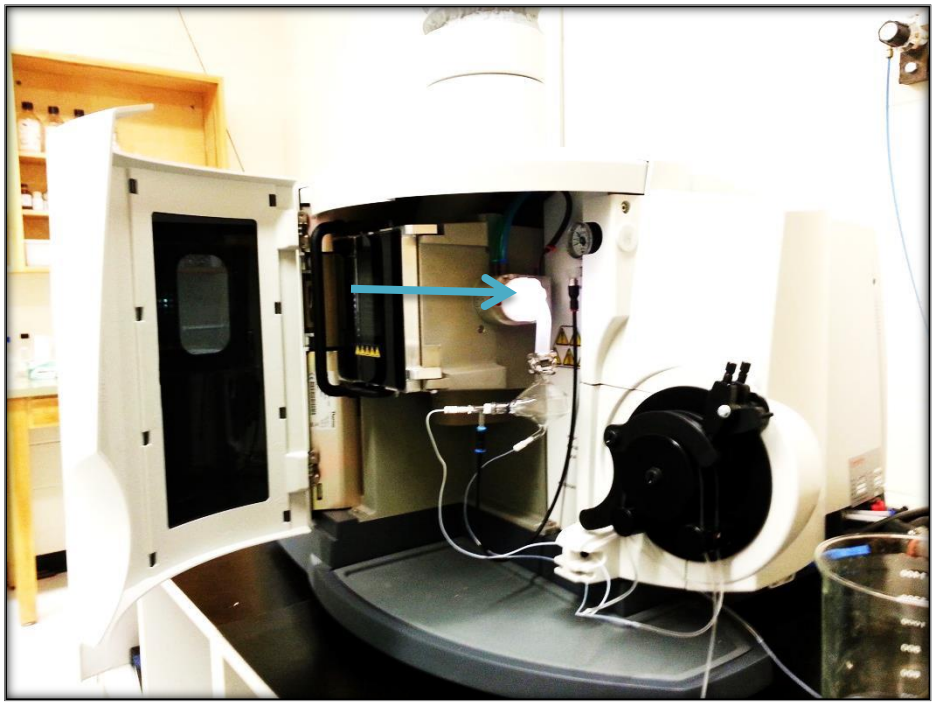

Figure 2.2: ICP-OES instrument showing carrier tube towards glowing plasma (refer to blue arrow).

2.4 Characterization of Chitosan-Glutaraldehyde Copolymers

2.4.1 FTIR Spectroscopy

DRIFT (Diffuse Reflectance Infra-red Fourier Transform) spectroscopy was used to measure the vibrational spectral signatures of the CH-GL copolymers. Solid chitosan copolymers were analyzed using a Bio-RAD FTS-40 Spectrometer in reflectance mode and the intensity was expressed as Kubelka-Munk units, since signals are related to the sample concentration and reflectance intensity [158-160].

Samples were prepared by mixing 2.00±0.01 mg of CH-GL copolymers (1:6, 1:1, 1:0.50, and 1:0.25) with spectroscopic grade KBr (20.00±0.01 mg) and grinding in a mortar and pestle. Spectra were obtained over a range of 4000-400 cm^{-1} by recording 16 scans with correction

against KBr as a background. While FTIR spectra of glutaraldehyde in liquid phase, was taken using CaF_2 window as the cell and the background.

2.4.2 Thermal Gravimetric Analysis

Thermal Gravimetric Analysis (TGA) of samples was measured with a TGA Q50. During the measurement of the TGA profile samples were heated in open aluminum pans to 30° C in an optical Evolved Gas Analyzer (EGA) furnace under controlled conditions and allowed to equilibrate for 5 min before further heating to 500° C at a scan rate of 5° C per min. Nitrogen gas was used for cooling and purging of the samples compartment [161].

2.4.3 Swelling Behaviour of the Copolymers

The swellability of the CH-GL copolymers in water was determined using a gravimetric approach. 20± 0.01mg of each copolymer was added to clean, lidless 6 dram vials and then 10.00 mL of deionized water was added to the vials. Then materials were shaken for 24 h at room temperature at 165 rpm. The materials were filtered using pre-weighed filter paper and then the weights of dried copolymers were determined.

Then filter papers and vials were weighed after 12 hours air drying after achieving constant weight. The weight of hydrated copolymer was calculated using weight of dry super absorbent and swollen samples in equation2.1. Where, m_s is weight of hydrated sample and m_d is weight of dry absorbent.

$$W_s = \left((m_s - m_d / m_d)\right) \times 100\% \qquad (2.1)$$

2.4.4 CHN Analysis

Carbon, Hydrogen, and Nitrogen (CHN) elemental analysis of chitosan and all polymers were obtained using a Perkin Elmer 2400 Elemental Analyzer. A mixture of pure oxygen and

helium gas was used to purge the instrument where the temperature of combustion oven was over 925˚ C while 640˚ C was elevated temperature in reduction oven.

2.4.5 Powder X-Ray Diffraction

Structural differences of the chitosan and chitosan polymers were studied using powder X-ray diffraction (PXRD). All spectra were obtained using PANalytical Empyrean powder X-ray diffractometer using monochromatic Cu-Kα1 radiation. The applied voltage and current were set to 45 kV and 40 mA, respectively. The samples were mounted as evaporated hexane film in a vertical configuration. PXRD patterns were measured in a continuous mode over a 2θ range of 5-45° with a scan rate of 5°/min.

2.5 Equilibrium Sorption Studies

2.5.1 Preparation of Buffer Solutions

2.5.1.1 Potassium Phosphate Buffer Solution

A. Preparation of Buffer at pH 8.5

An aqueous 10 mM KH_2PO_4 solution was prepared using 2.70±0.01 g of salt in 2 L Millipore water. Then solution was stirred and pH of the solution was adjusted with a 2 N NaOH solution up to pH 8.5. Thereafter, this buffer solution was stirred for one hour.

B. Preparation of Buffer at pH 5.0

10 mM KH_2PO_4 solution had been prepared using 2.70±0.01 g of salt in 2L Millipore water. This aqueous solution was stirred and pH was adjusted with a 2 N NaOH solution to raise the pH up to 5.0 and then stirred for one hour.

2.5.1.2 Bicarbonate Buffer solution

An aqueous solution of 0.1 mM sodium bicarbonate was prepared by dissolving 16.8±0.01 g of salt in 2 L Millipore water. Solution was then stirred and pH was adjusted to 8.5 using a 2 N NaOH aqueous solution and then stirred for one hour.

2.5.2 PNP Adsorption Studies at Equilibrium

Each powdered copolymer used was passed through 40 mesh sieve to get a homogeneous particle size. The concentration range of PNP was 0.10-20 mM in potassium phosphate monobasic buffer at pH 8.5 and 5.0 adjusted using 0.01 M NaOH. Nearly constant weights (0.02 ± 0.01 g) of the copolymer were mixed with 10 mL of PNP solution using 4 dram vials. Samples were equilibrated at room temperature on a horizontal shaker table (165 rpm) for 24 h to ensure that the sorbent is fully mixed with an aqueous adsorbate solution as described in another study [118]. In addition several vials containing only PNP solutions designated as blanks (i.e. no sorbent) were also placed on the shaker and used to determine the initial concentrations (C_o).

After 24 h, vials were removed from the shaker table and then the supernatant was transferred into clean vials and centrifuged at room temperature for 1 hour. The concentration of the unbound PNP (C_e) in the solution after sorption was determined using UV-Vis absorbance from the spectrum of the dye using a λ_{max} = 400 nm at pH 8.5 and 317 nm at pH 5.0. Uptake of the adsorbate was determined from the difference between the initial blank (C_o) and residual PNP (C_e) concentration in the solution using equation 2.2.

2.5.3 Arsenate Adsorption Studies at Equilibrium

2.5.3.1 Preparation of Arsenate Stock Solution in Buffer

A 1000 ppm stock solution of arsenate oxoanion was prepared by dissolving 2.2459 g sodium arsenate in 1000 mL phosphate or bicarbonate buffer solution at pH 8.5 or 5.0

accordingly. This solution was stirred for homogenous dissolution. Then arsenate working solutions were prepared in a concentration range from 1 ppm to 200 ppm using above stock solution by appropriate dilution.

2.5.3.2 Preparation of Un-buffered Arsenate Stock Solution

A 1000 ppm stock solution of arsenate was prepared by dissolving 2.2459 g sodium arsenate in 1000 mL deionized distilled water. This solution was stirred for homogenous dissolution. Then arsenate working solutions were prepared in the concentration range from 1 ppm to 200 ppm using above stock solution by appropriate dilution.

2.5.3.3 Arsenate Sorption Experiment

Chitosan and all copolymers were dried in the vacuum oven for 24 h, ground, and sieved through a 40 mesh sieve before weighing. A fixed amount ~20.0±0.01 mg of each polymer was mixed with 10 mL aqueous adsorbate solution (0.1-200 ppm at pH 8.5 and 5.0) in 4 dram vials and sealed with para film liner and capped. The samples were put on the shaker at room temperature for 24 h at 165 rpm. After 24 h, the vials were removed from the shaker and then the supernatant was transferred into other vials and centrifuged for 1 h followed by filtration through 0.45µm nylon syringe filter into glass vials for subsequent analysis using ICP-OES at SIAST (Saskatchewan Institute of Applied Science and Technology).

2.6 Equilibrium Sorption Models and Equations

2.6.1 Sorption Isotherms

The adsorption isotherm represents the equilibrium distribution of an adsorbate in the adsorbent phase relative to the equilibrium adsorbate in the aqueous phase at constant temperature. The equilibrium uptake of the adsorbate by the sorbent phase is expressed relative to the mass of the sorbent (Q_e: mmol/g or mg/g). The quantity Q_e is the amount of the adsorbate in the adsorbent phase at equilibrium, and can be defined by equation (1.1) where, C_o is the initial (before sorption) and C_e is the equilibrium concentration (after sorption), m is the mass of the adsorbent used and V is the volume of adsorbate containing solution in contact with the adsorbent.

2.6.2 Error Analysis

Differential error analysis was done to calculate the error in experimental Q_e values [4, 156, 157]. This error is contributed by uncertainties in mass (m) of adsorbent and concentration (ΔC_0 and ΔC_e) of adsorbate.

$$\Delta Q_e = 2 \left| \frac{(C_o - C_e) \times V}{m^2} \times \Delta m \right| \quad (2.2)$$

$$\Delta Q_e = 2 \left| \frac{V}{m} \times \Delta C_o \right| \quad (2.3)$$

$$\Delta Q_e = 2 \left| \frac{V}{m} \times \Delta C_e \right| \quad (2.4)$$

Where ΔC_o, ΔC_e, and Δm are "standard errors" associated with each measurement. The overall total ΔQ_e is sum of three standards error given in equations (2.2-2.4) and can be measured as an absolute value because there is a positive and negative error for each data point [4, 156]. The standard error ΔC_o and ΔC_e is coming from the uncertainty in absorbance, which can be calculated from the Beer's Law and uncertainty in mass (Δ m) is contributed by the uncertainty in weighing on an electric balance [4, 156].

2.6.3 Removal Efficiency

The percent removal of PNP from the aqueous solution was calculated using equation (2.5), where C_o is the initial concentration and C_e is the equilibrium liquid adsorbate concentration, as described above.

$$\varepsilon_R\% = \left(\frac{C_o - C_e}{C_o}\right) \times 100\% \qquad (2.5)$$

2.7 Synchrotron Methods

2.7.1 Sample Preparation

2.7.1.1 Phosphate Buffer System

A fixed amount (~20±0.01 mg) of chitosan and polymer CH-GL1:1 was mixed with 10 mL adsorbate (45 and 115 ppm) in 4 dram vial and then covered with the para film and sealed. These vials were put on the shaker at room temperature for 24 h at 165 rpm. After equilibration, the vials were removed from the shaker and gravity filtered. Both the residue on the filter paper and the adsorbate solution without polymers were analyzed. Liquid samples were loaded into 2 mm × 3 mm× 25 mm cuvettes and then immediately frozen in liquid nitrogen. Solid samples were loaded onto Teflon powder plates of 2 mm thickness (Fig.2.3). Experiment was performed

at the Stanford Synchrotron Radiation Lightsource (SSRL, Menlo Park, CA, USA) with the storage ring operating at a 3 GeV and 500 mA in top-up mode. Spectra were collected on beamline 7-3 using a Si (220) double crystal monochromator. An upstream Rh-coated mirror provided both the pre-collimation of the incident beam and also rejection of harmonic component. As K-edge XANES and EXAFS measurements of arsenic samples were obtained in fluorescence mode using a Canberra 30-element germanium detector. During measurements samples were held at 10 K in a liquid helium flow cryostat. Nitrogen-filled gas ionization detectors were used to monitor the incident and transmitted X-ray intensities and an arsenic metal foil was placed after the sample for internal energy calibration, energy of which was assumed to be 11867.0 eV.

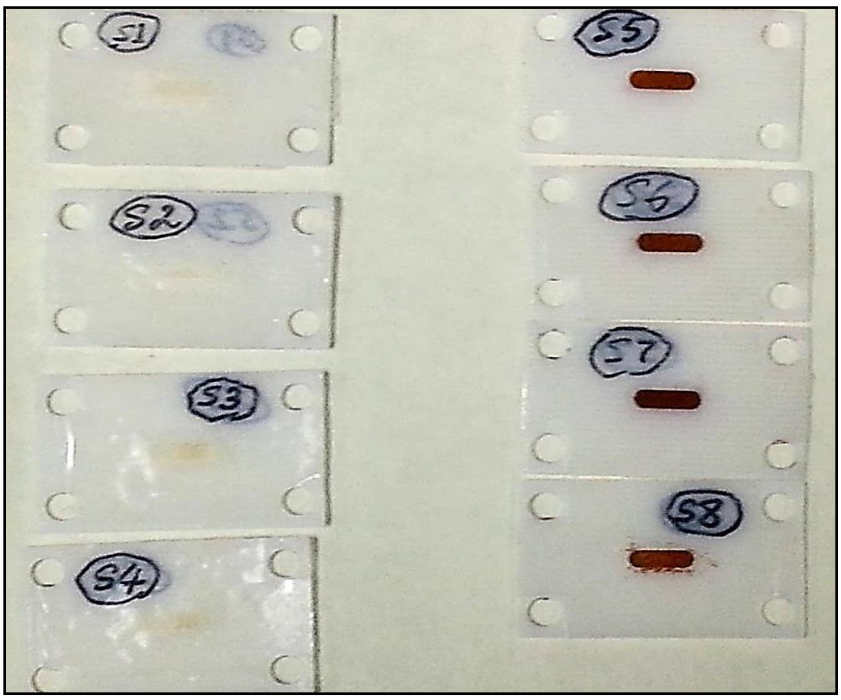

Figure 2.3: Solid samples (CH: S1, S2, S3, S4 CH-GL1:1: S5, S6, S7, S8) mounted in a small Teflon holder, with the sample occupying a small slot in the center, a small hold at each corner is for mounting screws.

2.7.1.2 Bicarbonate Buffer

A separate analysis was done using bicarbonate buffer at pH 8.5 to elucidate the effect of the phosphate buffer. A fixed amount of same polymer CH-GL1:1 (20±0.01 mg) was mixed with 10 mL of arsenate solution (45 ppm) in bicarbonate buffer in 4 dram screw vial and then covered with the para film and sealed. After equilibration, the vials were removed from the shaker and gravity filtered. The residue on the filter paper and adsorbate solution without polymers was analyzed. Liquid samples were loaded into 2 mm × 3 mm× 25 mm cuvettes and then immediately frozen in liquid nitrogen. However, solid sample were packed at room temperature in powder form.

EXAFSPAK program was used for data reduction. The pre-edge subtraction was done to remove the effects of background and other absorption edges. Then spline function was fitted to extract EXAFS. Near-edge spectra were also normalized to get an edge jump of unity. EXAFS was Fourier transformed and amplitude and phase shift functions were calculated after getting an initial "best- fit". Final phase and amplitude shift function were calculated from *ab initio* code feff [200]. The sum of the squares of the differences between experimental and calculated EXAFS was minimized by adjusting the structural parameters [199,200].

Chapter 3 RESULTS AND DISCUSSION: COPOLYMER SYNTHESIS AND CHARACTERIZATION

3.1 Synthetic Yield

The overall yield of chitosan-glutaraldehyde cross-linked polymers ranged from 84-88%, in agreement with previous reported values [4, 156, 157]. The potential loss of small particle sizes product occurred during the filtration and grinding of products. The percentage yields of each copolymer (CH-GL1:1, 1:0.50, and 1:0.25) are given in Table 3.1. The CH-GL1:1 copolymer displayed the greatest yield. The experimental yield calculation was based on the assumption that two monomers of the chitosan can react with one monomer of glutaraldehyde as reported previously [14,162].

The above assumption was based on the concept to ignore the self-polymerization of the glutaraldehyde and to control the level of cross-linking. Although, the self-polymerization of glutaraldehyde was indicated elsewhere [14,162], the stoichiometry obeys equation (3.1) where the ratios are indicative of the number of glutaraldehyde monomers for cross-linking.

$$\mathbf{2}\boldsymbol{Chitosan} + \boldsymbol{Glutaraldehyde} \rightarrow \boldsymbol{Glutaraldehyde} - (\boldsymbol{chitosan})_{\mathbf{2}} + \mathbf{2}\boldsymbol{H_2O} \qquad \textbf{(3.1)}$$

One chitosan monomer has an average molar mass of 161 g/mol and the molar mass of glutaraldehyde is 100.101 g/mol. According to the first step of scheme (Scheme 3.1) two chitosan monomers react with one glutaraldehyde monomer and it is also assumed that both carbonyl groups of the glutaraldehyde are involved in the cross-linking since two molecules of water are lost. The percentage yields of the each copolymer (CH-GL1:1, CH-GL1:0.50, CH-GL1:0.25, and CH-GL1:6) are given in Table 3.1.

Table3.1: The experimental yield (%) of various chitosan-glutaraldehyde (CH-GL) copolymers.

Crossed-linked copolymer	**Weight CH (g)**	**Volume* GL(mL)**	**Yield %**
CH-GL(1:1)	2.00	2.7±0.1	88
CH-GL(1:0.50)	2.00	1.4±0.1	84
CH-GL(1:0.25)	2.00	0.7±0.1	85
CH-GL(1:6)	2.00	13±0.1	N/D

*The density of the glutaraldehyde solution (50% aqueous solution, *w/v*) was 1.106 g/L.

N/D: Not determined

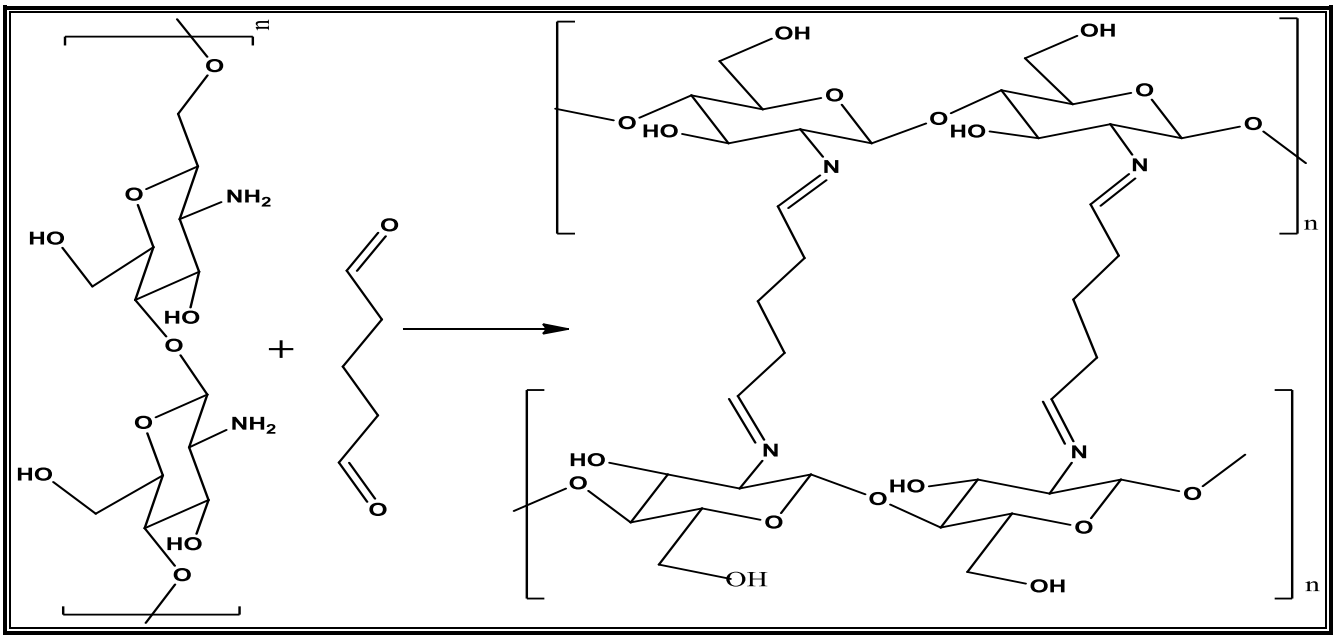

Scheme 3.1: Cross-linking reaction between the chitosan and glutaraldehyde via the amine groups of chitosan, where n represents the number of chitosan glucosamine monomers n×1/2.

3.2 Cross-linking Reactions and Synthesis Approach

Pristine chitosan gives hydrophilic hydrogels that swell under particular acidic conditions. This irreversible gel formation processes can be enhanced using any crosslinking agent or some organic solvent [162]. A schematic approach for the synthesis of copolymers is based on the following observations previously mentioned in the literature, that the $–NH_2$ groups present at position C_2 and sometimes the hydroxyl groups at C_4 and C_6 play important roles in the modification of chitosan during various reactions [162]. Generally during the gelation process, glutaraldehyde undergoes an aldol condensation depending on pH and temperature [4, 14, 162, 163] since the carbonyl group of the aldehyde reacts with primary amino group of the chitosan to generate imine or Schiff base adducts. The synthetic conditions under discussion represent a specific type of reductive amination [4, 164]. The mild acidic solution of chitosan is

viscous due to a polyelectrolyte affect [162] or protonation of the glucosamine units (Fig.3.3) and the viscosity of solution decreases with increasing solution pH [133,162].

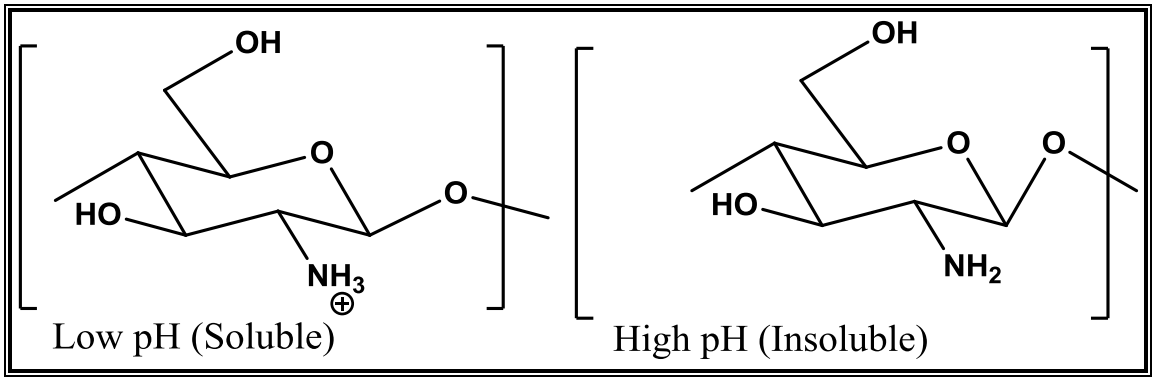

Figure 3.1: Various forms of chitosan in aqueous solution under different pH conditions, low pH < 6, and High pH > 6.5 (Modified from ref [133,135]).

In general, imine or Schiff base adducts generated from the reaction of the carbonyl groups of the aldehyde and primary amino groups of chitosan contain a carbon-nitrogen double bond. However, cross-linking of glutaraldehyde with primary amino group of chitosan follows a complex mechanism which can produce various oligomer products due to aldol condensation, where further polymerization results in gel formation [14,162]. The kinetics of the chitosan glutaraldehyde cross-linking reaction is affected by pH, temperature, and stirring rate of the reaction [14, 162-165].

Insight regarding the reaction mechanism starts from the first step of synthesis starting with the preparation of 2% solution of chitosan in acetic acid. At that stage the pH of the solution is in the range of 3.5-4.5 and only 10% of amino groups are available for nucleophilic addition to the carbonyl group of glutaraldehyde. At this pH, addition of NaOH solution increases the number of deprotonated amino groups without precipitation of chitosan and enables 50% of amino groups to take part in aldol condensation reaction [14, 162,163].

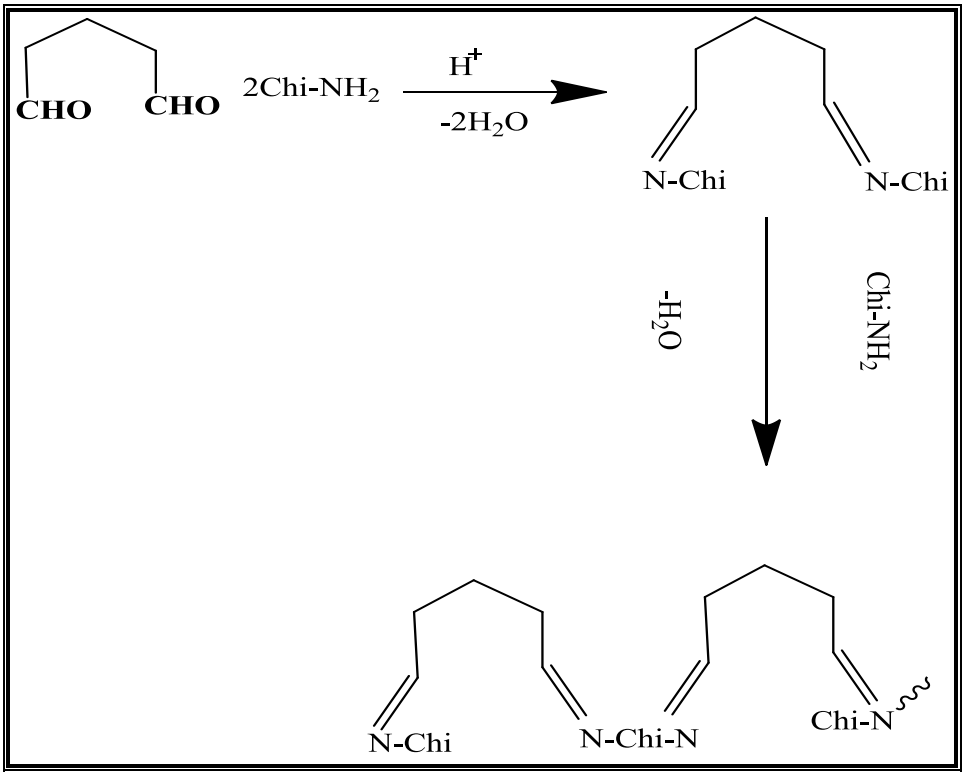

Scheme 3.2: Open chain glutaraldehyde (GL) is attacked by amine group of chitosan (Chi-N) under acidic conditions; self-polymerization of glutaraldehyde was not taken under consideration and N-acetyl group is also involved in the second step of the reaction (modified from ref [166]).

The role of the acetamide groups of chitosan at this pH is unknown. On the other side, glutaraldehyde is present in various isomeric forms such as monomer, bicyclic, and α, β-unsaturated polymerized forms (refer to Chapter 1, section 1.4.5) which undergo hydration because of conjugation stability of the carbonyl forms [14,162,163]. The reactivity of glutaraldehyde towards amino groups of chitosan is greater than hydroxyl groups [167-168]. A previous study indicated that ethylenic double bonds of glutaraldehyde are involved in the aldol condensation reaction but these types of addition reactions are more favourable when excess amino groups are available [163]. The pH condition of this cross-linking reaction ranged from

acidic to neutral based on the fact that glutaraldehyde exists in two major forms free aldehyde and hemiacetal structure [14,169]. These two forms undergo the aldol condensation reaction and form products as shown in the reaction Scheme 3.2 and 3.3. However reaction via hemiacetal and amino group of chitosan was previously observed [170]. During gel formation, the Schiff base adduct is the major product which is unstable under acidic condition. A stable product is obtained at greater pH of the solution by the addition of NaOH [14,169].

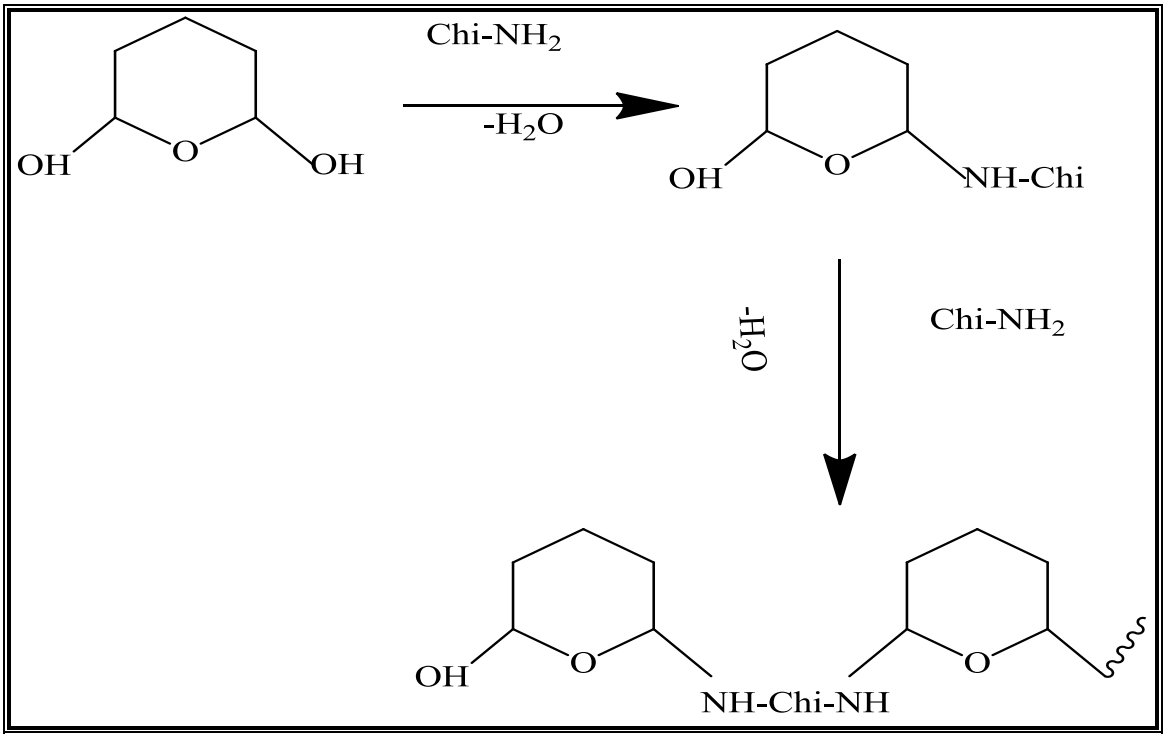

Scheme3.3: Cyclic form of glutaraldehyde (GL) is attacked by amine nucleophile of chitosan (Chi-N) under acidic or neutral conditions, glutaraldehyde underwent self-polymerization and N-acetyl group is also involved in the reaction. Self-polymerization of glutaraldehyde was not taken under consideration and acetyl group is also involved in the second step of the reaction

3.3 Physical Appearance

The synthesis of chitosan-glutaraldehyde copolymers was carried out according to previously reported methods [4, 156] with some modification, i.e. pH adjustment, reactant ratios followed by stirring, drying, and grinding of products. Commercial chitosan is available as high, medium, and low molecular weight; where the water solubility of low molecular weight chitosan is greatest [4, 156]. Chitosan (CH) can be cross-linked with glutaraldehyde (GL) at various mole ratios, and it has been reported that cross-linking affects the physicochemical properties such as the sorption capacity [4]. This can be understood according to the illustration of the copolymer product shown in Scheme 3.1. To test this hypothesis, the synthesis of copolymer materials was carried out at four weight ratios of chitosan and glutaraldehyde [4, 156, 171]**.** The pH of the solution was monitored at regular time interval before and after addition of glutaraldehyde.

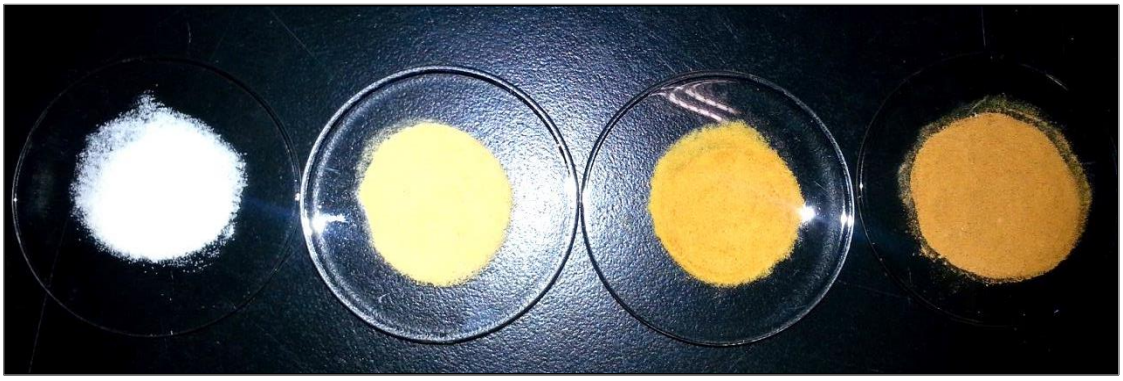

Figure 3.2: Color variation of chitosan and its CH-GL copolymers (From left to right CH, CH-GL1:1, 1: 0.50, and 1:0.25).

In addition to stirring and drying, the occasional grinding of the sample was required to achieve efficient drying of product. Overall, light brown CH-GL copolymers were collected after grinding (Fig.3.2). Darker colored products were obtained with color intensity varying according to increased levels of glutaraldehyde with other reaction conditions held constant. Previously, it was observed that increased in the darker color confirmed the presence of chromophore group

i.e., -C=N- [165]. Previous results [4, 156,171] indicate that the color intensity of the products increased according to the level of glutaraldehyde employed.

Figure 3.3: Chitosan-glutaraldehyde copolymer (CH-GL1:1) after vacuum filtration. Color of the same product after drying in oven (CH-GL1:1 in Fig. 3.2).

3.4 Elemental Analysis

The composition of the CH-GL copolymers was estimated using CHN analysis. The percent deacetylation, and average molecular weight of the chitosan monomer units was applied (as used previously) to find the nitrogen content in 1 monomer unit of chitosan [4, 162]. The empirical formula was determine from the CHN data and then the total carbon contents of polymers were estimated as contributed from chitosan and glutaraldehyde while nitrogen contents were fixed. It was supported from compositions of copolymers that 1 mole of

glutaraldehyde react with 2 glucosamine monomers of chitosan. The error in the calculated value was determined by considering the volumetric errors (±0.1 ml) of dispensing glutaraldehyde.

Table 3.2: The CHN Elemental Analysis and experimental estimates of CH-GL copolymers.

Polymer	Experimental			Calculated		
	%C	%H	%N	%C	%H	%N
Chitosan	41.8	6.70	7.47	41.9	6.47	7.47
CH-GL(1:0.25)	46.1	6.39	6.43	45.5	6.56	6.43
CH-GL(1:0.50)	48.17	6.68	5.50	48.1	6.79	5.56
CH-GL(1:1)	51.5	5.83	4.63	51.4	6.17	4.72

3.5 Solubility and Swelling Behavior of the copolymers

It has been reported in the literature that crystallinity of chitosan and its derivatives can be estimated from the percentage of swelling [59]. Cross-linking can alter the crystalline behaviour of polymers by changing the number of "crystalline domains of the polymer chain" [59] as anticipated by changing in the degree of intermolecular H-bonding for such polysaccharides. The swelling results for CH and CH-GL copolymers are shown in Fig.3.4. The degree of swelling was determined in distilled water and 10 mM potassium phosphate buffer at room temperature. There is decrease in the percentage of swelling with the increase of the

glutaraldehyde content as shown in Fig.3.4. The degree of the swelling for each polymer is greater in distilled water than buffered solution. These results are in agreement with previous reported results [59] where Chitosan-GLA beads with lower degree of swelling show greater adsorption. Chitosan is showing percentage lower degree of swelling in both phosphate buffer and distilled water.

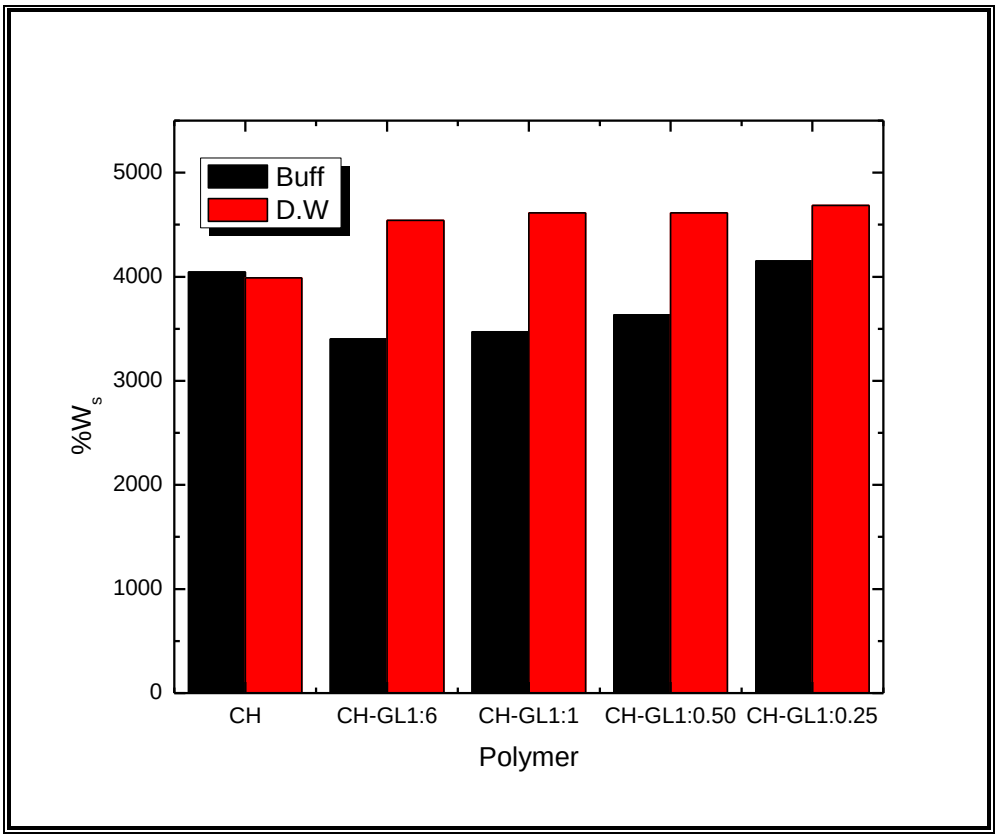

Figure 3.4: Swelling data for chitosan and glutaraldehyde copolymers in distilled water (D.W) and 10 mM potassium phosphate buffered solution (Buff) at room temperature.

3.6 Powder X-ray Diffraction

The effect of crosslinking on the crystallinity of CH-GL copolymers was determined. PXRD spectra of chitosan and polymers (CH-GL1:1, CH-GL-1:0.50, CH-GL1:0.25, and CH-GL1:6) are shown in Fig. 3.5. As shown in Fig. 3.5, chitosan diffractogram has two characteristic

reflections occurring at 2θ =11 and 20°. These two reflection indicate the crystal forms I, and II respectively as also observed by Lazaridis et al. during the year 2007 [165]. Chitosan cross-linked polymers have only one broad peak at 2θ= 21°. Okuyama et al. explained the orthorhombic unit cell of the "tendon chitosan" where chains of chitosan twofold helix have a repeat period of 10.34 Å. In the "zigzag" structure, there are two chains stabilized by hydrogen bonding with packing in an antiparallel pattern [172]. This is supported since cross-linking alters the hydrogen bonding network between the hydroxyl and amino group of chitosan framework. This is understood because of the steric hindrance coming from the GL side chain as observed by Lazaridis et al. [165]. One polymer CH-GL 1:6, contains the highest content of glutaraldehyde shows very different behavior as compared to other copolymers (Fig. 3.5) but the precise reason is unknown. Diffraction results were reported by Silva et al. for chitosan glutaraldehyde cross-linked membranes, where 2-D WAXS (Wide-Angle X-ray Scattering) results for highly cross-linked chitosan membrane show highly amorphous structure [173].

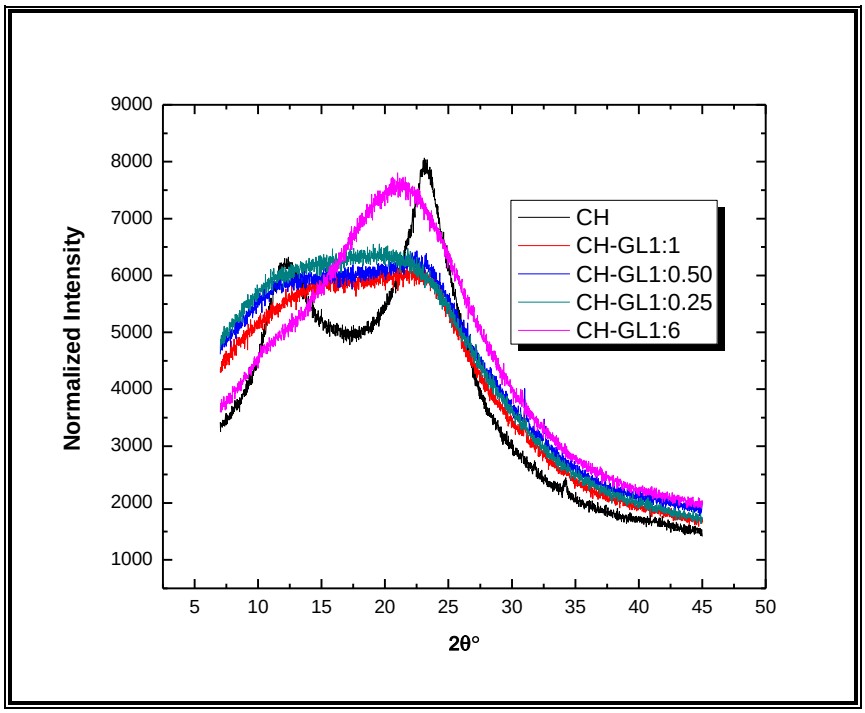

Figure 3.5: PXRD diffraction pattern for chitosan-glutaraldehyde polymers (CH, CH-GL1:1, CH-GL-1:0.50, CH-GL1:0.25, CH-GL1:6).

3.7 Thermal Gravimetric Analysis

The first derivative plots *vs.* temperature for chitosan and each copolymer material are given in Fig. 3.6. Generally chitosan has only one major peak of thermal degradation with increase heating rate [132, 162]. The results of thermogravimetric analysis of chitosan and chitosan copolymers (CH, CH-GL1:1, CH-GL-1:0.50, CH-GL1:0.25, CH-GL1:6) in nitrogen show two different decomposition stages. The major peak indicates the thermal degradation of chitosan at ~300° C, while weight loss at less than 100° C is attributed to loss of adsorbed or bound water or some solvents loss [162].

It can be inferred that chitosan degradation in nitrogen is one step process. The decomposition temperature at 225-275° C and 425° C is related to effect and the level of cross-

linking. The bands at 425°C are indicative of the amount of cross-linking in CH-GL copolymers, and it can be seen in Fig. 3.6 that the peak area increases with an increase of GL content [132, 162]. It is noted that there is a shift in temperature with an increasing content of GL since the CH-GL 1:6 copolymer has a high content of glutaraldehyde which results in shift towards lower temperature in the thermogram [132].

The lower temperature event observed for the copolymers relative to the secondary degradation temperature of the chitosan indicated that copolymers are less thermally stable on the basis that copolymers contain less primary amino groups [162]. The reduced availability of the H-bond donor/acceptor sites due to cross-linking may result in materials that are more amorphous with reduced temperature stability [162].

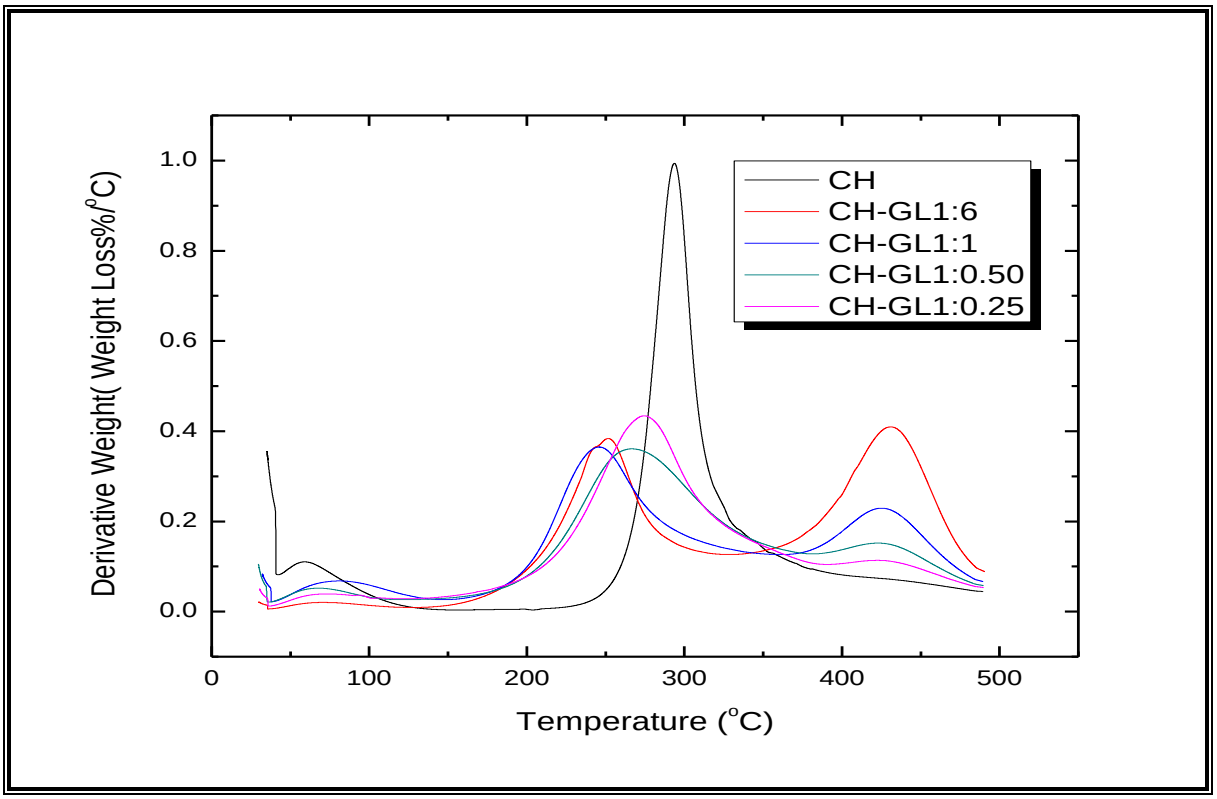

Figure 3.6: The first derivative TGA plots of chitosan and copolymers (CH, CH-GL1:1, CH-GL-1:0.50, CH-GL1:0.25, CH-GL1:6). CH-GL1:6 copolymer has high content of glutaraldehyde shift towards lower temperature. TGA results for GL is not shown here.

3.8 Fourier Transform-Infrared Spectroscopy

FTIR spectra of chitosan, glutaraldehyde and CH-GL copolymers are shown in Fig. 3.7, 3.8, and 3.9. There is a clear difference between the FTIR profile of chitosan, GL and each respective CH-GL copolymer material. The broad band from 3000 cm^{-1} to 3500 cm^{-1} is attributed to the stretching vibration of O-H and N-H of chitosan (Fig. 3.8). Some characteristics IR bands for pure chitosan occur at 1155, 1070, 824cm^{-1} (Fig. 3.7, 3.8, and 3.9) and correspond to the stretching vibration of the glucosidic bridge of the polysaccharide. The stretching vibrations of

the amide I band appear in the 1604-1655 cm^{-1} range (Fig. 3.9). Asymmetric and symmetric C-H stretching occurs at 2879 cm^{-1} (Fig. 3.6, 3.9) [174].

The FTIR spectra of glutaraldehyde has characteristics bands at 1720 cm^{-1} (refer to expanded region of Fig. 3.9) which indicates the presence of free carbonyl groups of glutaraldehyde before the reaction. However this signature is evident for CH-GL1:6 which suggests self-polymerization of glutaraldehyde. The intensity band at 1075 cm^{-1} shows evidence of an ether group corresponding to a cyclic form of glutaraldehyde (*cf.* Scheme3.2 and 3.3) [59, 175, and 178].

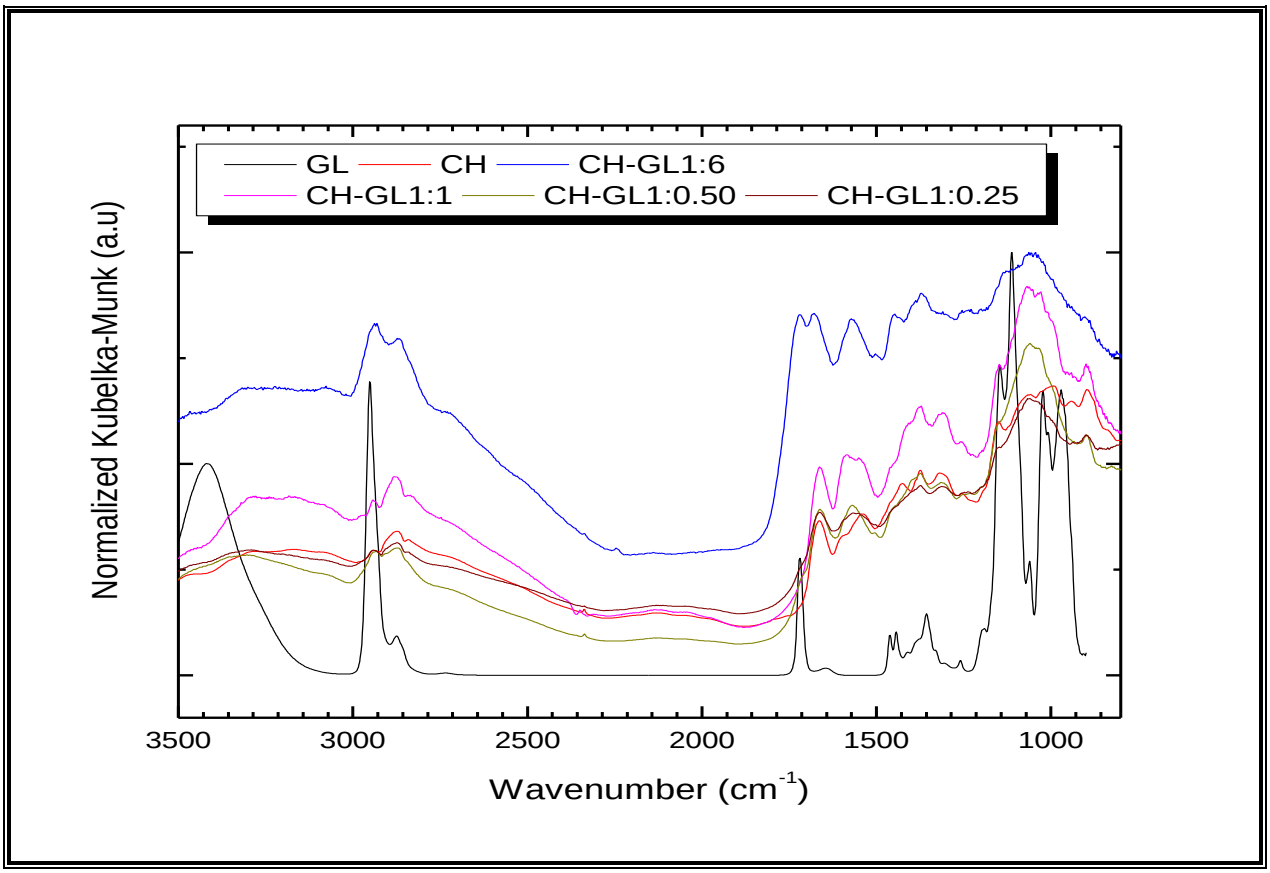

Figure 3.7: The FTIR spectra of chitosan and glutaraldehyde copolymers (CH, GL, CH-GL1:1, CH-GL-1:0.50, CH-GL1:0.25, CH-GL1:6).

The IR bands provide support that the linear form of glutaraldehyde is reacting with the chitosan monomer units. Structural differences exist between the chitosan and its cross-linked copolymers since the IR band at 1660 cm^{-1} indicates cross-linking between the amino group of CH and GL, including the disappearance of the N-H_2 bending (1579 cm^{-1}) signature, which provides further evidence of cross-linking between the chitosan and glutaraldehyde [184]. The range of values from 1324 cm^{-1} to 1380 cm^{-1} are attributed to the stretching vibration of the C-N band (amide) and the C-H bending modes of methylene [4, 156, 171].

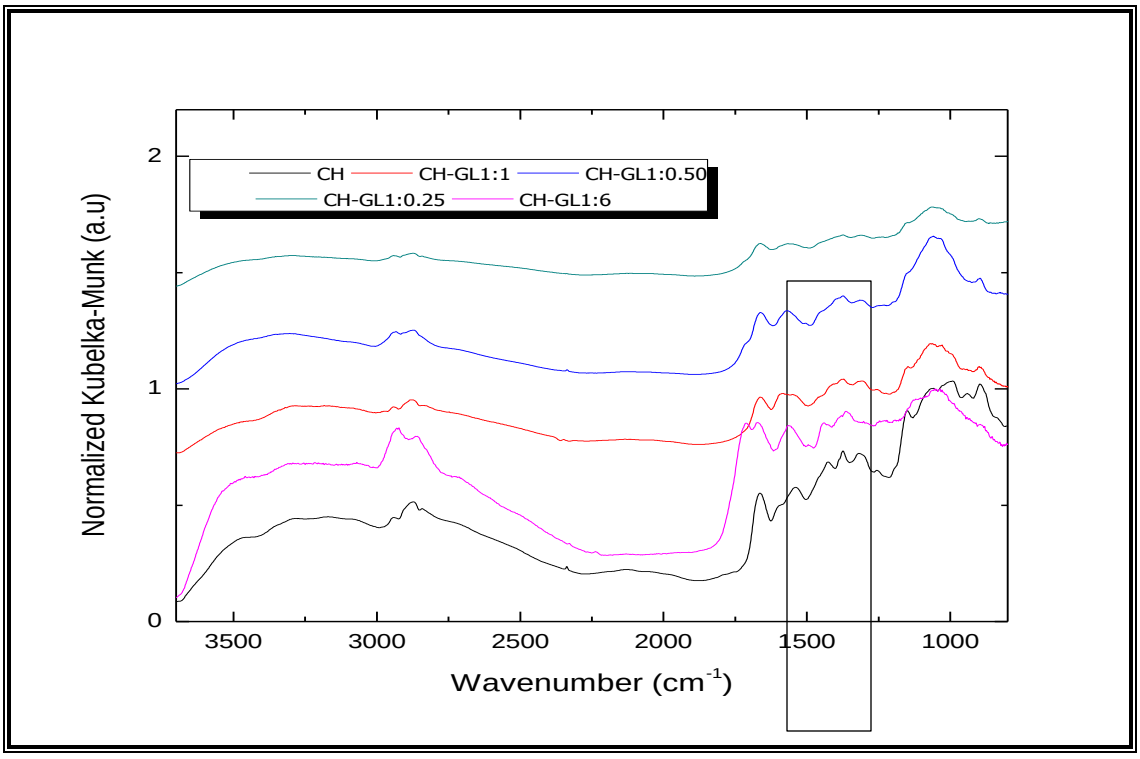

Figure 3.8: The FTIR spectra of chitosan and glutaraldehyde copolymers (CH, GL, CH-GL1:6, CH-GL1:1, CH-GL1:0.50, and CH-GL1:0.25).

The emergence of the new IR signature at 1720 cm^{-1} indicates stretching vibrations of C=N of a Schiff base adduct, in agreement with the presence of cross-linking between glutaraldehyde and chitosan (refer to arrow in Fig.3.9).

Table 3.3: The FTIR bands and frequencies for chitosan-glutaraldehyde copolymers

Polymers	**Frequency (cm^{-1})**					
Vibrational mode	**CH**	**GL†**	**CH-GL(1:6)**	**CH-GL(1:1)**	**CH-GL(1:0.50)**	**CH-GL(1:0.25)**
ν_{as} (C=N)	N/D	N/D	1680	1660	1654	1658
C=C	1540	N/D	1560	1565	1542	N/A
$\nu_s(CH_2)$	2878	2840	2841	2839	2838	NA
ν(O-H)	2970	N/D	3300	3280	3246	3168
C=O	N/D	1720	N/D	N/D	N/D	N/D
δ (CH_2)	1035	1198	1084	1079	1077	1077

N/D Not determined

†Analyzed as liquid film using CaF_2 window as the cell and the background.

ν and δ denote the bands involved the stretching, bending, or deformation of bonds, respectively.

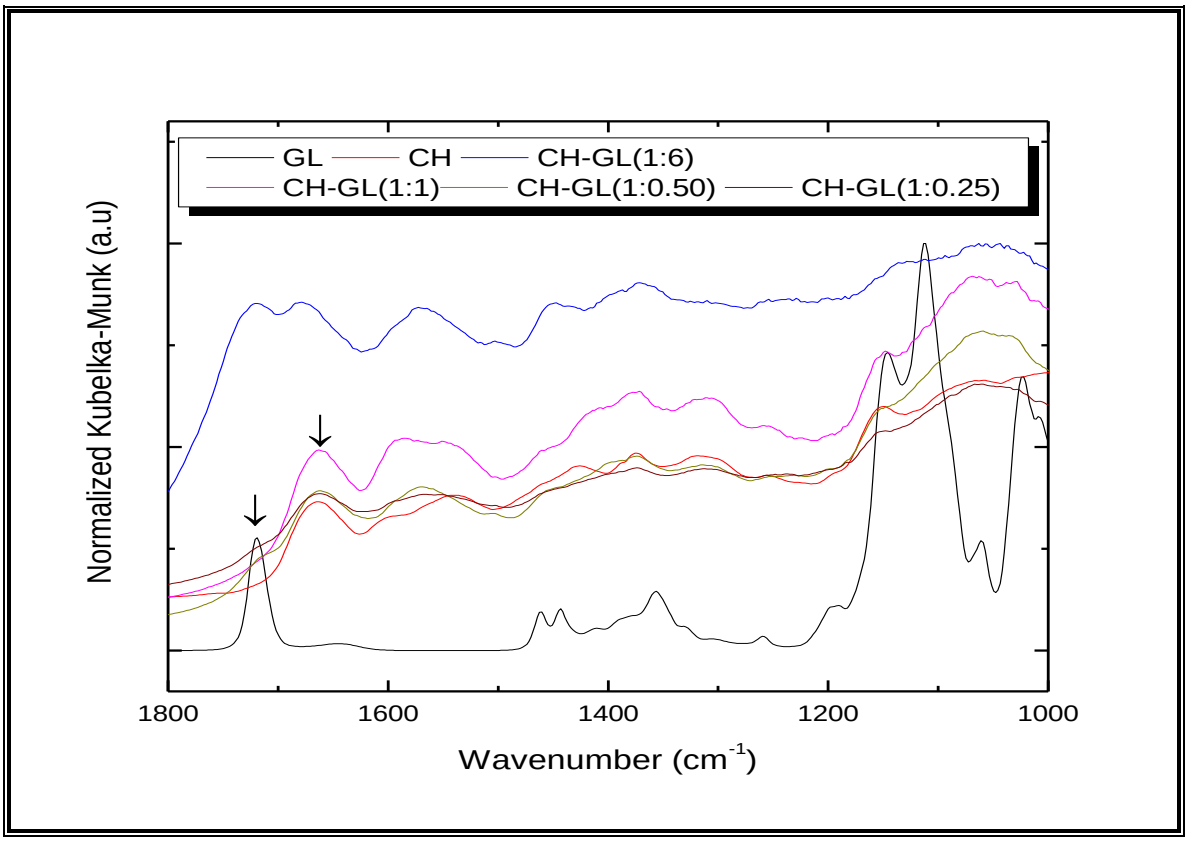

Figure 3.9: Expansion for 1000-1500 cm^{-1} region of the FTIR spectra of chitosan and glutaraldehyde copolymers (CH, GL, CH-GL1:1, CH-GL-1:0.50, CH-GL1:0.25, and CH-GL1:6).

Vibrational bands at 1664 cm^{-1} and 1660 cm^{-1} reveal that chitosan is cross-linked with glutaraldehyde [59, 157,166]. Thus, FTIR bands shifts help to support the Schiff base mechanism for cross-linking between the chitosan and glutaraldehyde [14,157,177]. The doublet in the range of 2800 cm^{-1} to 2900 cm^{-1} can be attributed for the symmetric stretching and asymmetric stretching of the methylene groups. The bands between the region 3200 cm^{-1} to 3400 cm^{-1} show the hydrogen bonded of O-H groups [162].

Chapter 4 RESULTS AND DISCUSSION: EQUILIBRIUM SORPTION STUDIES

4.1 PNP Equilibrium Sorption Results

PNP can exists as neutral or anion (*p*-nitrophenoxide or *p*-nitrophenolate, PNP^-) species depending upon the pH conditions. PNP absorbs at 317 nm in acidic solution and absorbs strongly at 400 nm when pH of the solution is more alkaline (pH > 7). This shift in absorbance depends on the amount of PNP species (neutral or anion) in the solution as the pK_a value of PNP is 7.14 [162]. The effect can be observed by change in intensity of the yellow color, as shown in Fig. 4.1 and Fig. 4.2 [178].

Figure 4.1: Comparison of color intensity of 10mM of PNP and PNP^- at pH 5.0 and 8.5, in 10 mM phosphate buffer.

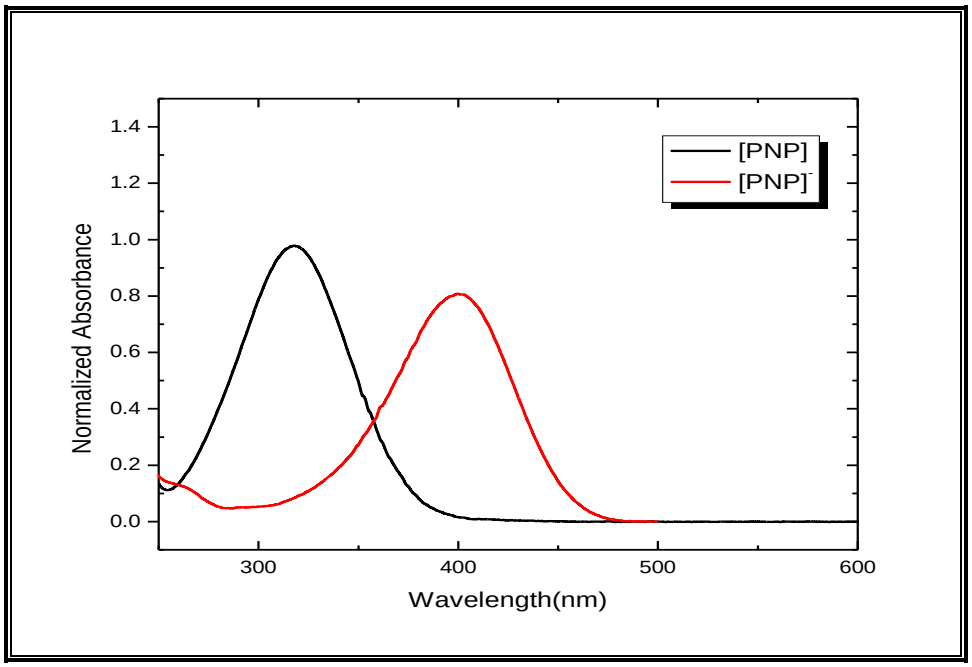

Figure 4.2: UV-Vis absorbance spectra of 10 mM [PNP] and $[PNP]^-$ at pH 5.0 and 8.5.(refer to Figure 1.3 for the molecular structure of PNP)

The adsorption of various dyes using chitosan based materials was reported in the literature [171,175,179]. As mentioned in Chapter 1, many chitosan based sorbents were used for the removal of PNP from water [70-72]. The sorption of PNP was carried out at different pH (5.0 and 8.5) conditions and room temperature (295 K) using a fixed amount (~ 20.0± 0.01) mg of each polymer in 10 mL of PNP adsorbate in 10 mM potassium phosphate buffer. The results were plotted by measuring concentration of the unbounded PNP using a double beam spectrophotometer (Varian Cary 100).

4.1.1 Adsorption of PNP at pH 8.5

The molar absorptivity (ε) of PNP (18,030 and 10,252 L mol^{-1} cm^{-1}) was estimated using the Beer-Lambert law at pH 8.5 and 5.0 in 10 mM potassium phosphate buffer, respectively,. The results are in agreement with previous studies [4, 71-72]. The sorption isotherms of the chitosan-glutaraldehyde (CH-GL) polymers at pH 8.5 are illustrated in Fig.4.3 and Fig.4.4.

In general, the polymer with high content of glutaraldehyde (CH-GL1:1) show high adsorption. The adsorption capacities; Q_e (mmol/g) at pH 8.5 for all polymers are listed in the following order: CH-GL1:1>CH-GL1:0.50>CH-GL1:0.25. Table 4.1 summarizes the best fit parameters using the Sips model at pH 8.5. The sorption capacity is highest for CH-GL (1:1) and lowest for CH-GL (1:0.25). The value of n_s is greater than unity for each of the polymer which indicates that the adsorption deviates from the monolayer adsorption behavior and that the possibility of interaction between the anions of PNP. The removal efficiency for each of the copolymers: CH-GL1:1(4.8-17%), CH-GL1:0.50(3.2-16%), CH-GL1:0.25(1.8-170%) and for CH (0.8-10.1%). By comparison, the removal efficiencies at pH (5.0) are greater compared to the values of obtained at pH 8.5.

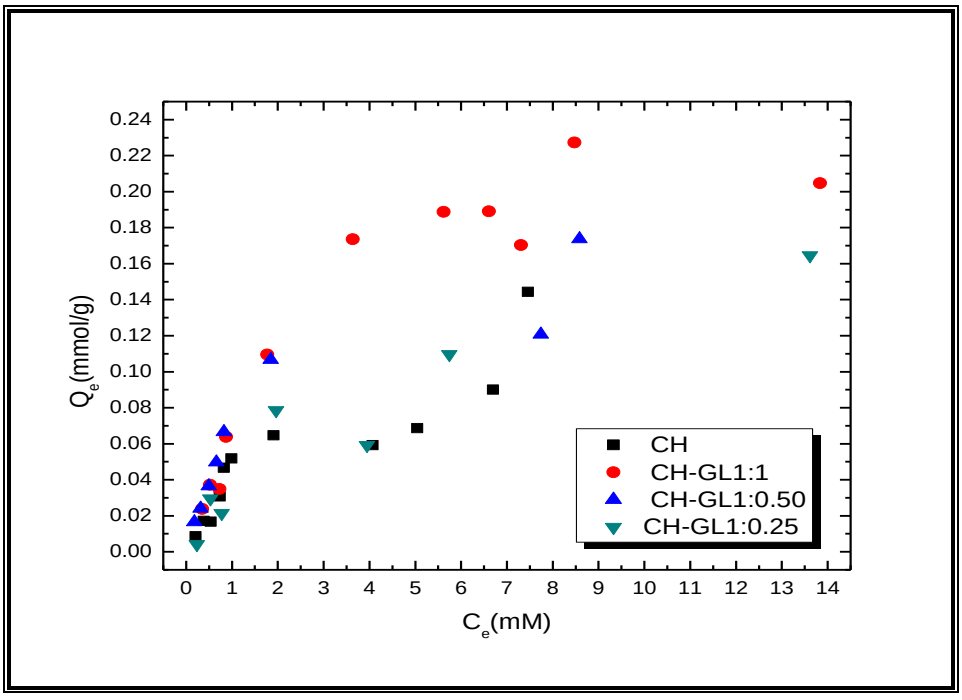

Figure 4.3: Adsorption isotherm results of PNP using CH-GL polymers (CH, CH-GL1:1, CH-GL1:0.50, CH-and GL1:0.25) at pH 8.5 and 295 K.

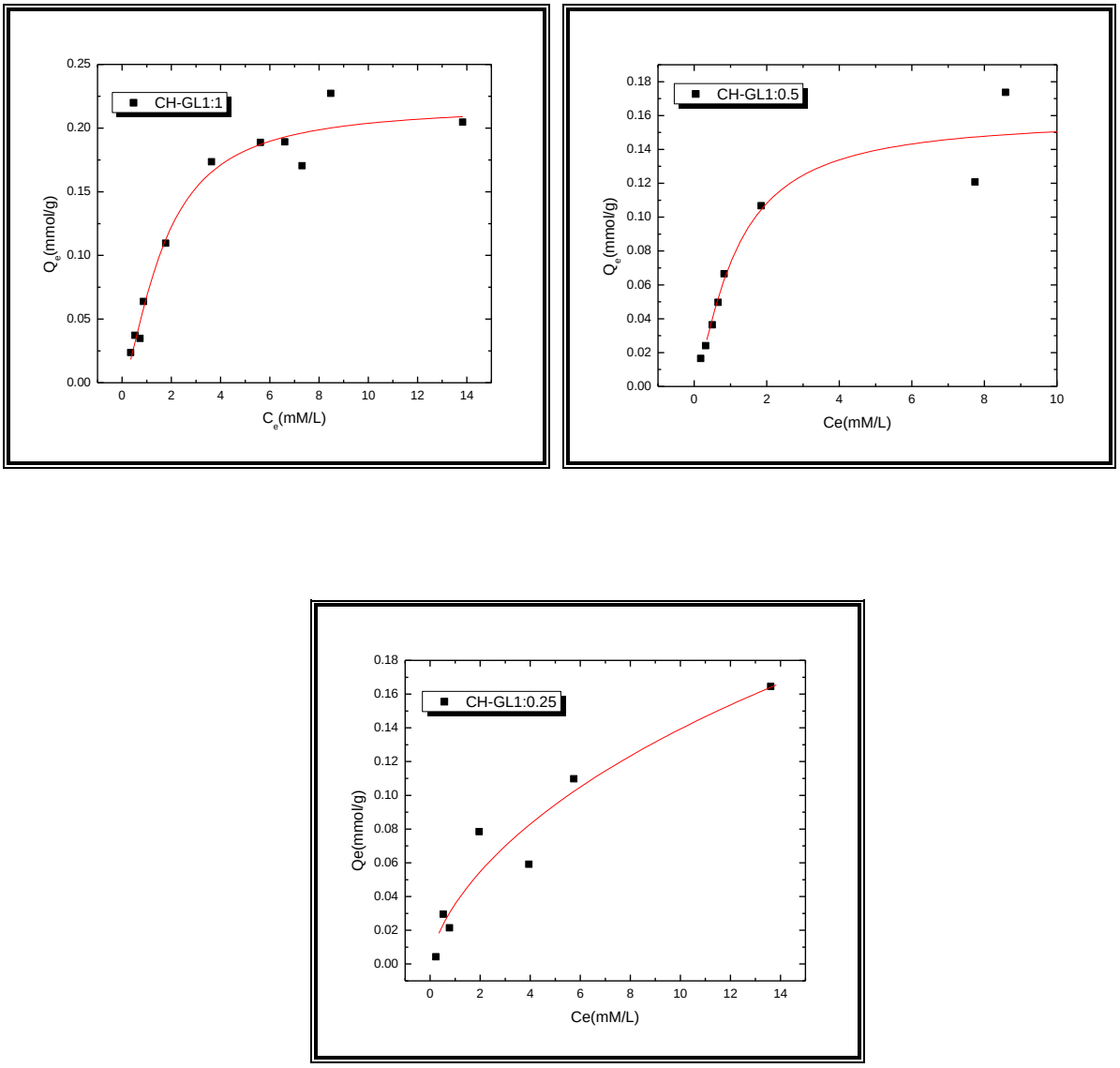

Figure 4.4: Sorption isotherms for PNP using CH-GL(~ 20 ±0.01mg) polymers at 8.5 pH and 295K in 10 mM potassium phosphate buffer (a) CH-GL1:1, (b) CH-GL1:0.5, and (c) CH-GL1:0.25. The solid lines represent the best-fit by the Sips model where the isotherm data is the same as shown in Figure 4.3. The error estimates associated with these best-fits are not shown here because of apparent scatter of the data.

Table 4.1: Sorption isotherm results of PNP with CH-GL copolymers (20.0±0.01 mg) at pH 8.5 (295 K) in 10 mM potassium phosphate. These parameters were calculated from Sips Isotherm Model (Data from Fig. 4.3).

Polymer	Q_m (mmol/g)	K_s (L/mmol)	R^2	n_s
CH-GL(1:1)	0.218	0.452	0.97	1.5
CH-GL(1:0.5)	0.159	0.854	0.93	1.3
CH-GL(1:0.25)	0.077	0.048	0.92	0.66
CH	N/D	N/D	N/D	N/D

*N/D: Not determined due to the limit concentration dependence of Q_e.

4.1.2 Adsorption of PNP at pH 5.0

In this study, greater adsorption capacities of PNP are noted with decreasing pH of the solution (Fig. 4.5). However, it was difficult to fit all isotherms with the Sips model (results are not shown here)**.** The change in sorption capacity with the change of pH of solution can be attributed to the surface charges of both PNP and chitosan. It is known that amino groups of chitosan are positively charged near its pK_a value and chitosan polymer shows an attraction for PNP. Thus, adsorptive uptake is greater at lower pH (5.0) values, as expected for surface with lower surface charge. Poon has also reported the high adsorption capacities (0.0095-0.066 mmol/g) at low pH rather than high pH and greater adsorption with increasing GL content for chitosan and its polymers cross-linked polymers [4, 162]. Ngah et al. also reported the removal of PNP with chitosan beads [59]. However opposite results were reported since increasing pH

values of the solution resulted in an increase in the adsorption of PNP [165]. At greater pH values, the deprotonation of amino groups of chitosan results in higher adsorption of PNP [165].

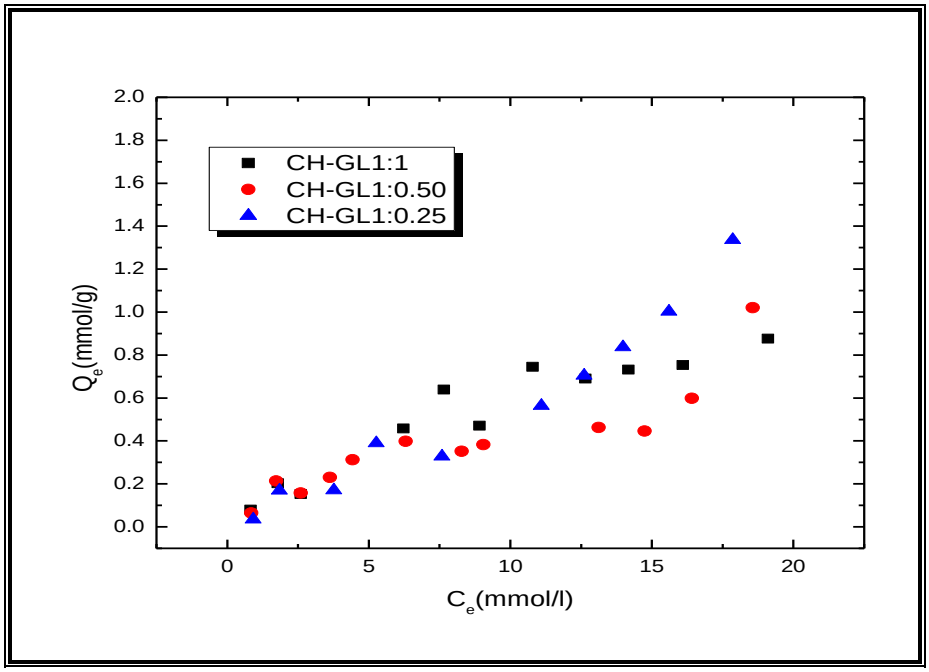

Figure 4.5: Sorption results of PNP using CH-GL polymers (CH-GL1:1, CH-GL1:0.50, CH-GL1:0.25, CH-GL1:6) at pH 5.0 and 295 K.

4.1.3 Adsorption of PNP at pH 8.5 (Bicarbonate Buffer)

Adsorption of PNP in bicarbonate was studied at pH 8.5. Sorption isotherm results show that the adsorption of PNP increased with bicarbonate buffer, as shown in Fig. 4.7. In a separate study [180], the sorption properties of similar sorbent materials with roxarsone were investigated by Poon et al. [180]. Roxarsone (ROX) is an organic arsenical a phenyl and arsenate functional groups (*cf.* Section 1.1.4.1). Roxarsone has three pK_a values (3.49, 5.74, 9.13) [54,56, 180, 181] and AsO_4^{-3} is one of the degradation by-products of ROX. The adsorption properties of ROX were investigated with chitosan-glutaraldehyde cross-linked polymers (CG) at various pH

conditions, since a comparative study using commercial granular activated carbon (GAC) and two phenolic dyes was also done as shown in Fig. 4.6 [180]. The effect of salt concentration, salt type, and various adsorbates was determined along with the effect of cross-linking density [180]. Single point sorption using 1 mM ROX was done at neutral and acidic conditions. Poon reported greater sorptive uptake occurs with CG polymers and relatively high uptake was obtained by GAC [180]. The results of that study support the effect of phosphate on adsorption of ROX with various adsorbent (CH, GAC, and CG) materials.

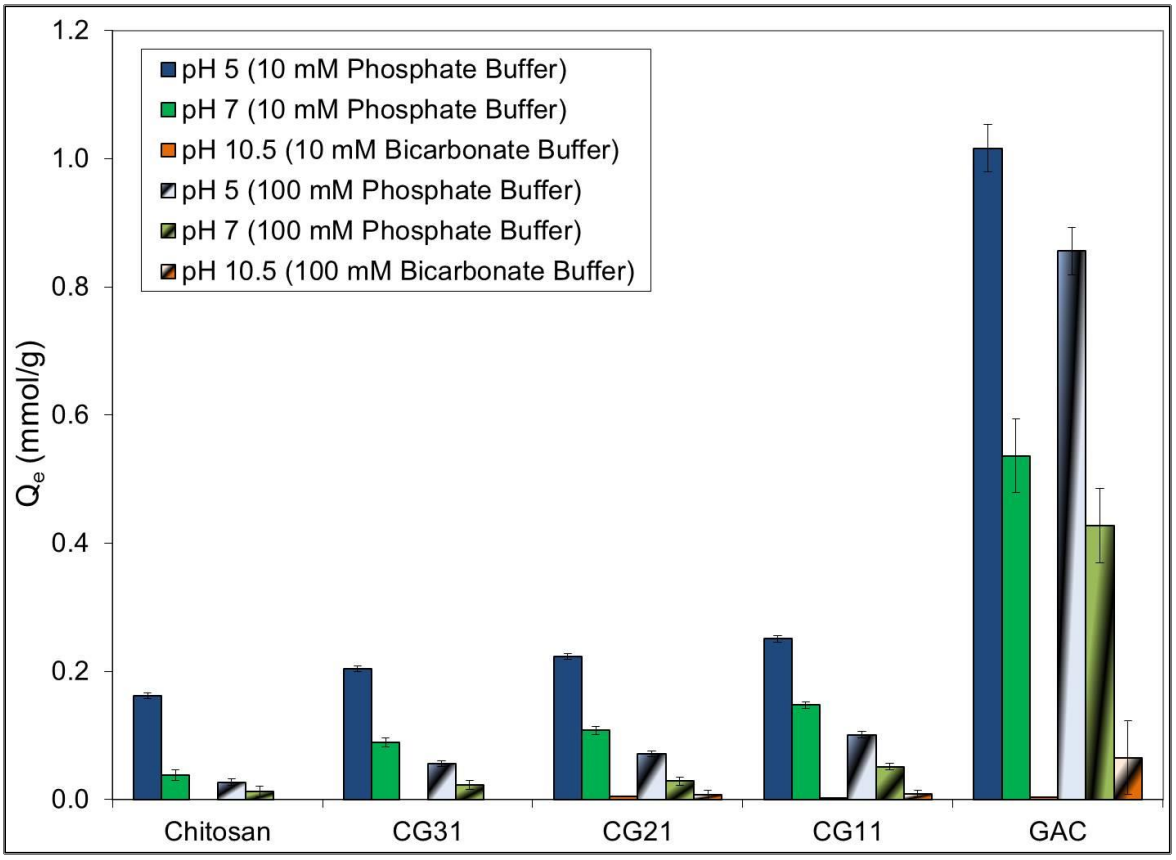

Figure 4.6: Single-point sorption of ROX at various pH and salt concentration for various sorbent systems [obtained from ref. 180].

It was inferred that ROX and phosphate compete for adsorption sites when the pH of the solution is acidic (pH < 5.0) and the phosphate concentration increases from 10 to 100 mM. A decrease in the adsorption of ROX adsorption was observed at high phosphate concentration (at 100 mM) and pH 7.0, as shown in Fig 4.6 [180]. Opposing effects were observed using bicarbonate buffer where sorption increased as the salt concentration increased from 10 mM to 100 mM at pH 10.5 (Fig. 4.6). The trend was attributed to "salting out" effects which occur when the precipitation of hydrophilic polymers occur due to an increased salt concentration [180].

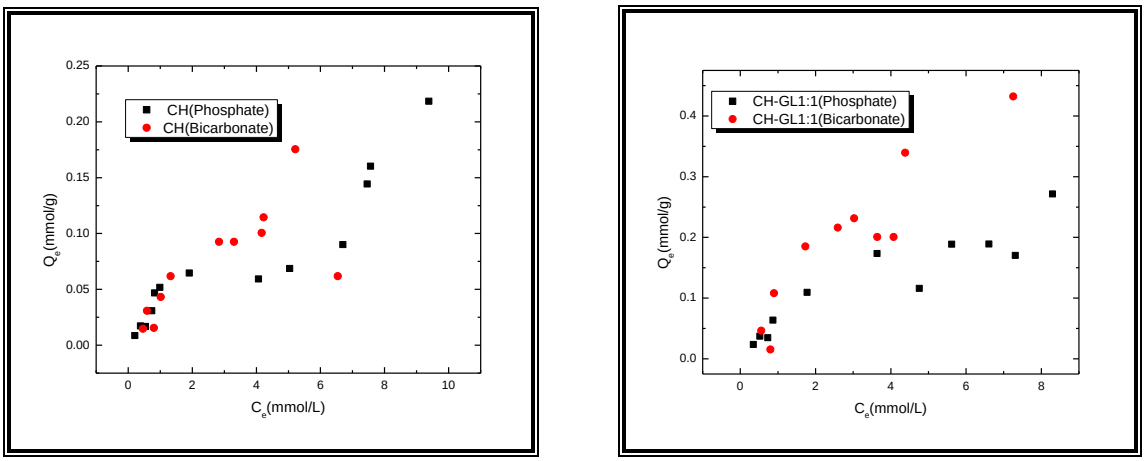

Figure 4.7: Sorption of PNP using CH-GL polymers at 8.5 pH and 295K in10 mM potassium phosphate buffer and bicarbonate buffer.

4.2 Arsenate Equilibrium Sorption Results

A fixed amount ~ 20.00 ± 0.01 mg of each polymer was mixed with 10 mL of adsorbate (arsenate oxoanion) in concentration range 0.1 to 200 ppm to obtain arsenate adsorption isotherms. After 24 h of equilibration at room temperature, each solution was filtered and the equilibrium concentration of arsenate was determined using ICP-OES. The sorption experiments

were studied without buffer and in 10 mM potassium phosphate at pH 5.0 and 8.5. The sorption isotherms were presented by plotting the levels of adsorbed arsenate (Q_e) vs the unbound equilibrium concentration (C_e), as shown in Fig. 4.8.

4.2.1 Adsorption of Arsenate in Un-buffered Solutions

The adsorption of arsenate anions by pristine chitosan is relatively low (ca. 0.41 mg/g), in agreement with the literature [180]. Therefore, the best fit results are not shown for chitosan with arsenate due to the low level of uptake. The low uptake for chitosan is related to the reduced accessibility of chitosan active sites (amino groups) while reduced stability of chitosan may also occur under acidic conditions [141]. It is also known that adsorption by unmodified chitosan depends on temperature and composition of the solution [141].

The surface charge of chitosan and its derivatives depends on the properties of surrounding solution such as pH. Chitosan and its cross-linked polymers (CH-GL) show variable surface charge with the protonation of the amino groups or deprotonation of hydroxyl groups under different pH conditions. These surface charges are electrostatic "sites" for adsorption of the adsorbate species (arsenate species or other anionic or neutral species present in the solution). Electrostatic interactions are often spontaneous processes and may occur via the adsorption of ion species on the surface of the chitosan [171]. Adsorption (chemisorption) may also involve irreversible binding as a result of covalent bonding [171]. Amino groups of chitosan show affinity toward positive cations under basic pH. Adsorption of anion species from the solution is favored when chitosan is protonated in the case of acidic conditions (pH ~5.0 < pK_a) or in a neutral protolytic form as seen in this thesis research.

The adsorption capacity (Q_m: mg/g) of chitosan copolymers for arsenate are listed in the following order: CH-GL1:1 > CH-GL1:0.50 > CH-GL1:0.25 > CH-GL1:6 for solution without

buffer as illustrated by Fig.4.8. The value of Q_m for each polymer is listed in descending order: CH-GL1:1(14.5), CH-GL1:0.50 (12.0), CH-GL1:0.25(10.3), CH-GL1:6(2.24).

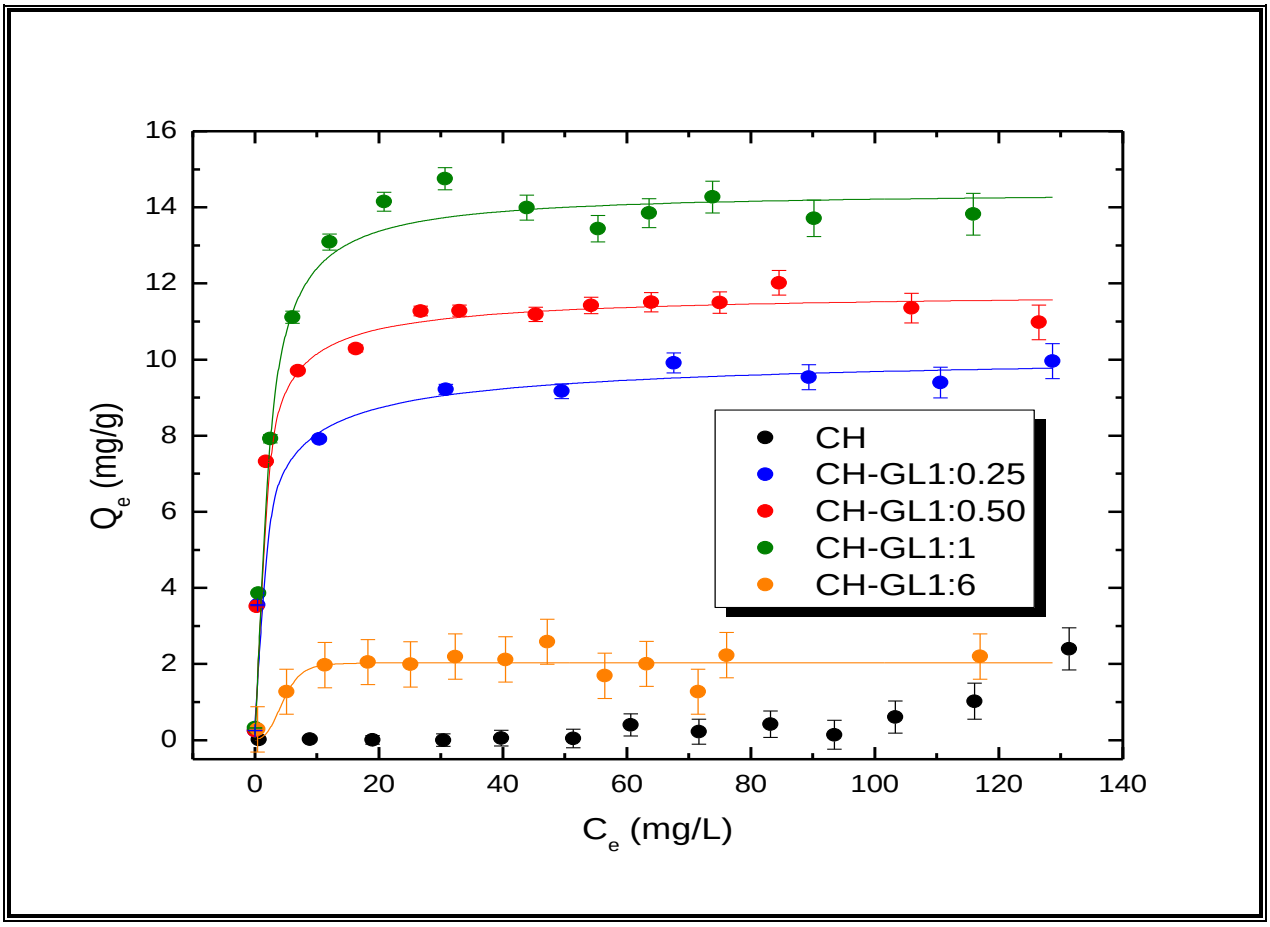

Figure 4.8: Adsorption isotherm data of arsenate anion sorption using CH-GL polymers (CH-GL1:1, CH-GL1:0.50, CH-GL1:0.25, CH-GL1:6) at 295 K in un-buffered solutions. The solid lines represent the best fit using the Sips isotherm model.

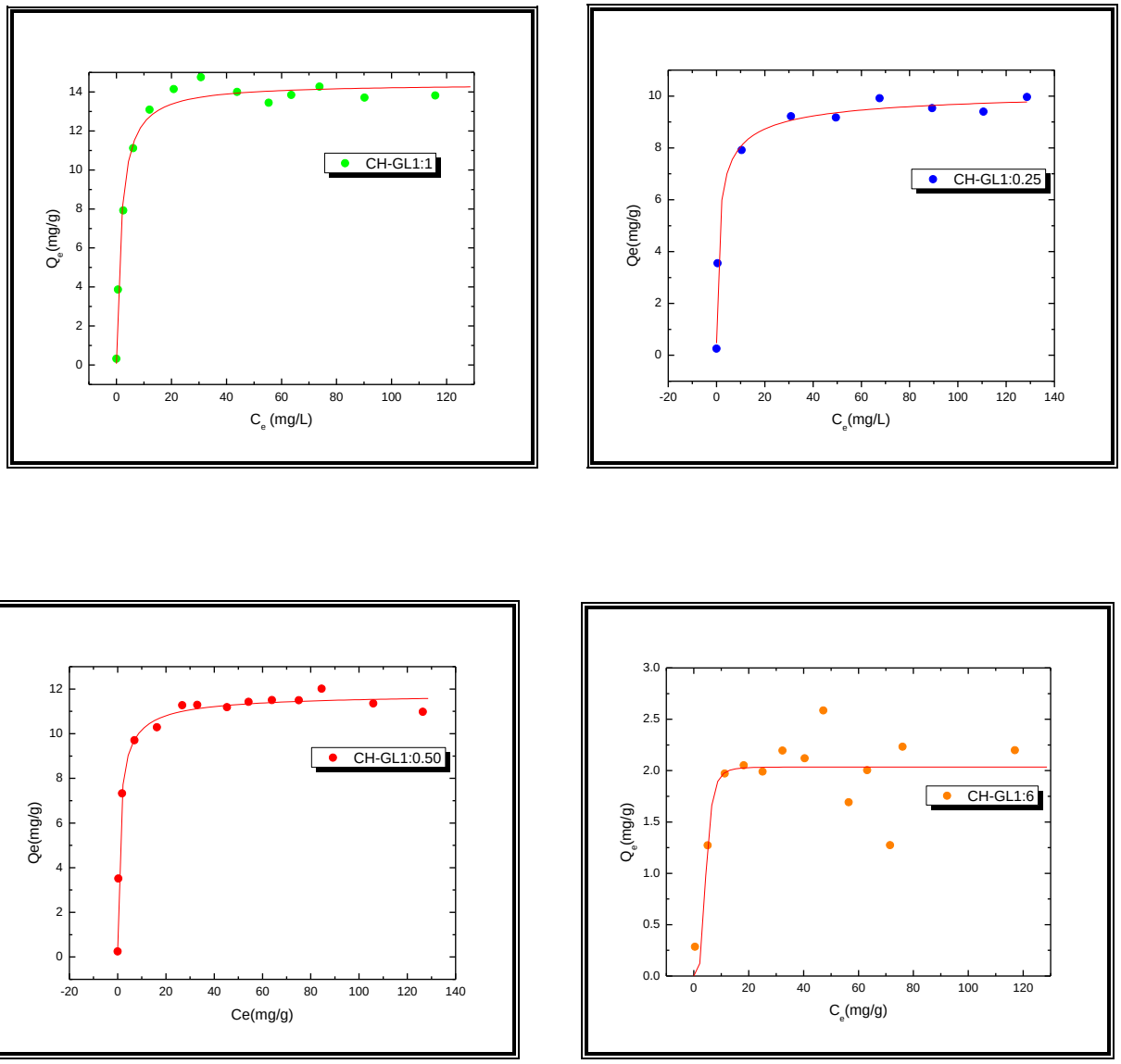

Figure 4.9: Sorption results of arsenate anions using CH-GL polymers (CH-GL1:1, CH-GL1:0.50, CH-GL1:0.25, CH-GL1:6) at 295 K in un-buffered solutions.

The increase in the adsorption capacity addresses the hypothesis related to the effect of glutaraldehyde content on the cross-linking ratios during synthesis. By contrast, Pratt et al. reported that the adsorption capacities were "inversely related to the contents of glutaraldehyde" at pH 8.5 in 10 mM potassium phosphate buffer [4,156]. Pratt reported the adsorption capacities as: 228mg/g for copolymers (CPL-1) with the lowest cross-linking; whereas, a lower value

(39.9mg/g) was obtained for a highly cross-linked polymer(CPL-3). Greater arsenate adsorption capacity (*ca.* 96.4 mg/g) was reported by Boddu et al. [182].

Table 4.2: Sips isotherm sorption parameters for arsenate (10 mL of adsorbate) with CH-GL copolymers (20.0±0.01mg) at 295 K in aqueous solution without buffer solution.

Polymer	Q_m (mg/g)	n_s	K_s (L/mol)
CH-GL(1:6)	2.24	1.23	$3.16x10^4$
CH-GL(1:1)	14.4	1.04	$7.70x10^4$
CH-GL(1:0.50)	12.0	0.743	$1.35x10^5$
CH-GL(1:0.25)	10.3	0.619	$1.17x10^5$
CH	N/D	N/D	N/D

N/D: Not determined due to low concentration dependence of Q_e.

A comparison of the sorption capacity and best fit parameters for the polymers is shown in Table 4.2. Likewise, a comparison of adsorption capacities according to the Langmuir and Sips models is shown in Table 4.3. According to the Langmuir model, a better fitting is observed with increasing GL content. There is a decrease in the values of the equilibrium constant K_L (L/mol) which relates to the strength of the sorptive interaction between the adsorbate and the surface of the adsorbent. The decreased value of K_L for CH-GL (1:1) indicates that weak adsorption occurs for this polymer, while stronger adsorption occurs for CH-GL (1:0.25) [183]. The removal efficiency (Fig. 4.10) of the CH-GL copolymers (CH-GL1:1 > CH-GL1:0.50 > CH-GL1:0.25) in un-buffered solutions was in the range of 10-98%.

Table 4.3: Comparison of the best fits parameters of Sips and Langmuir Models for the adsorption of arsenate oxoanions with CH-GL (20.0±0.01 mg, 10 mL of adsorbate, and ambient temperature 295 K) in aqueous solution without buffer.

Langmuir parameters					**Sips parameters**			
Polymer	**Q_m (mg/g)**	**K_L (L/mg)**	**K_s (L/mol)**	**R^2**	**Q_m(mg/g)**	**K_s (L/mol)**	**n**	**R^2**
CH-GL(1:6)	2.04	0.00309	430	0.866	2.24	$3.16x10^4$	1.23	0.866
CH-GL(1:1)	14.5	0.576	$8.00x10^4$	0.987	14.4	$7.70x10^4$	1.04	0.997
CH-GL(1:0.50)	11.5	1.07	$1.49x10^5$	0.987	12.0	$1.35x10^5$	0.743	0.994
CH-GL(1:0.25)	10.2	1.25	$1.75x10^5$	0.995	10.3	$1.17x10^5$	0.619	0.984
CH	N/D	N/D	N/D	N/D	N/D	N/D	N/D	N/D

*N/D: Not determined due to the low concentration dependence of Q_e.

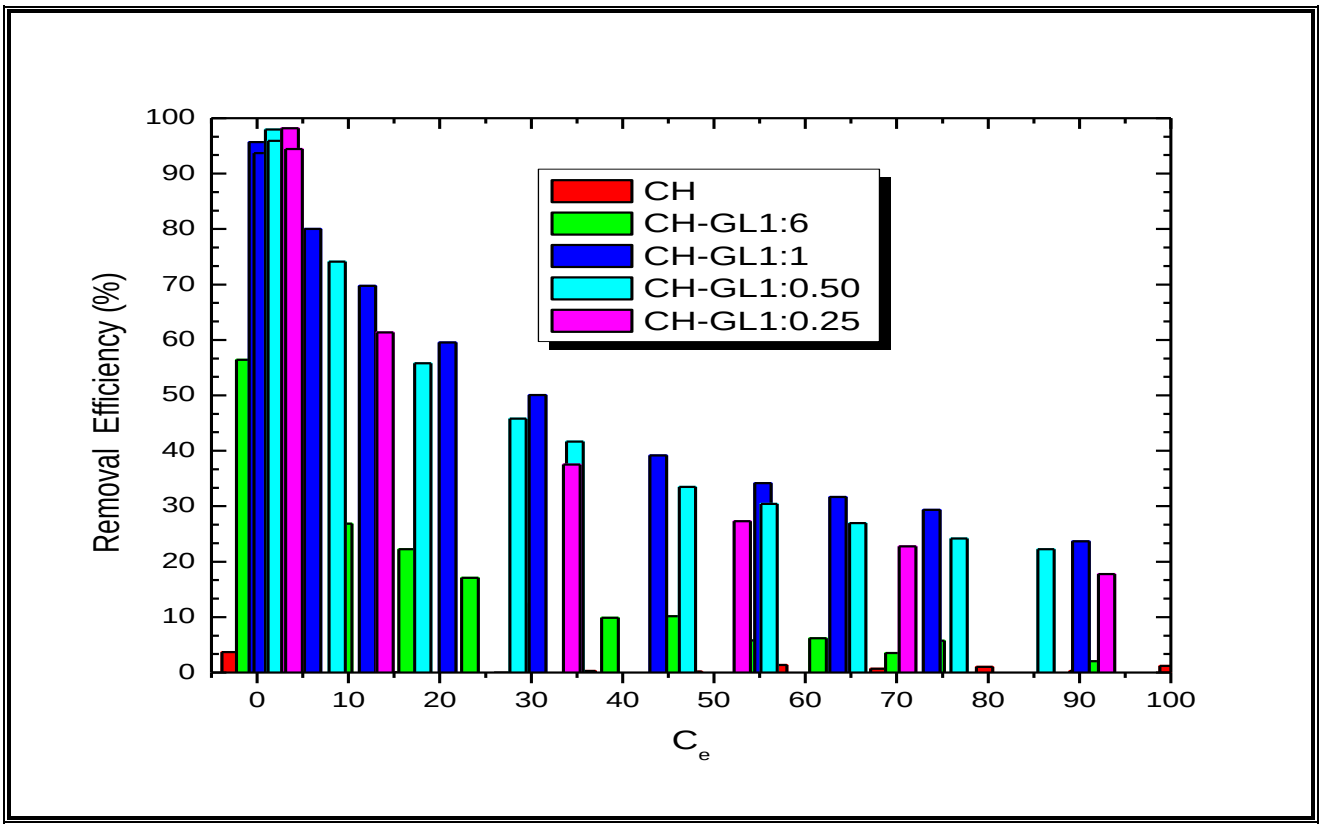

Figure 4.10: Removal Efficiencies (%) for a fixed mass of (~20 mg) of the CH-GL copolymers (CH, CH-GL1:1, CH-GL1:0.50, CH-GL1:0.25 and CH-GL1:6) for arsenate in un-buffered solution at 295K.

4.2.2 Adsorption of Arsenate in Potassium Phosphate Buffer

4.2.2.1 Adsorption of Arsenate at 8.5 pH (Potassium Phosphate Buffer)

Figure 4.11 illustrates the adsorption isotherms of arsenate in 10 mM potassium phosphate buffer at pH 8.5. By comparison, the removal efficiency of pristine chitosan was in the range 0.007-3.0 % and CH-GL1:6 had a 2-57% removal efficiency as shown in Table 4.4.There is clear evidence that removal efficiency is a function of equilibrium concentration (C_e) which decrease for each polymer at higher values of C_e.

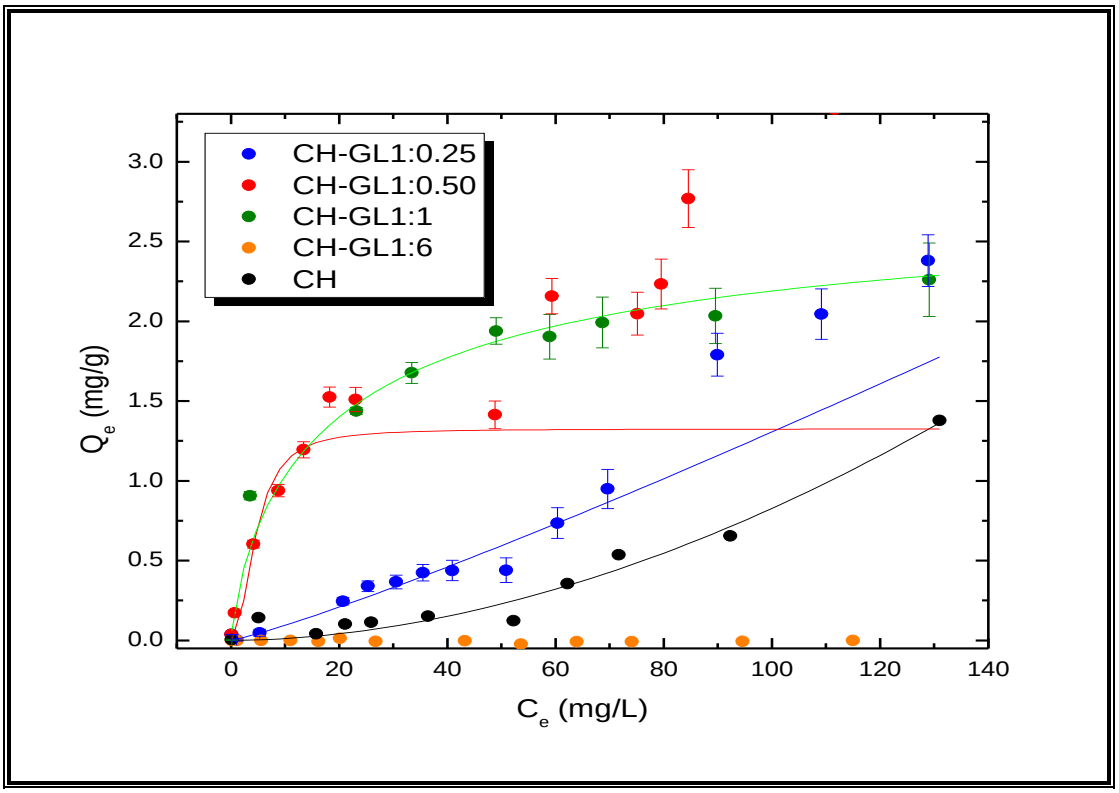

Figure 4.11: Sorption results of arsenate oxoanion using CH-GL polymers (CH-GL1:1, CH-GL1:0.50, CH-GL1:0.25, and CH-GL1:6) at 295K in 10 mM potassium phosphate buffer at pH 8.5.

4.2.2.2 Adsorption of Arsenate at 5.0 pH (Potassium Phosphate Buffer)

Adsorption of arsenate was increased with decreasing pH of the solution (Fig. 4.12). This pronounced increase in the adsorption capacity is related to the nature of arsenate species in the solution. As indicated in Chapter 1, arsenic species have pH dependent speciation in aqueous solution. Figure 1.1 indicates that arsenate species are present in the form of $H_2AsO_4^-$ and $H_2AsO_4^{-2}$ at different pH conditions [119].

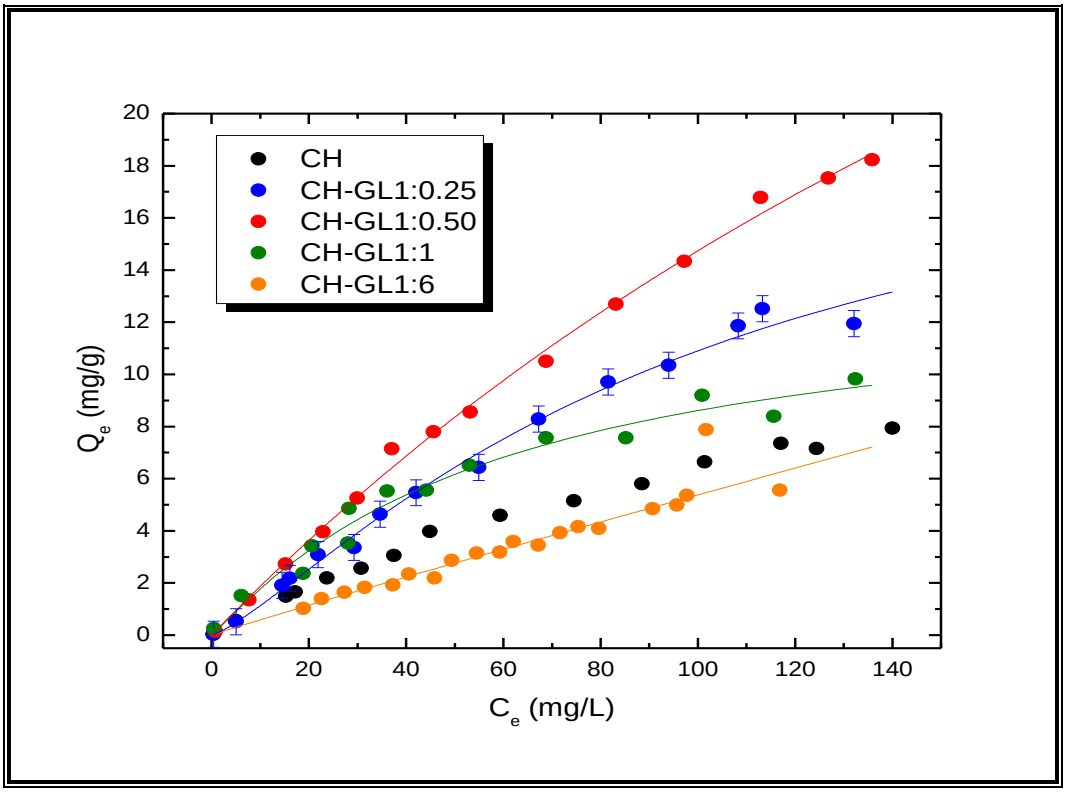

Figure 4.12: Isotherm adsorption data of arsenate oxoanion using CH-GL polymers (CH-GL1:1, CH-GL1:0.50, CH-GL1:0.25, and CH-GL1:6) at 295 K in 10 mM potassium phosphate buffer at pH 5.0.

The CH-GL polymers show relatively higher value of ε_R% in un-buffered solution, as compared to phosphate buffer at higher concentration. Overall, the removal efficiencies for the polymers (Table 4.4.) are listed in the following order: un-buffered > buffered (pH. 5.0) > buffered (pH. 8.5). The overall uptake of arsenate (14-8 mg/g) in un-buffered aqueous solution exceeds buffered solution, where phosphate ions are present as the buffer media. There is a significant decrease in the values of Q_m by a factor of 20% for aqueous solutions containing potassium phosphate buffer compared to the un-buffered solutions. An increased adsorption capacity for arsenate (V) was reported for acid-washed crab shells by Niu et al. [184]. Niu reported an increase in the arsenate uptake with a decreased solution pH where arsenate uptake at

pH 2.51±0.02 was 1.5-7 As/g absorbent because of arsenate adsorbed by amide groups of acid-washed crab shells.

Tofan-Lazar et al. studied the effect of arsenate on phosphate adsorption on surface of Fe (oxyhydr) oxide film in presence of arsenate and dimethylarsenic acid (DMA). However, the rapid kinetics study was done under neutral pH conditions [185]. Similarly, a significant decrease (ca. 90 %) in As (V) uptake was reported [186].

Table4.4: Removal Efficiencies (ε_R %) at variable pH for a fixed mass (20±0.01 mg) of the CH-GL copolymers in aqueous solution without buffer over a concentration range of 0.1-200 ppm.

pH condition / Polymer	**Un-buffered**	**8.5**	**5.0**
CH-GL(1:6)	2.0-56%	N/D	8-13%
CH-GL(1:1)	20-95%	3-35%	17-53%
CH-GL(1:0.50)	14-97%	5-50%	21-23%
CH-GL(1:0.25)	10-98%	0.4-5.8%	15-22%
CH	0.007-3.9%	0.4-2.0%	10-18%

N/D: Not determined

4.2.3 Adsorption of Arsenate at 8.5 pH (Bicarbonate Buffer)

It has been concluded so far (based on the adsorption experiments) that phosphate ion has significant effect on adsorption of arsenate by CH-GL polymers. Similarly effect of phosphate anion on the adsorption of arsenate was determined by So et al. [187]. The adsorption properties of phosphate and arsenate on calcite were evaluated [187]. A competitive adsorption study

revealed that arsenate adsorption on calcite was reduced due to the presence of phosphate anions in the solution [187]. Both arsenate and phosphate compete for binding sites because of their comparable tetrahedral structure and physicochemical properties such as pK_a values (7.0 for arsenate and 7.2 for phosphate). Based on the above details, it was concluded that phosphate ions are competing with the arsenate anions for adsorption. To demonstrate this effect, the adsorption properties of CH and CH-GL (1:1) were determined in bicarbonate buffer system where it was observed that the adsorption capacities increased in bicarbonate buffer (Fig.4.13). However, the increase was modest and the results were in agreement with an independent study [187]. Competitive adsorption occurs between phosphate and arsenate with goethite under pH [188]. Carabante et al. reported the reduction in adsorption capacities of arsenate on synthetic ferrihydrite in presence of phosphate [189]. This study was done at various phosphate and arsenate concentration levels where D_2O was used as the solvent to evaluate ATR-FTIR spectra on iron oxide surfaces [189]. Tofan-Lazar et al. reported kinetics of adsorption of phosphate on iron (oxyhydr) oxides [185] and the effect of various arsenic species (inorganic and organic) on the adsorption of phosphate. It was concluded that the rate of phosphate adsorption was a dependent on the arsenate coverage of the iron oxide surface [185].

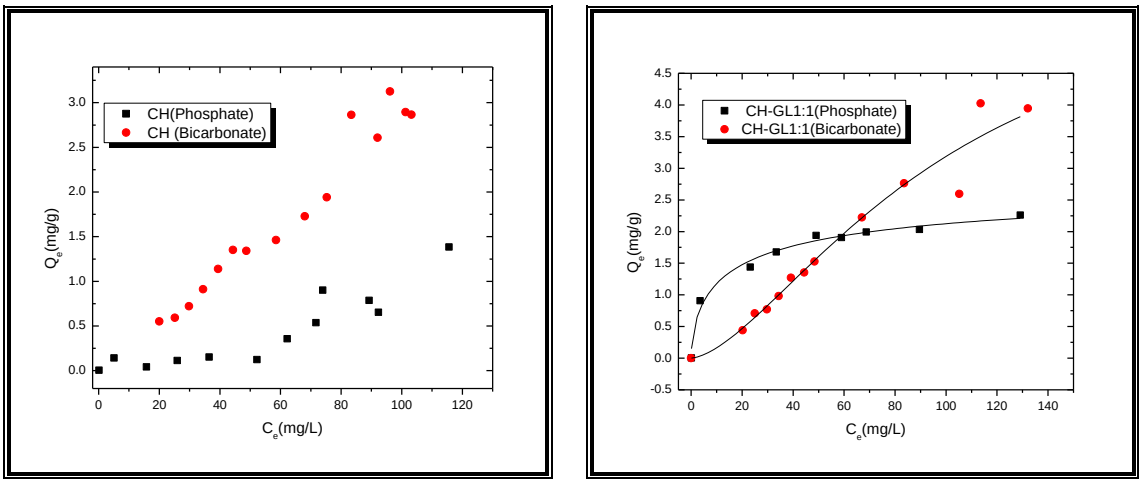

Figure 4.13: Isotherm adsorption data of arsenate oxoanion using CH-GL polymers (CH, CH-GL1:1) in 10 mM potassium phosphate buffer and bicarbonate buffer at pH 8.5.

Chapter 5 RESULTS AND DISCUSSION: SYNCHROTRON STUDIES

5.1 Synchrotron XAS Results

In the past, after identification of arsenic as a toxic element, total arsenic levels were determined using various traditional spectroscopic methods. With the passage of time, it was revealed that actual toxicity levels of arsenic is a function of its chemical speciation in water under various pH conditions and it was also identified that inorganic form of arsenic is more toxic than organic form; although it is also well known that arsenite As(III) is more toxic than arsenate As (V).

Various methods were developed by other researchers to measured specific level of arsenic species in given water sample or other compounds. However these were time consuming or indirect methods and required some pre-treatment of samples (solvent extraction or acid digestion), and also there were possibilities for the change in chemical form or features of arsenic originally present in the sample. Elemental speciation of arsenic has been done using various analytical techniques such as electrochemical, atomic absorption spectroscopy [190], graphite furnace atomic absorption spectroscopy [24], atomic emission spectroscopy, and inductively coupled plasma spectroscopy. ICP-AES, and ICP-MS coupled with HPLC [191] were used to determine and characterize various forms of arsenic [24, 190-194-196].

X-ray absorption spectroscopy (XAS) provides very feasible experimental conditions for analysis of any biological sample. One of major advantage is to use sample in any form: liquid, solid, frozen liquids, dry powder or a slurry[197]. Recently XAS was used for detection and characterization of arsenic species in various environmental samples [198-200] such as plant sap [201] or plant [94] roots and minerals [95]. XAS, in this project was used to examine the arsenic speciation and its coordination environment in liquid samples and sorbed samples.

5.1.1 Near-edge Spectra of Arsenic Species in Various Samples

X-ray absorption spectroscopy at the arsenic K-edge was used for the liquid and solid phase speciation of arsenic. The solid sorbed residue (after adsorption) was collected after gravity filtration of adsorption solution at variable pH; 5.0 and 8.5 in two buffer systems.

5.1.1.1 Adsorption of Arsenate in Potassium Phosphate Buffer

Generally, a typical XAS scan of arsenate solid residue (CH-GL1:1) as shown in Fig. 5.1, shows three main regions; pre-edge region indicates insufficient X-ray energy to eject 1s core-electrons, whereas, near-edge indicates the K edge absorption for arsenic that involves ejection of core-electron. Extended X-ray absorption fine structure is extended XAS region where oscillation in signal occurs because of backscattered photoelectrons of neighboring atoms.

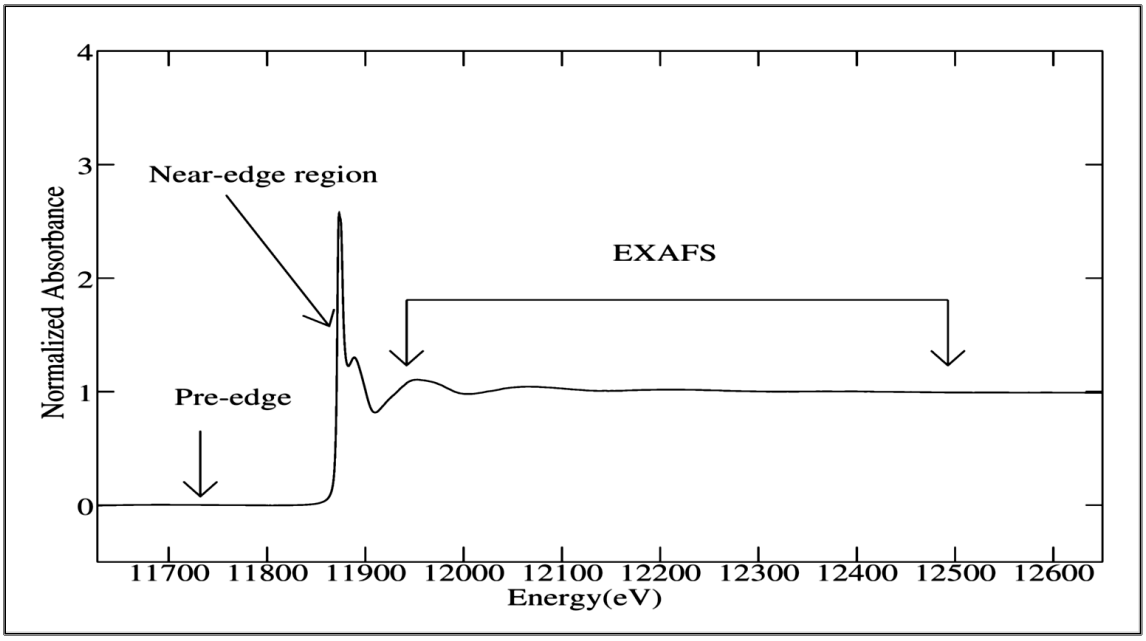

Figure 5.1: Typical background-subtracted and normalized X-ray absorption Arsenic K edge spectra showing various spectral regions. CH-GL sample was analyzed as a solid residue obtained from a solution at pH 5.0.

Arsenic K near-edge spectrum of arsenate shows one major peak at around 11876.3 eV, which is characteristic of a dipole-allowed transition from 1s to 4p of core electron and indicate the four coordinate arsenate was reported previously [94, 95, 191-198, 201]. Fig. 5.2 illustrates the edge spectra of liquid samples before and after filtration of 115 ppm arsenate solution in 10 mM potassium phosphate buffer in comparison with the arsenate and arsenite standards at pH 8.0 (all arsenate and arsenite standards were taken from a previous study by Andrahennadi et al.) [199,200].

As observed in Fig. 5.2 that arsenate peaks for the sample have been split and this splitting is consistent in both liquid and solid samples before and after adsorption in Fig. 5.3. However, the edge scans are more similar to the arsenate standard than arsenite which further supports that no change in oxidation state occurred during the adsorption process.

All arsenic K near-edge spectra in phosphate buffer (10 mM) show a splitting of the major peak, which is not characteristic of the arsenate near-edge spectra measured previously [94, 199,200]. Arsenate has a single characteristic peak in the near-edge spectrum (as mentioned before). The possibility that phosphate anions form a complex with arsenate species in the solution (actual mechanism and reason in unknown) was hypothesized. In a previous study, synchrotron radiation X-ray absorption spectroscopy was used to determine the speciation of sulfur in situ. Figure 1 (ref. 202) illustrates that the splitting of the sulfate ester peak where oxygen is bridging to another atom (i.e carbon, in case of ester) while sulfate shows a single peak. As sulfate is the tetrahedral analogue to arsenate or AsO_4^{-3}, it can be inferred that splitting of the arsenate peak may occur because the oxygen single bridge analogue to sulfate ester coordination.

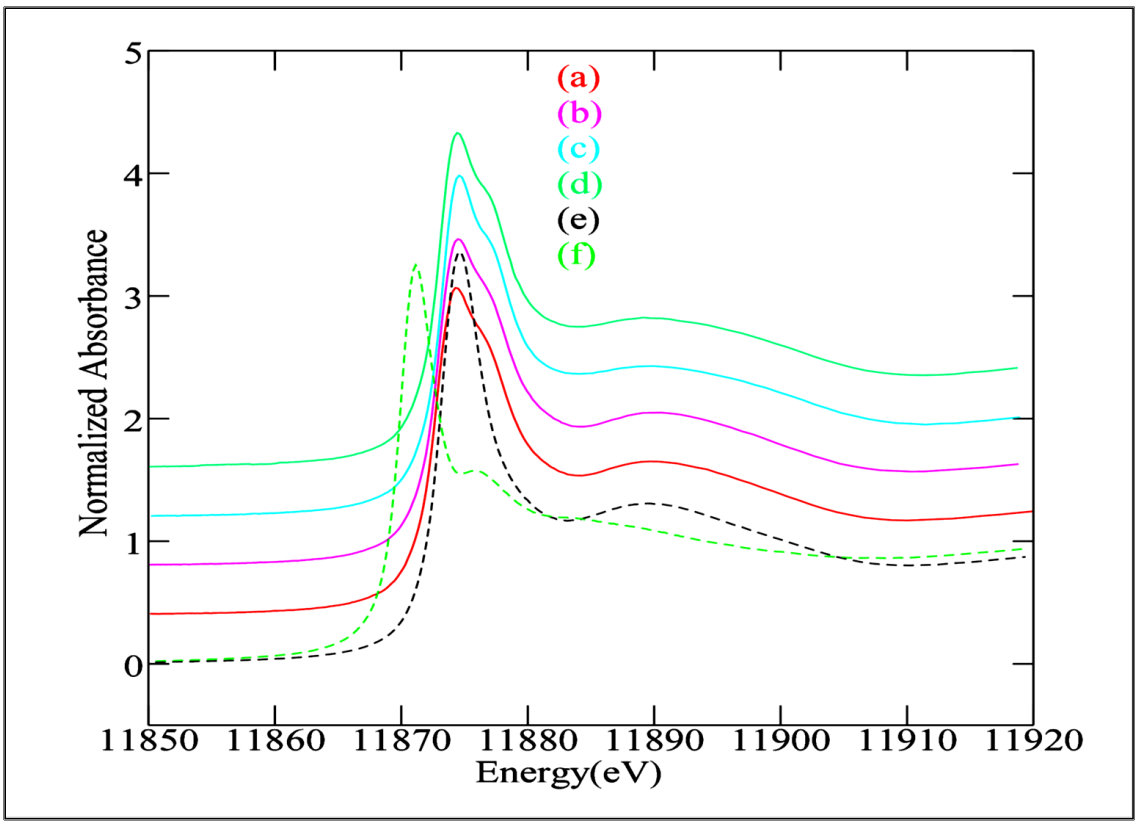

Figure 5.2: Arsenic K-edge spectra of liquid samples in 10 mM phosphate buffer at pH 8.5 and 5.0. [(a) CH, 115 ppm arsenate solution before adsorption at pH 8.5 (b) CH, 115 ppm arsenate adsorption filtrate solution at pH 8.5 (c) CH, 115 ppm arsenate solution before adsorption at pH 5.0 (d) CH, 115 ppm arsenate adsorption filtrate solution at pH 5.0, (e) Arsenate standard at pH 8.0 (f) Arsenite standards at 8.0 pH]. All spectra were normalized to get an edge jump of unity.

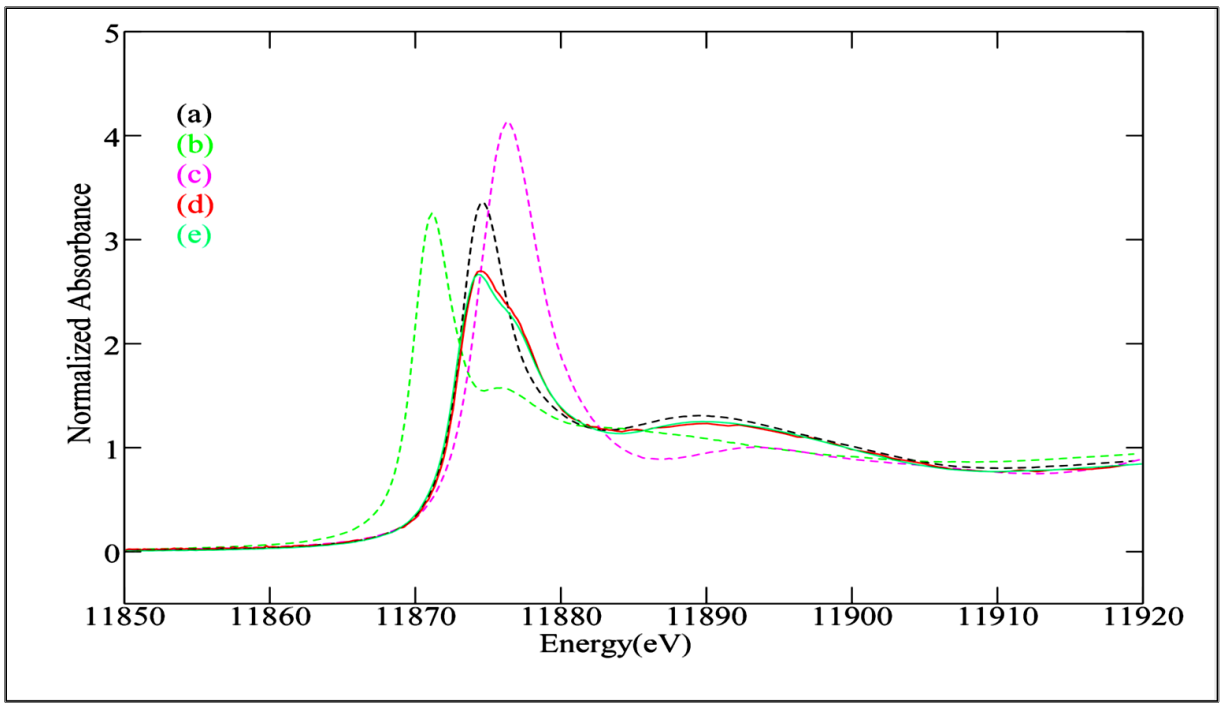

Figure 5.3: Arsenic K-edge spectra of three standards, one solid, and one liquid samples in 10 mM phosphate buffer at pH 8.5. [(a) Arsenate standard at pH 8.0 (b) Arsenite standard at 8.0 pH (c) Arsenate-glycerol complex solution at pH 0, (d) CH, solid residue after adsorption at 8.5 pH, and (e) CH, liquid sample before adsorption.]

In Fig.5.3, sample (c) is an arsenate-glycerol complex in solution where the data was taken from a previously reported study [198]. The peak at 11876.3 eV corresponds to arsenate equilibrated with glycerol at pH ~0, indicating that the "aliphatic" dihydroxyl groups reside on the "vicinal hydrocarbon" [198]. It was recently reported that arsenic was coordinated in an octahedral (6-coordinate) environment with oxygen instead of the 4-coordinated environment expected for arsenate. Arsenic K-edge spectra of samples in phosphate buffer show similar spectra as compared to arsenate standard samples at pH 9.0. The results indicate that arsenate is coordinated with 4 oxygen atoms.

5.1.1.2 Adsorption of Arsenate in Bicarbonate Buffer

In a separate experiment bicarbonate buffer was used at pH 8.5. The solid residue was collected from filter paper after adsorption (refer to Chapter 2, section 2.7.1.2). The As near-edge spectra in bicarbonate buffer show a single peak in Fig. 5.4 and 5.5. Fig. 5.4 shows the As K edge spectra of CH-GL polymers in bicarbonate buffer solution. This comparison of spectra indicates that arsenate solution in bicarbonate buffer is not forming any complex. The absorbance is similar to an arsenate standard at pH 8.0, shown in Fig. 5.4(a) and is different from an arsenite standard at pH 8.0 and an arsenate glycerol mixture at pH ~0. Fig. 5.5 illustrates the K edge spectra of arsenate in phosphate and bicarbonate buffer systems along with a comparison with three standards samples.

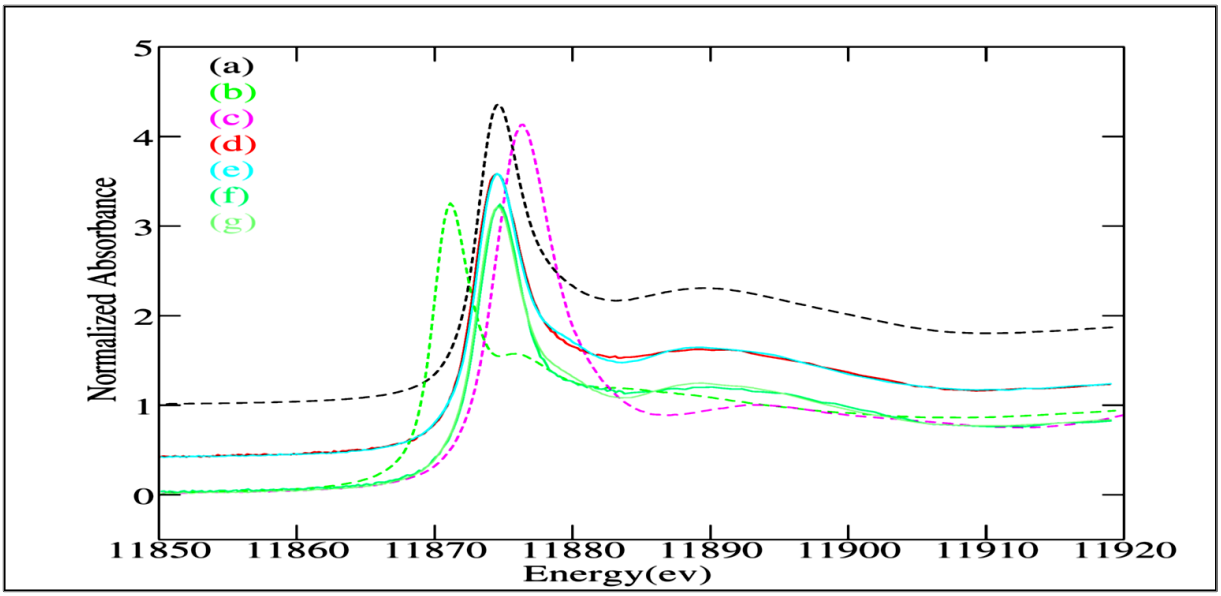

Figure 5.4: Arsenic K-edge spectra of three standards (dashed lines), two solid, and two liquid samples in bicarbonate buffer at pH 8.5. All spectra were also normalized to get an edge jump of unity. [(a) Arsenate standard at pH 8.0 (b) Arsenite standard at pH 8.0 (c) Arsenate-glycerol complex solution at pH 0 (d) CH, liquid sample after adsorption at pH 8.5. (e) CH-GL1:1 liquid sample after adsorption (f) CH, solid residue after adsorption at pH 8.5. (g) CH-GL1:1 solid residue after adsorption.]

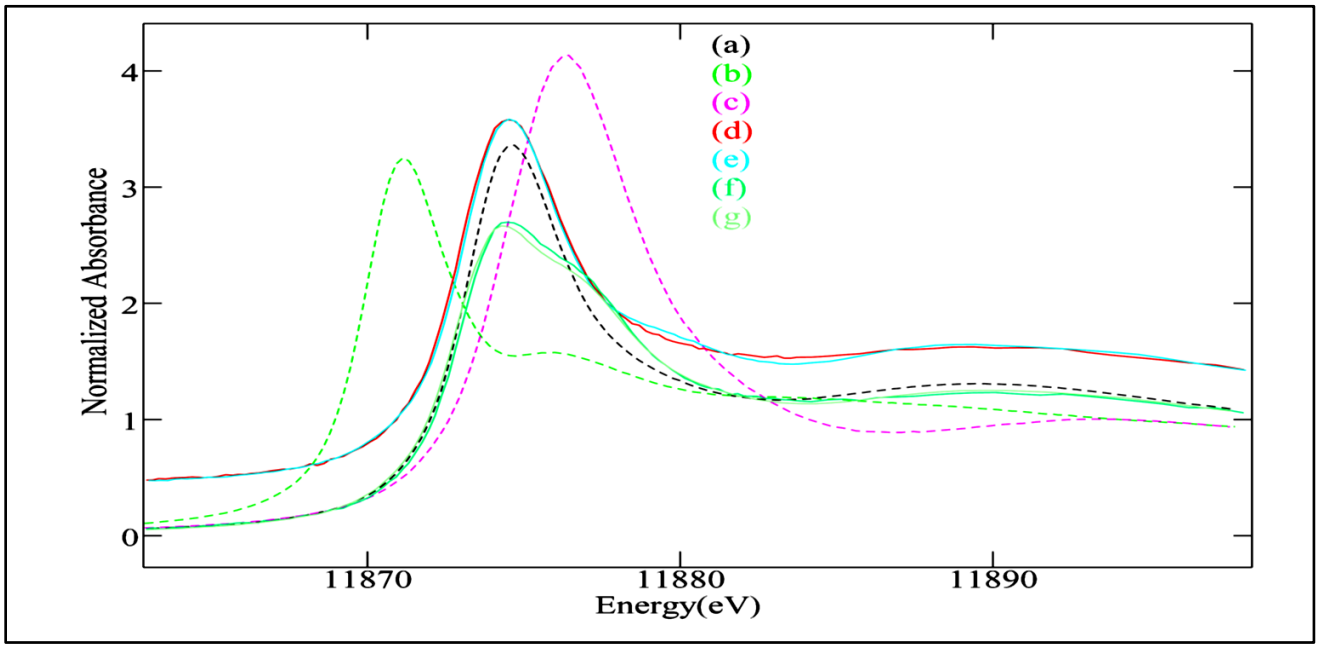

Figure 5.5: Arsenic K-edge X-ray absorption spectra of three standards (dashed lines), one adsorbed solid, and one liquid sample in 10 mM phosphate buffer and bicarbonate buffer at pH 8.5. (a) Arsenate standard at pH 8.0, (b) Arsenite standard at pH 8.0, (c) Arsenate-glycerol complex solution at pH 0. **Bicarbonate buffer:** (d) CH-GL1:1 liquid sample after adsorption, (e) CH-GL1:1 solid sample after adsorption. **Phosphate buffer:** (f) CHGL1:1 liquid sample after adsorption in phosphate buffer, and (g) CH-GL1:1 solid residue after adsorption in phosphate buffer. All spectra were also normalized to get an edge jump of unity.

5.1.2 Extended X-ray Absorption Fine Structure (EXAFS)

The EXAFS provide detailed structural information about electronic environment of a compound. Herein, the aim was to explore the chemical environment of the arsenate species before and after adsorption on the CH-GL polymers. Fig. 5.6 shows the EXAFS of CH-GL1:1 exposed to arsenate in phosphate buffer and bicarbonate buffer in comparison with the arsenate solution and arsenate-glycerol complex standard.

The best fits of the EXAFS spectra in each case are shown as dashed lines. In Fig.5.7, the EXAFS Fourier transform spectra of the CH-GL1:1 in phosphate buffer and bicarbonate buffer are compared against an arsenate-glycerol solution at pH 0 and 9. The numerical results are shown in Table 5.1. In Fig. 5.7, all Fourier Transform spectra have a single peak which indicates the nature of the first coordination shell.

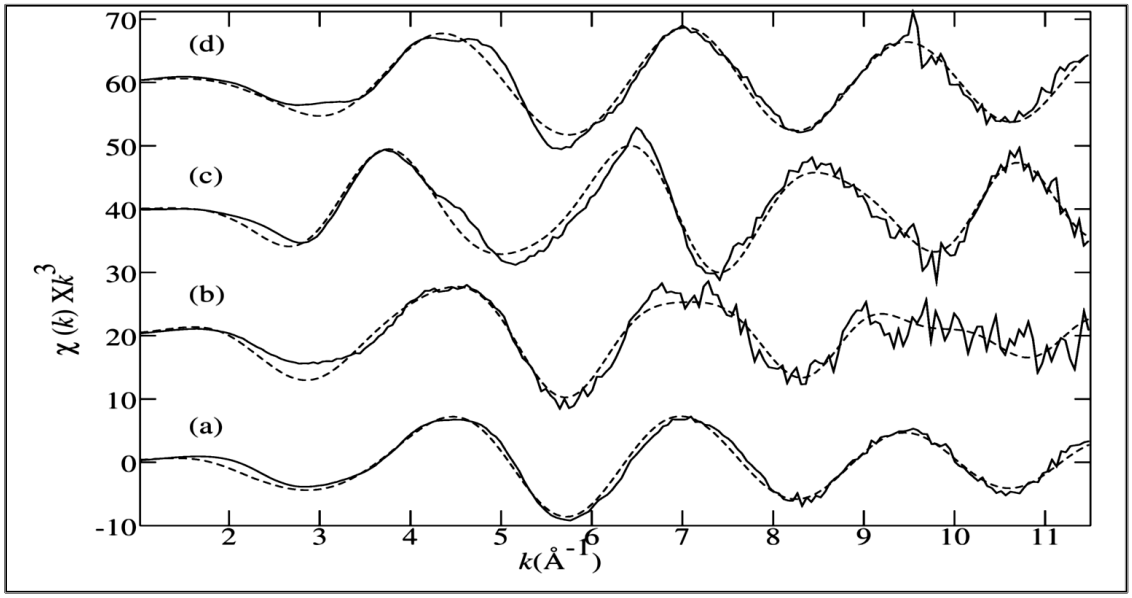

Figure 5.6: k^3-Weighted EXAFS of arsenic sorbed on the CH-GL polymers in phosphate buffer and bicarbonate buffer solution. Solid lines represent the data while the best fits are shown with dash lines. $\chi(k)$is the magnitude of the Fourier transform signal as a function of *R*. (a) CH-GL1:1, phosphate buffer, (b) CH-GL1:1 bicarbonate buffer, (c) arsenate-glycerol at pH 0, and (d) arsenate at pH 9. The quality of data presented herein was not optimal because liquid samples had very low arsenic concentration and a very small volume was used for sample preparation. For bicarbonate buffer the lower signal to noise ratio was because of the lower concentration of the arsenic after adsorption [199,200].

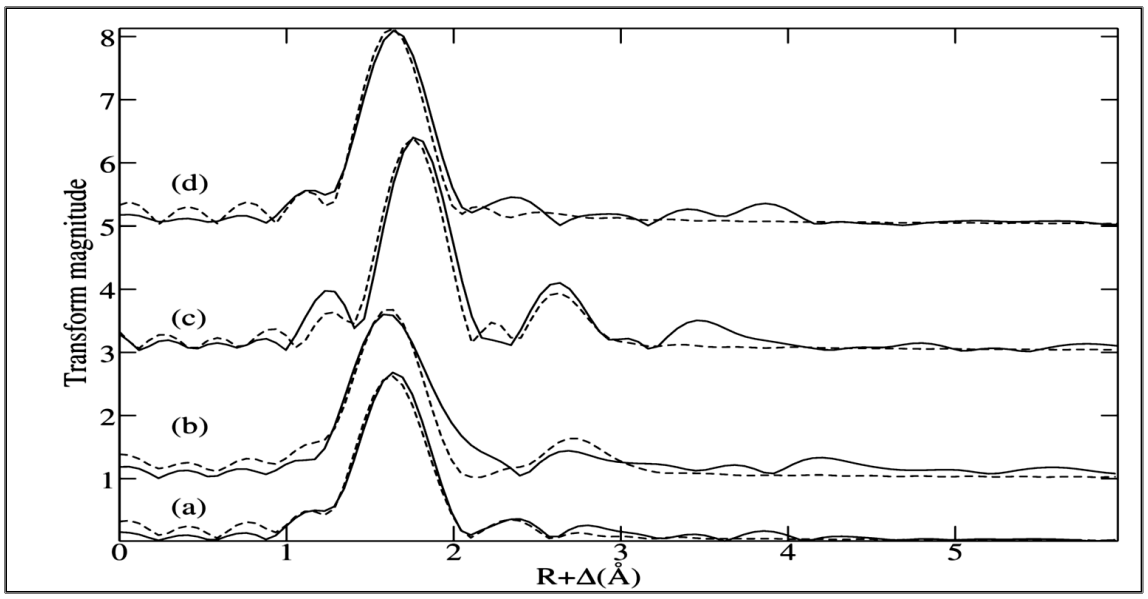

Figure 5.7: Fourier transforms, phase corrected for the first shell As-backscatterer pair. Solid lines represent the data while best fits are with dash lines: (a) CH-GL1:1, phosphate buffer, (b) CH-GL1:1, bicarbonate buffer, (c) arsenate-glycerol at pH 0, (d) arsenate at pH 9. (Data for c and d was taken from ref.203-204).

According to numerical results shown in Table 5.1 that arsenate in phosphate buffer has approximately ~4 oxygen atoms at a distance of 1.68 Å. The first shell of arsenic in bicarbonate buffer shows ~4 As-O at a distance of 1.68 Å. However, in a previous study, it was determined that arsenate-glycerol has six As-O at a mean distance of 1.833 Å [198].

Table5.1: EXAFS curve-fitting results for As in phosphate buffer and bicarbonate buffer. Where X, means type of bonded atom. N, means coordination number. R is interatomic distance of bounded atom. σ^2 is Debye-Waller factor. Numbers in parenthesis represents three times the estimated standard deviation in the last digit (some data was used from reference198, 199).

Sample	**As-X**	**N**	**R (Å)**	**σ^2(Å^2)**	**Ref**
Arsenate, pH 9.0	**As-O**	4.7(3)	1.688(2)	0.0036(5)	198,199
Arsenate-glycerol, pH 0	**As-O** **As-C**	5.1(6) 4.5(2)	1.81(3) 2.73(2)	0.0039(5) 0.004(3)	Data taken from ref.19,199
Arsenate (Solid sorbed residue phosphate buffer)	**As-O**	3.9(3)	1.68(3)	0.0039(3)	This study
Arsenate (Solid sorbed residue bicarbonate buffer)	**As-O** **As-C**	5.5(6) 2.1(2)	1.68(6) 2.74(2)	0.0076(1) 0.0019(3)	This study

It was observed from adsorption measurements (Chapter 4 section 4.2) that arsenate adsorption capacities in the phosphate buffer were much lower than in aqueous solution without buffer or/and bicarbonate buffer. Accordingly, it was inferred that phosphate ion was competing with arsenate for the sites on adsorbent and there is less effect of counter ions in un-buffered solutions. However, from the XAS results, it was inferred that arsenate interacts directly with phosphate. Thus, phosphate buffer system is not an optimal choice for adsorption isotherm, whereas; bicarbonate may be better due to reduced interaction with arsenate.

Chapter 6 CONCLUSIONS AND FUTURE WORK

6.1 Conclusions

In general, the aim of this project was to synthesize several chitosan-glutaraldehyde copolymers at controlled levels of cross-linking ratios and to evaluate such effects on the adsorption properties of the polymers relative to pristine chitosan. The polymer materials were characterized, and their sorption properties for arsenate oxoanions and *p*-nitrophenol at various pH conditions were evaluated.

Cross-linking at various weight ratios of glutaraldehyde was carried out according to methods previously reported [4, 157, 162, 180]. The yield of cross-linked polymers was 84-88%. The solubility and swelling behaviour of the polymers indicate that the degree of swelling (%) increased with increasing glutaraldehyde content, in accordance with the previous reports [165, 173]. TGA enabled estimates of the effect of crosslinking on the thermal stability of polymers. Further evidence of cross-linking was shown by FTIR results according to the disappearance of the glutaraldehyde signature and the presence of imine bond signatures due to cross-linking. Sorption experiments for PNP using CH-GL polymers showed that sorption capacities are a function of relative initial concentrations of adsorbate and pH of solution since sorption increased with increase in adsorbate concentration and has greater adsorption occurred at pH 5.0 relative to 8.5.

The sorption studies of CH-GL polymers in buffered systems indicated that sorption is pH dependent evidence by the greater uptake of arsenate oxoanions at pH 5.0. Greater adsorption (both in phosphate and bicarbonate buffer) was observed at pH 5 relative to pH 8.5.

Sorption results for un-buffered solution show greater Qm values 14.5 mg/g and removal efficiency covered a range of values (20-95%) for 20 mg of adsorbent material. Adsorptive

uptake is also a function of adsorbate concentration. The CH-GL1:1 copolymer show highest adsorption capacity among the polymers studied where it can be inferred that a gradual increase in the cross-linking improves the sorption capacities of the CH-GL polymers. Such polymers are suitable uptake of arsenate and PNP, and may have wider applications in the removal of waterborne contaminants for environmental remediation.

6.2 New Insight in Adsorption of Arsenate

A survey of the literature reveals a number of methods for the estimation and determination of arsenate (V) and As (III) using spectroscopic techniques and simultaneous determination of arsenate and phosphate and relative effect of phosphate on the adsorption behaviour of arsenate oxoanions. However, these methods indicate the effect of phosphate anion on adsorption of arsenate but there was no evidence of any interaction between arsenate species and phosphate anions [185,187, 188]. It was observed that arsenate was interacting with phosphate buffer system and potentially forming a complex (i.e. arseno-phosphate; reason is not known) due to the attenuation of unbound arsenate. As well, phosphate anions may compete for arsenate binding sites on the chitosan polymers. Evidence of peak splitting for the arsenate peak in the XAS results confirm that phosphate anions interfered with the arsenate sorption by directly interacting with arsenate before the adsorption process, according to experimental results.

6.3 Future Work

Based on observations and results mention above, some future studies are proposed to better understand the adsorption properties between chitosan sorbents and arsenate oxoanions.

- **Improved CH-GL Copolymers**

One of the goals proposed was to evaluate the effect of weight ratios of cross-linkers with chitosan and their resulting sorption properties. Poon has described more about the gelation base synthesis of CH-GL copolymers, however; it may be helpful to do gelation based synthesis under specific pH conditions (5.6) to attain maximum cross-linking (*cf.* Chapter 3; section 3.2). To open the door for industrial applications, synthetic method modification such as high scale synthesis should be under considered.

- **Characterization of Adsorbents before and after Sorption**

To develop a better understanding of adsorption mechanism of adsorbate (arsenate oxoanions) with CH-GL polymers, FTIR analysis of the adsorbed material (solid residue) will establish if any spectral shifts (IR, XAS, etc) to characterize the nature of the adsorptive interactions.

- **Improvement in Adsorption Kinetics**

It was noticed that stirring time of stock solution in phosphate buffer has a significant effect on reduced adsorption of arsenate (results are not shown and reason is not known). A systematic approach towards an understanding of the adsorptive or complex formation between arsenate and phosphate can be achieved from systematic kinetic studies. A comparative and quantitative study can be done using different buffer systems such as bicarbonate and sulphate.

To minimize the interferences from particles and other ions, an improved isolation method can be achieved. A good calibration can be achieved using arsenic concentrations in ppb levels to get a complete isotherm covering a wide range of concentration.

- **Some other Techniques for Arsenate Anion Analysis**

The mechanistic approach for the adsorption can be achieved using solid high field ^{75}As NMR. This technique is not suitable for compounds containing structural H_2O or protonated arsenate species [203]. As indicated above, phosphate anions may influence the sorption of arsenate oxoanions on chitosan based materials. ATR analysis can help to determine the quantitative effect [204]. Preliminary ATR measurements were carried out to determine the effect of phosphate anions using D_2O as reference material but inconclusive results were obtained due to the solubility of CH-GL polymers film in D_2O (results are not shown here). The effect of phosphate and bicarbonate anions can be explored in detail by using some traditional colorimetric spectroscopic for arsenate kinetic uptake experiments. The interaction of phosphate with chitosan glutaraldehyde polymers or arsenate can be evaluated using potentiometric titrations [205].

- **Sorption Properties of other Arsenic Species**

A comparative study can be done using an organic arsenical with suitable spectrophotometric properties as good reference to optimize the sorption protocols for greater accuracy.

- **Future Work for Synchrotron XAS**

Synchrotron XAS is a suitable technique for providing new insights into adsorption of arsenate. The adsorption properties of CH-GL copolymers have been evaluated in un-

buffered solution since the XAS analysis of that system was not studied. XAS will help to study the comparative phosphate effect on the adsorption properties of these polymers. Similarly, the adsorption of roxarsone (ROX) has been studied using same polymers in a separate study [180]. Synchrotron XAS measurements may help to determine whether if inorganic anion species of ROX (AsO_4^{-3}) interact with phosphate buffer.

REFERENCES

1. United Nations, Ensure Environmental Sustainability, http://www.un.org/millenniumgoals/environ.shtml (accessed May 29, 2014).

2. Chitosan: Commercial uses and potential applications. In: Chitin and Chitosan: Sources, Chemistry, Biochemistry, Physical Properties and Applications, eds. G. Skjak- Break, T. Anthonsen, and P. Sandsord, 1989, pp 1-69. England: Elsevier Applied Sci.

3. Ravi Kumar, M. N.V.; Muzzarelli, R.A.A.; Muzzarelli, C.; Sashiwa, H.; Domb, A. *J.* Chitosan Chemistry and Pharmaceutical Perspective *Chem. Rev*. **2004**, *104*, 6017-6084.

4. Pratt, D.Y.; Wilson, L. D.; Kozinski, J.A. Preparation and sorption studies of glutaraldehyde cross-linked chitosan copolymers *J. Colloid. Interface. Sci*. **2013**, *395*, 205-211.

5. Michael Anto, S.; Annadurai, G. Arsenic Adsorption from Aquoeus Solution Using Chitosan Nanoparticles *Res. J. Nanosci. Technol*. **2012**, *2*(2), 31-45.

6. Zha, F.; Li, S.; Chang, Y. Preparation and adsorption properties of chitosan beads bearing β-cyclodextrin cross-linked by 1,6-hexamethylene diisocyanate *Carbohyd. Polym*. **2008**, *72*, 456-461.

7. Chang, X.; Chen, D.; Jiao, X. Chitosan-based aerogels with high adsorption performance *J. Phys. Chem. B* **2008**, *112*, 7721-7725.

8. Crini, G.; Badot, P.-M. Application of chitosan, a natural aminopolysaccharide, for dye removal from aqueous solution by adsorption processes using batch studies : A review of recent literature *Prog. Polym. Sci.* **2008**, *33*, 399-447.

9. Guibal, E. Interactions of metals ions with chitosan-based sorbents: a review *Sep. Purif. Tech*. **2004**, *38*, 43-74.

10. Chassary, P.; Vincent, T.; Guibal E. Metal anion sorption on chitosan and derivative materials: a strategy for polymer modification and optimum use *React. Funct. Polym*. **2004**, *60*, 137-149.

11. Rana, M.S.; Halim, M.A.; Waliul Hoque, S.A.M.; Hasan, Kamrul.; Hossain, M. K. Bioadsorption of Arsenic by Prepared and Commercial Crab Shell Chitosan, *Biotechnol*. **2009**, *8*(1), 160-165.

12. Renault, F.; Sancey, B.; Badot, P.-M.; Crini, G. Chitosan for coagulation/flocculation processes –An eco-friendly approach *Eur. Polym. J.* **2009**, 1*45,* 13371348.

13. Poon, L.; Wilson, L. D.; Headley, J.V. Chitosan-glutaraldehyde copolymers and their sorption properties, *Carbohyd. Polym*, **2014**, *109*, 92-101.

14. Kildeeva, N. R.; Perminov, P. A.; Vladimirov, L.V.; Novikov, V.V.; Mikhailov, S.N. About Mechanism of Chitosan Cross-linking with Glutaraldehyde *J. Bioorganic. chem*. **2009**, *35*(3), 397-407.

15. Ishii, T.; Sorita, A.; Sawamura, M.; Kusunose, H. Ukeda, H. Determination of the reaction-product of glutaraldehyde and amine based on the binding ability of Coomassie brilliant blue *Anal. Sci*. **1997**, *13*, 5-9.

16. Chen, C.-C.; Chung, Y. -C. Arsenic Removal Using a Biopolymer Chitosan Sorbent *J. Environ. Sci. Heal. A* **2006**, *41*, 645.

17. Piepenbrock, M. M.; Lloyd, G.; Clarke, N.; Steed, J.W. *J. Metal- and anion-binding superamolecuar gels Chem, Rev*. **2010**, *110*(4), 1960-2004.

18. Boyle, R.W.; Jonasson, I. R. The geochemistry of arsenic and its use as an indicator element in geochemical prospecting *J. Geochem. Explor*. **1973**, *2*, 251.

19. National Research council (1999) Arsenic in Drinking Water, Washington DC, National Academy Press, pp 27-82.

20. Arsenic and Arsenic compounds, Environmental Health criteria 224. 2nd Ed, Geneva, International Programme on Chemical Safety.

21. Periodic Table Home page http://www.rsc.org/periodic-table/element/33/arsenic (accessed May 05, 2014).

22. Hazardous Substances Data Bank. National Library of Medicine http://toxnet.nlm.nih.gov/cgi-bin/sis/htmlgen (accessed May 05, 2014).

23. Brooks, W. E. Minerals Yearbook, Arsenic http://minerals.usgs.gov/minerals/pubs/commodity/arsenic/myb1-2007-arsen.pdf (accessed May 06, 2014).

24. Toxicological profile for Arsenic. Agency for Toxic Substances and Disease Registry. http://www.atsdr.cdc.gov/toxprofiles/tp2.pdf (accessed May 06, 2014).

25. ATSDR http://www.atsdr.cdc.gov/tfacts2.pdf (accessed May 06, 2014).

26. Hasegawa, H.; Matsui, M.; Okamura, S.; Hojo, M.; Iwasaki, N.; Sohrin, Y. Speciation including 'hidden' arsenic in natural waters *Appl. Organometal. Chem*. **1999**, *13*, 113.

27. Skinner, J.T.; McHargue, J. S. Supplementary of arsenic and manganese on copper in synthesis of hemoglobin *Am. J. Physiol*. **1946**, *145*, 500-6.

28. Nielsen, F. H.; Uthus, E.O. S.H. *Biochemistry of Essential Trace Elements*: Arsenic, **1984**, *3*, 319-340.

29. Jain, C. K.; Ali, I. Arsenic occurrence, toxicity and speciation techniques *Water Res*. **2000**, *34*, 4304-43-12.

30. Harper, T.R.; Kingham, N.W. Removal of arsenic from wastewater using chemical precipitation methods *Water. Environ. Res*. **1992**, *65*, 200-203.

31. United Sates Environmental Protection Agency. Basic information about arsenic in drinking water http://water.epa.gov/drink/contaminants/basicinformation/arsenic.cfm (accessed May 05, 2014).

32. Sounderajan, S.; Udas, A. C.; Venkataramani. B. Characterization of arsenic (V) and arsenic (III) in water samples using ammonium molybdate and estimation by graphite furnace atomic absorption spectroscopy *J. Hazard. Mater*. **2007**, *149*, 238-242.

33. Badal, K. M.; Kazuo, T. S. Arsenic round the world: a review *Talanta*. **2002**, *58*, 201-235.

34. Mohan, D.; Pittman, C.U. Jr. Arsenic removal from water/wastewater using adsorbents Acritical review *J. Hazard. Mater*. **2007**, *142*, 1-53.

35. Smedley, P. L.; Nicolli, H.B.; Macdonad, D.J.; Barros, A.J.; Tullio, J.O. A review of the source, behaviour and distribution of arsenic in natural waters *Appl. Geochem.* **2002**, *17*, 517-568.

36. Chen, C. J.; Kuo, T. L.; Wu, M. M. Arsenic and cancers *Lancet*. **1988**, *1*, 414-415.

37. Berg, M.; Tran, H.C.; Nguyen, T. C.; Pham, H. V.; Schertenleib, R.; Giger, W. Arsenic contamination of groundwater and drinking water in Vietnam: a human health threat *Environ. Sci. Technol*. **2001**, *35*, 2621-2626.

38. Mandal, B. K.; Suzuki, K. T. Arsenic around the world: a review *Talanta*. **2002**, *58*, 201-235.

39. Hricko, A. Environmental problems behind the Great Wall *Environ. Health Persp*. **1994**, *102*, 154-159.

40. Shen, Y. S. Study of arsenic removal from drinking water *J. Am. Water Works Assoc*. **1973**, *65*(8), 543-548.

41. Das, D.; Chattered, A.; Samanta, G.; Mandal, B.K. Arsenic contamination in ground water in six districts of West Bengal, India: The biggest arsenic calamity in the world *Analyst*. **1994**, *119*, 168N-70N.

42. McGuigan, C. F.; Hamula, C. L. A.; Huang, S.; Gabos, S.; Chris Le, X. A review on arsenic concentration in Canadian drinking water *Environ. Rev.* **2010**, *18*, 291.

43. Gibbons, M. K.; Gagnon, G. A. Adsorption of arsenic from Nova Scotia ground water onto water treatment residual solids *Water. Research*, **2010**, *44*(19), 7540-7549.

44. Farmer, J.G.; Johnson, L. R. Assessment of Occupational Exposure to Inorganic Arsenic Based on Urinary Concentrations and Speciation of Arsenic *Br. J. Ind. Med*. **1990**, *42*, 342-348.

45. Lorenzen, L.; Van Deventer, S. J.; Landi W. M. Factors affecting the mechanism of adsorption of arsenic species on activated carbon *Miner Eng*. **1995**, *8(45)*, 557-569.

46. Lagerkvist, B. J.; Zetterlund, B. Assessment of exposure to arsenic among smelter workers: A five follow-up *Am. J. Ind. Medicin*. **1994**, *25*, 477-488.

47. Arial, Y.; Lanzirotti, A.; Sutton, S.; Davis, J. A.; Sparks, D. L. Arsenic Speciation and reactivity in poultry litter *Environ. Sci. Technol*. **2003**, *37*, 4083-4090.

48. Nachman, K.E.; Raber, G.; Francesconi, K.A.; A. Navas-Acien, A.; Love, D. C. Arsenic species in poultry feather meal *Sci. Tot. Environ*. **2012**, *417-418*, 183-188.

49. Hu, J.; Tong, Z.; Hu, Z.; Chen, G.; Chen, T. Adsorption of roxarsone from aqueous solution by multi-walled carbon nanotubes *J. Colloid. Interface. Sci*. **2012**, *377*, 355-361.

50. Thirunavukkarasu, O.S.; Viraraghavan, T.; Subramanian, K. S.; Tanjore, S. Organic arsenic removal from drinking water *Urban Water*. **2002**, *4*, 415-421.

51. Liu, X.; Zhang, W.; Hu, Y.; Cheng, H. Extraction and detection of organoarsenic food additives and common arsenic species in environmental matrices by HPLC-ICP-MS *Microchem. J*. **2013**, *108*, 38.

52. WHO Arsenic in drinking-water http://www.who.int/water_sanitation_health/dwq/chemicals/arsenic.pdf (accessed May 29, 2014).

53. EPA, Basic Information about Arsenic in drinking Water, http://water.epa.gov/drink/contaminants/basicinformation/arsenic.cfm (accessed May 29, 2014).

54. Hasegawa, H.; Sohrin, Y.; Matsui, M.; Hojo, M.; Kawashima, M. Speciation of arsenic in natural waters by solvent extraction and hydride generation atomic absorption spectrometry *Anal. Chem*. **1994**, *66*, 3247-3252.

55. Mondal, P.; Majumder, C. B.; Mohanty, B. Laboratory based approaches for arsenic remediation from contaminated water: Recent development *J. Hazard. Mater*. **2006**, *137*, 464-479.

56. Kwon, J. Study of Surface Modified Carbon nano-materials, Ph.D. Dissertation, University of Saskatchewan, Saskatoon, CA, 2014.

57. Binoy, S.; Yunfei, X.; Megharaj, M.; Gummuluru, S.R.K.; Ravi, Naidu. *J. Colloid. Interf. Sci*. **2012**, *350*, 295.

58. Li, J. -M.; Meng, -X. -G.; Hu, C. -W.; Du, Adsorption of phenol, *p*-chlorophenol, and *p*-nitrophenol onto functional chitosan *J. Bioresource. Technol*. **2009**, *100*, 1168-1173.

59. Bowers, G. N.; McComb, R.B.; Christensen, R.G.; Schaffer, R. High-purity 4-nitrophenol: purification, characterization and specification for use as spectrophotometric reference material *Clin. Chem*. **1980**, *26*(6), 724-729.

60. Anirudhan, T. S.; SreeKumari, S. S.; Bringle, C. D. Removal of phenol from water and petroleum industry refinery effluents by activated carbon obtained from coconut coir pith *Adsorption*. **2009**, *15*, 439-451.

61. Olcay, F.; Sagban, T. Impacts of wastewater sludge amendments in restoring nitrogen cycle in *p*-nitrophenol contaminated soil *J. Environ. Sci*. **2011**, *23*(40), 616.

62. Hong, Q.; Zhang, Z. H.; Hong, Y. F.; Li, S. P. A microcosm study on bioremediation of fenitrothion-contaminated soil using *Burkholderia sp*. FDS-1 *Int. Biodeter. Biodegr.* **2007**, *59*,155-161.

63. Gemini, V. L.; Gallego, A.; De Oliveira, V.M.; Gomez, C.E.; Manfio, G.P.; Korol, S. E. Biodegradation and detoxification of *p*-nitrophenol by *Rhodococcus wratislaviensis Int. Biodeter. Biodegr*. **2005**, *55*, 103-108.

64. World Health Organization Guidelines for Drinking-Water Quality http://whqlibdoc.who.int/publications/2011/9789241548151_eng.pdf (accessed date May, 29 2014).

65. McKav, G.; Bino, M.G.; Altamemi, A. R. The adsorption of various pollutants from aquoeus solution on to activated carbon *Water Res*. **1985**, *19*(4), 491.

66. Radovic, L.R.; Moreno-Castilla, C.; Rivera-Utrilla, J. Carbon materials as adsorbents in aqueous solutions *Chem. Phys. Carbon*. **2000**, *27*(4), 227-406.

67. Spiker, J. K.; Crawford, D.L.; Thiel, E. Oxidation of phenolic and nonphenolic substances by the lignin peroxide of Streptomyces viridosporus *J. Appl. Microb. Biotech.* **1992**, *37*,518-523.

68. Maugans, C. B.; Akgerman, A. Catalytic wet oxidation of phenol over a Pt/TiO catalyst *Water Res*. **1997**, *4*, 3116-3124.

69. Kavita, V.; Palanivelu, K. The role of ferrous ion in Fenton and photo-Fenton processes for the degradation of phenol *Chemosphere*. **2004**, *55*, 1235-1243.

70. Fan, L.; Li, M.; Lv, Z.; Sun, M.; Luo, C.; Lu, F.; Qiu, H. Fabrication of magnetic chitosan nanoparticles grafted with β-cyclodextrin as effective adsorbents toward hydroquinol *J. Colloid. Sur. B* **2012**, *95*, 42-49.

71. Wilson, L.D; Mohamed, M.H.; Berhaut, C. L. Sorption of Aromatic Compounds with Copolymer Sorbent Materials Containing β-Cyclodextrin *Materials.* **2011**, *4*, 1528-1542.

72. Mohamed, M. H.; Wilson, L. D.; Headley, J.V. Peru, K.M. Investigation of the sorption properties of β-cyclodextrin-based polyurethanes with phenolic dyes and naphthenates *J. Colloid. Interface. Sci*. **2011**, *356*(1), 217-226.

73. Kwon, J. H.; Wilson, L. D. Surface-modified activated carbon with β-cyclodextrin part II adsorption properties *J. Environ. Sci. Health. Part A* **2010**, *45*(13), 1793-1803.

74. Hermosin, M.; Martin, P.; Cornejo, J. Adsorption mechanism of monobutyltin in clay minerals *Environ. Sci. Technol.* **1993**, *27*, 2606-2611.

75. Banergee, K.; Cheremisinoff, P.N.; Cheng, L.S. Adsorption kinetics of O-Xylene by flyash *Water Res*. **1997**, *31*, 249-261.

76. Wang, K.; Furney, T.D.; Halway, M. C. *Chem. Eng. Sci*. **1995**, *50*, 2883-2897.

77. Ngah, W.S.W.; Fatinathan, S. Chitosan-flakes and chitosan-GLA beads for adsorption of *p*-nitrophenol in aquoeus solution *Colloid. Surface A* **2006**, *277*(1-3), 214-222.

78. Hering, J. G.M. Elimelech. Arsenic Removal by Enhanced Coagulation and Membrane Processes *J. AWWA*. Denver, 1996.

79. Edward, M. A. Chemistry of Arsenic Removal during Coagulation and Fe-Mn Oxidation *J.AWWA*, September, **1994**, 64-77.

80. Renault, F.; Sancey, B.; Badot, P.-M.; Crini, G. Chitosan for coagulation/flocculation processes –An eco-friendly approach *Eur. Polym. J.* **2009**, 1*45*, 13371348.

81. Logsdon, G.S.; Sorg, T. J. Symon, J. M. (1974). "Removal of Heany Metals by Conventional Treatment," Proc.16th Water Quality Conference- Trace Metals in Water Suplies: Occurrence, Significance and Control, University Bulletin no71, U. of Illinois.

82. McNeill, L.S.; Edwards. M.A. Soluble Arsenic Removal at Water Treatment Plants *J. AWWA*. **1995**, 105-113.

83. Vickers, J. C.; Braghetta, A.; Hawkins, R.A. "Bench Scale Evaluation of Microfiltration for Removal of Particles and Natural Organic Matters," Proceeding Membrane Technology Conference, Feb 23-26, 1997, New Orleans, LA.

84. Harper, T. R.; Kingham, N.W. Removal of arsenic from wastewater using chemical precipitation methods *Water. Environ. Res*. **1992**, *64*, 200-203.

85. Chutia, P.; Kato, S.; Kojima, T.; Satokawa, S. Arsenic adsorption from aqueous solution on synthetic zeolites *J. Hazard. Mater*. **2009**, *162*, 440-447.

86. Ming, D.W.; Dixan, J. B. Quantitative determination of Clinoptilolite in soils by a cation-exchange capacity method *Clays. Clay. Miner*. **1988**, *35*(60), 463-468.

87. Dhar, R. K.; Zheng, Y.; Rubenstone, J.; Geen, A.V. A rapid colorimetric method for measuring arsenic concentrations in ground water *Anal. Chem. Acta*. **2004**, *526*, 203-209.

88. Coedo, A. G.; Dorado, M. T. Application of Flow Injection Inductively Coupled Plasma Mass Spectrometry to the Simultaneous Determination of Arsenic, Antimony, Tin, Selenium and Tellurium in Steels *J. Anal. Atom. Spectrom.* **1994**, *19*, 1111-1115.

89. Shraim, A.; Chiswell, B.; Olszowy, H. Speciation of arsenic by hydride generation-atomic absorption spectrometry (HG-AAS) in hydrochloric acid reaction medium *Talanta*, **1999**, *50*, 1109-1127.

90. Coelho, N. M. M.; Cosmen da Silva, A.; Moraes da Silva, C. Determination of As(III) and total inorganic arsenic by flow injection hydride generation atomic absorption spectrometry *Anal. Chem. Acta*. **2002**, *460*, 227.

91. Sigrist, M.E.; Beldome nico, H.R. Determination of inorganic species by flow injection hydride generation atomic absorption spectrometry with variable sodium tetrahydroborate concentrations *Spectrochem. Acta*. B **2004**, *59*, 1041-1045.

92. Delgado-Andrate, C.; Navarro, M.; Lopez, H.; Lopez, M. C. Determination of total arsenic levels by hydride generation atomic absorption spectrometry in food from south-east Spain: estimation of daily dietary intake *Food. Addit. Contam.* **2003**, *20*(10), 923-932.

93. Hou, X.; Jones, B.T. Inductively Coupled Plasma/Optical Emission Spectrometry, Encyclopedia of the Analytical Chemistry, R. A. Meyer (ED), John Wiley & Sons Ltd, Chichester, 200, pp. 9468-9485.

94. Pickering, I. J.; Prince, R. C.; George, M. J.; Smith, R. D.; George, G. N.; Salt, D.E. Reduction and Coordination of Arsenic in Indian Mustard *Plant Physiology*. **2000**, *122I*, 1171-1177.

95. Farquhar, M. L.; Charnock, N. J. M.; Livens, F. R.; Vaughan, D. Mechanism of Arsenic Uptake from Aqueous Solution by Interaction with Goethite, Lepidocrocite, Meckinawite, and Pyrite: An X-ray Absorption Spectroscopy Study *J. Environ. Sci. Technol*. **2002**, *36*, 1757-1762.

96. Meirer, F.; Pepponi, G.; Streli, C.; Wobrauschek, P.; Mihucz, V. G.; Zaray, G.; Czech, V.; Broekaert, J. A. C.; Fittschen, U. E. A., Falkenberg, G. Arsenic speciation in cucumber (Cucumber sativus L.) xylem sap by K-edge TXRF-XANES *X-Ray Spectrum*. **2007**, *36*, 408-412.

97. Cheremisinoff, P.N.; Angelo, C. M. Carbon adsorption applications, in: Carbon Adsorption Handbook, Ann Arbor Science Publishers, Inc., Ann Arbor, MI, 1980, 1-54.

98. Bawn, C.E. H. The adsorption of gases and vapors on plane surfaces *J. Am. Chem. Soc*. **1932**, *54*, 72.

99. Atkins, P.; DePaula, J. Physical Chemistry. Oxford University Press, New York. 2002; P. 515-529.

100. Kwon, J. Sorption studies of surface modified activated carbon with β-cyclodextrin, M.Sc. Thesis, University of Saskatchewan, Saskatoon, CA, 2007.

101. Ruthven, D.M. Principles of adsorption and adsorption and adsorption processes. John Wiley & Sons: New York, USA, 1984; p. 30

102. Gregg, S. J.; Sing, SK. S. Adsorption, Surface Area and Porosity, 2nd Ed.; Academic Press: New York, USA, 1982; p 4.

103. Langmuir, I. The Constitution and Fundamental Properties of Solids and Liquids Part I Solids *J. Am. Chem. Soc*. **1916**, 2221.

104. Langmuir, I. The Constitution and Fundamental Properties of Solids and Liquids Part II Liquids *J. Am. Chem. Soc*. **1917**, 1848.

105. Sips, R. On the structure of a catalyst surface *J. Chem. Phys*. **1948**, *16*, 490.

106. Wang, L.; Chen, A.; Field, K. Arsenic Removal from Drinking Water by Ion Exchange and Activated Alumina Plants, Report EPA-600/R00-/088, United states Environmental Protection Agency; 2000.

107. Gupta, S.K.; Shen, K. Y. Arsenic removal by adsorption *J. Wat. Pollut. Control Fed.* **1978**, 493-506.

108. Pattanayak, J.; Mondal, K.; Mathew, S.; Lalvani, S.B. A parametric evaluation of the removal of As(V) and As(III) by carbon based adsorbents *Carbon*. **2000**, *38*, 589-596.

109. Rajakovic, L.V. Sorption of arsenic onto activated carbon impregnated with metallic silver and copper *Sep. Sci. Technol*. **1992**, *27*(11), 1423-1433.

110. Bailey, S. E.; Olin, T. J.; Bricka, R.M.; Adrian, D. D. A review of potentially low-cost sorbents for heavy metals *Water Res.* **1999**, *23*, 2469.

111. Grover, M.; Narayanaswam, Y. M.S. Removal of hexavalent chromium by adsorption on fly ash *J. Inst. Eng. (India) Environ.***1982**.

112. Bailey, R. P.; Bennett, T.; Benjamin, M. M. Sorption onto and recovery of Cr (v) using iron-oxide coated sand *Water Sci. Technol*. **1992**, *26*(5-6), 1239-1244.

113. Masri, M. S.; Friedman, M. Effect of chemical modification of wool on metal ion binding *J. Appl. Polymer Sci*. **1974**, *18*, 2367-2377.

114. Roberts, E. J.; Rowland, S. P. Removal of mercury from aqueous solutions by nitrogen-containing chemically modified cotton *Environ. Sci. Technol*. **1973**, *7*(6), 552-555.

115. Randall, J.M.; Bermann, R.L.; Garret, V.; Waiss, A. C. Jr. Use of bark to remove heavy metals ions from waste solutions *J. Forest Prod*. **1974**, *24* (9), 80-84.

116. Vazquez, G.; Antrorrena, G.; Gonzalez. Adsorption of heavy metal ions by chemically modified *Pinus pinaster* Bark *Bioresour. Technol*. **1994,** *48(3)*, 251-255.

117. Srivastava, S. K.; Singh A.K.; Sharma, A. Studies on the uptake of lead and zinc by lignin obtained from black liquor- a paper industry waste material *Environ. Technol*. **1994,** *15*, 353.

118. Cadena, F.; Rizvi. R.; Peters, R.W. Feasibily studies for the removal of heavy metals from soltution tailored bentonite. *In Hazardous and industrial Waste*, Proceeding of the Twenty-Second Mid-Atlantic Industrial Waste Conference, Drexel University, 1990, 77-94.

119. Dambies, L.; Vincent, T.; Guibal, E. Treatment of arsenic-containing solution derivatives: uptake mechanism and sorption performances *Water Res.* **2002**, *36*, 3699-3710.

120. Islam, M.; Mishra, P.C.; Patel, R. Arsenate removal from aquoeus solution by cellulose-carbonated hydroxyapatite nanocomposites *J. Hazard. Mater*. **2011**, *189*, 755-763.

121. Berkeley, R.C.W. *Chitin, Chitosan and their Degradative enzymes. In Microbial Polysaccarides*, Academic press: 1979, New York, P. 205-236.

122. George, T.S.; Guru, K.S.S.; Vasanthi, N.S.; Kannan, K.P. Extraction, Purification and Characterization of Chitosan from Endophytic Fungi Isolated from Medicinal Plants *World. J. Sci. Technol*. **2011**, *1*(40), 43.

123. Tokura, S.; Tamura, H. Chitin and chitosan. In Comprehensive Glycoscience, eds. H. Kamerling, G. Boons, Y.C. Lee, A. Suzuki, N. Taniguchi, A. G. J. Voragen, 2007, pp. 449-475. Elsevier Ltd., Amsterdam, the Netherlands.

124. Zhang, M.; Haga, A.; Sekiguchi, H.; Hirano, S. Structure of insect chitin isolated from beetle larva cuticle and silkworm (*Bombyx mori*) pupa exuvia *Int .J. Biol. Macromol*. **2000**, *27*, 99-105.

125. Zamani, A.; Edebo, L.; Niklasson, C.; Taherzadeh, M. J. Temperature shifts for Extraction and Purification of Zygomycetes chitosan with Dilute Sulfuric Acid *Int. J. Mol. Sci*. **2010**, *11*, 2976-2987.

126. Peniston, Q.P.; Johnson, E. Process for the Manufacture of Chitosan. US Patent4, 195, 175, 5pp 1980.

127. Hirano, S. Chitin biotechnology applications *Biotechnol. Annu*. Rev. **1996**, *2*, 239-258.

128. Gao, X.; Kim, K. S.; Liu, D. Nonviral gene delivery: What we know and what is next *AA P S. J.* **2007**, *9*, 92-104.

129. Felt, O.; Buri, P.; Gurny, R. Chitosan: A unique polysaccharide for drug delivery *Drug .Dev. Ind .Pharm*. **1998**, *24* (110), 979-993.

130. Bratby, J. Coagulation and flocculation in water and wastewater treatment. 2nd ed. IWA Publishing; 2007.

131. Hirohara, H.; Takehara, M.; Fukita, A.; Kansai, K.K.K, Hirohara H. Flocculant and sludge treatment method. Japanese Patent JP 2001129310, 1999.

132. Hong, P.-Z.; Li, S.-D.; Ou, C.-Y.; Li, C.-P.; Yang, L.; Zhang, C.-H. Thermogravimetric Analysis of Chitosan *J. Appl. Polym. Sci*. **2007**, *105*, 547-551.

133. Park, J.W.; Choi, K.-H.; Park, K. K. Acid-Base Equilibria and Related Properties of Chitosan *B. Kor. Chem. Soc*. **1983**, *4*, 2.

134. Singla, A. K; Chawla, M. Chitosan: some pharmaceutical and biological aspects-an update *J. pharm. pharmacol*. **2001**, *53*(8), 1047-1067.

135. Dash, M.; Chiellini, F.; Ottenbrite. R.M; Chiellini, E. Chitosan- A versatile semi-synthetic Polymer in biomedical applications *Prog. Poly. Sci*. **2011**, *36*, 981-1014.

136. Kawamura, Y.; Mitsuhashi, M.; Tanibe. H. Adsorption of metal ions on polyaminated highly porous chitosan chelating resin *Ind. Eng. Chem. Res*. **1993**, *32(2)*, 386-391.

137. Yang, T. C; Zall, R. R. Adsorption of metals by natural polymers generated from seafood processing wastes *Ind. Eng. Chem. Prod. Res. Des*. **1984**, *23*, 168-172.

138. Varma, A. J.; Deshpande, S.V.; Kennedy, J. F. *Metal complexation by chitosan and its derivatives : a review Carbohydr. Polym. Sci*. **2004**, *55*,77-93.

139. Masri, M. S.; Reuter, F. W. Binding of metal cations by natural substances *J. Appl. Polymer. Sci*. **1974**, *18*, 675-681.

140. Hsien, T. Y; Rorrer, G.L. Effects of acylation and crosslinking on the material properties and cadmium ion adsorption capacity of porous chitosan beads *Separ. Sci. Technol*. **1995**, *30* (12), 2455-2475.

141. Pontoni, L.; Fabbricino, M. Use of chitosan and chitosan-derivatives to remove arsenic from aqueous solutions A mini review *Carbohyd. Res.* **2012**, *356*, 86-92.

142. Inoue, K.; Baba, Y.; Yoshizuka, K.; Noguchi, H.; Yoshizaki, M. Selectivity series in the Adsorption of Metal Ions on a Resin prepared by cross-linked copper(II)-complexed chitosan *Chem. Lett.* **1988**, 1281-1284.

143. Muzzarelli, R. A. A.; Tubertini, O. Chitosan for collection from seawater of naturally occurring zinc, cadmium, lead and copper *Talanta*. **1971**, *18(9)*, 853-858.

144. Koyama, Y.; Taniguchi, A. Study on Chitin X Homogeneous cross-linking of chitosan for Enhanced Cupric ion Adsorption *J. Appl. Polym. Sci*. **1986**, *31*(6), 1951-1954.

145. Martinez, L.; Agnely, F.; Leclerc, B. Siepmann, J.; Cotte, M.; Geiger, S.; Couarraze, G. Cross-linking of Chitosan and Chitosan/poly(ethylenoxide) beads: a theoretical treatment *Eur. J. Pharm. Biopharm.* **2007**, *67*, 339-348.

146. Oshita, K.; Oshima, M.; Goa, Y. -H.; Lee, K. -H.; Motomizu, S. Adosprtion behaviour of Mercury and Precious Metals on cross-linked chitosan and the removal of ultratrace Amounts of Mercury in concentrated Hydrochloride Acid by a column Treatment with cross-linked chitosan *Anal. Sci*. **2002**, *18*, 1121-1125.

147. Jubinka, L.; Rajakovic, V. The sorption of the arsenic onto activated carbon impregnated with metallic silver and copper *Sep. Sci. Technol*. **1992**, *27*(11), 1423-1433.

148. Rorrr, G.L.; Hsien, T. Y.; Way, J.D. Synthesis of porous magnetic-chitosan beads for removal of cadmium ions from waste water *Ind. Eng. Chem. Res*. **1993**, *32*, 2170-2178.

149. Guibal, E.; Milot, C.; Tobin, J. M. Metal anion sorption by chitosan beads: equilibrium and kinetic studies *Ind. Eng. Chem. Res*. **1998**, *37*, 1454-1463.

150. Ruiz, M.; Sastre, A. M.; Guibal, E. Palladium sorption on glutaraldehyde-crosslinked chitosan *React. Funct. Polym*. **2000**, *44*(3), 155-173.

151. Verbych, S.; Bryk, M.; Alpatova, A.; Chornokur, G. Ground water treatment by enhanced ultrafiltration *Desalination* **2005**, *179*, 237-244.

152. McCarrick, P.; Tobin, J. Guibal, E. Comparative sorption of dyes on chitosan and activated carbon. *Sep. Sci. Technol*. **2003**, *38*, 3049.

153. Bosinco, S.; Guibal, E.; Roussy, P.; LeCloirec, P. Adsorption of Hexavalent Chromium ion Chitosan beads: Sorption Isotherm and Kinetics *Min. Pro. Ext. Met. Rev*. **1998**, *19*, 277-291.

154. Elson, C. M.; Davies, D. H.; Hayes, E.R. Removal of Arsenic from Contaminated Drinking Water by a Chitosan/Chitin Mixture *Water .Res.* **1980**, *14(9)*, 1307-1311.

155. Zhao, S.; Zhou, F.; Li, L.; Cao, M.; Zuo, D.; Liu, H. Removal of anionic dyes from aquoeus solutions by adsorption of chitosan-based semi-IPN hydrogel composites *Composites. B* **2012**, *43*, 1570-1578.

156. Pratt, D.Y. Sorption of Arsenic Species using Chitosan based Biosorbents Materials, M.Sc. Thesis, University of Saskatchewan, Saskatoon, CA, 2011.

157. Wilson, L.D.; Xue, C. Molecular sorbent materials for urea capture *J. Appl. Polym. Sci*. **2013**, *128*, 667-675.

158. Aruldhas, G. "*Molecular Structure and Spectroscopy*"6th ed Prentice-Hall of India Private Ltd.: New Delhi 2005.

159. Brian, C.; Smith. *"Fundamentals of Fourier Transform Infrared spectroscopy",* C, Boca Raton, 1996.

160. Sliverstein, R. M.; Webster, F.; Kiemle, D. "Spectroscopic Identification of Organic Compounds", 7th ed., John Wiley & Sons Inc. Hoboken. 2005, Pg. 96-98.

161. Huang, H.; Wang, K.; Wang, S.; Klein, M. T.; Calkins, W.H. Application of the thermogravimetric analysis in the study of Fossil fuels, Am. Chem. Soc., Div. Fuel. Chem *Am. Chem. Soc. Div. Fuel. Chem*. **1996**, *41*, 1-17.

162. Poon, L. Synthesis of β-cyclodextrin and chitosan-based copolymers for the removal of naphthenic acids, M.Sc. Thesis, University of Saskatchewan, Saskatoon, Canada, 2013.

163. Richards, F. M.; Knowles, J. R. Glutaraldehyde as a protein cross-linkage reagent *J. Mol. Biol*. **1968**, *37*, 231-233.

164. Rinaudo, R. Chitin and chitosan: Properties and application *Prog. Polym. Sci*. **2006**, *31*, 603.

165. Lazaridis, N.K.; Kyzas, G.Z.; Vassilion, A. A.; Bikiaris, D. N. Chitosan derivatives as biosorbents for basic dyes *Langmuir*. **2007**, *23*, 7634-7643.

166. Migneault, I.; Dartiguenave, C.; Bertrand, M. J.; Waldron, K.C. Glutaraldehyde : behaviour in aquoeus solution, reaction with protein, and application to enzyme crosslinking *Biotechniques*. **2004**, *37*(5), 790.

167. Hopwood, D.; Callen, C. R.; McCabe, M. The reaction between glutaraldehyde and various proteins. An investigation of their kinetics *J. Histochem*. **1970**, *2*, 137-150.

168. Alexa, G.; Chisalita, D.; Chirita, G. Reaction of dialdehyde with functional group in collagen *Rev. Tech. Ind. Cuir*. **1971**, *63*, 5-14.

169. Peters, K.; Richards, F.M. Chemical cross-linking: reagent and problems in studies of membrane structure *Annu. Rev. Biochem*. **1977**, *46*, 523-551.

170. Knaul, J. Z.; Hudson, S. M.; Creber, K. A. M. Crosslinking of chitosan fibers with dialdehyde: proposal of new reaction mechanism *J. Polym. Sci*. B **1999**, *37*, 1079.

171. Chiou, M.S.; Li, H.Y. Adsorption behaviour of reactive dye in aqueous solution on chemical cross-linked chitosan beads *Chemosphere.* **2003**, *50*, 1095-1105.

172. Okuyama, K.; Noguchi, K.; Miyazawa, T.; Yui, Y.; Ogawa, K. Molecular and crystal structure of hydrated chitosan *Macromolec*. **1997**, *30*, 5849-5855.

173. Silva, R.M.; Silva, G.A.; Coutinho, O.P.; Mano, J.F.; Reis, R. L. Preparation and characterization in stimulated body conditions of glutaraldehyde crosslinked chitosan membranes *J. Mater. Sci*. **2004**, *15*, 1105-1112.

174. Bhumkar, D. R.; Pokharkar, V.B. Studies on effect on pH on cross-linking of chitosan with sodium tripolyphosphate: a technical note *AAPS Pharm. Sci. Tech*. **2006**, *7*, 1.

175. Kyzas, G. Z.; Bikiaris, D. N.; Lazaridis, N. K. Low-swelling chitosan derivatives as biosorbents for basic dyes *Langmuir*. **2008**, *24*(9), 4791-4799.

176. Takayama, K.; Hirata, M.; Michida, Y.; Masada, T.; Sannan, T.; Nagai, T. Effect of interpolymer complex formation on bioadhesive property and drug release phenomenon of compressed tablets consisting of chitosan and sodium hyaluronate *Chem. Pharm. Bull*. **1990**, *38*, 1993-1997.

177. Hardy, P. M.; Nicholls, A.C.; Rydon, H.N. The nature of glutaraldehyde in aquoeus solution *J. Chem. Soc.: Chem. Commum*. **1969**, *10*, 565-566.

178. Woods, B.L.; Walker, R.A. pH effects on molecular adsorption and solvation of *p*-nitrophenol at silica/aquoeus interfaces *J. Phys. Chem. A* **2013**, *117*, 6224-6233.

179. Li, J.-M.; Meng, X. -G.; Hu, C. -W.; Du, J. Adsorption of phenol, *p*-chlorophenol and *p*-nitrophenol onto functional chitosan *Bioresource Technol*. **2009**, *100*, 1168.

180. Poon, L.; Younus, S.; Wilson, L.D. Adsorption study of an organo-arsenical with chitosan-based sorbents, *J. Colloid. Interface. Sci*. **2014**, *420*, 136-144.

181. Liu, X.; Zhang, W.; Hu, Y.; Cheng, H. Extraction and detection of organoarsenic feed additives and common arsenic species in environmental matrices by HPLC-ICP-MS. *Microchem. J*. **2013**, *108*, 38-45.

182. Boddu, V. M.; Abburi, K.; Talbott, J. L.; Smith, E.D.; Haasch, R. Removal of arsenic(III) and arsenic(V) from aquoeus medium using chitosan-coated biosorbents *Water. Res*. **2008**, *42*(3), 633-642.

183. Jovanovic, B. M,; Vukasinovic-pesic, V. L.; Veljovic, D. N.; Rajakovic, L. V. Arsenic removal from water using low-cost adsorbents- a comparative study *J. Serb. Chem. Soc*. **2011**, *76*(10), 1437-1452.

184. Niu, C. H.; Volesky, B.; Cleiman, D. Biosorption of arsenic (V) with acid-washed crab shell *Water. Res*. **2007**, *41*, 2473.

185. Tofan-Lazar, J.; Al-Abedleh, H. A Kinetic ATR-FTIR Studies on Phosphate Adsorption on Iron (Oxyhydr) oxide in the Absence and Presence of Surface Arsenic: Molecular-Level Insight into the Ligand Exchange Mechanism *J. Phys. Chem*. A **2012**, *116*, 10130-10149.

186. Li, R.; Li, Q.; Gao, S.; Shang, J.K. Exceptional arsenic adsorption performance of hydrous cerium oxide nanoparticles: Part A Adsorption capacity and mechanism *Chem. Engineer. J*. **2012**, *185-186*, 127-135.

187. So, H. U.; Postma, D.; Jakobsen, R.; Larsen, F. Sorption of phosphate onto calcite; results from batch experiments and surface complexation modeling *Geochim. Cosmochim. Acta.* **2012**, *93*, 2911-2923.

188. Manning, B. A.; Goldberg, S. Modeling Competitive Adsorption of Arsenate with Phosphate and Molybdate on Oxide Minerals *Soil. Sci. Soc .Am J*. **1996**, *60*, 121-131.

189. Carabante, I.; Grahn, M.; Holmgren, A.; Hedlund, J. In situ ATR-FTIR studies ofn the competitive of arsenate and phosphate on ferrihydrite *J. Colloid. Interface. Sci*. **2010**, *351*, 523-531.

190. Behari, J. R.; Prakash, R. Determination of total arsenic content in water by atomic absorption spectroscopy (AAS) using vapour generation assembly (VGA) *Chemosphere*. **2006**, *63*, 17-21.

191. Hymer, C.B.; Caruso, J. A. Arsenic and its speciation analysis using high-performance liquid chromatography and inductively coupled plasma mass spectrometry *J. Chrom. A* **2004**, *1045*, 1-14.

192. Ritsema, R.; Dukan, L.; Navarro, T. R.; Van Leeuwan, W.; Oliveria, N.; Wolfs, P.; Lebret, E. Speciation of arsenic compounds in urine by LC-ICP-MS *Appl. Organomet. Chem*. **1998**, 12(8-9), 591-599.

193. Svancara, I.; Vytras, K.; Bobrowski, A.; Kalcher, K. Determination of arsenic at a gold-plated carbon paste using constant current stripping analysis *Talanta*. **2002**, *58*, 45-55.

194. Mohan, M.S.; Zingara, R. A.; Micks, P.; Clark, P. O. Analysis and Speciation of Arsenic in Herbicide-Treated soils by DC Helium Emission Spectrometry *J. Environ. Anal. Chem.* **1982**, *11*, 175-187.

195. Amran, M. B.; Lagarde, F.; Leroy, M. J.F. Determination of arsenic species in marine organism by HPLC-HG- QFAAS *Mikrochim. Acta* **1997**, *127*(3-4), 195-202.

196. Howard, A. G.; Comber, S. D. W. Hydride-Trapping techniques for the speciation of arsenic *Mikrochim. Acta* **1992**, *109*, 27-33.

197. Ascone, I.; Meyer-Klaucke, W.; Murphy, L. Experimental aspects of biological X-ray absorption spectroscopy *J. Synchrotron. Rad*. **2003**, *10*, 16-22.

198. Andrahennadi, R.; Pickering, I. J. Arsenic accumulation, biotransformation and localization in bertha armyworm moths *Environ. Chem.* **2008**, *5*(6), 413-419.

199. Andrahennadi, R. Biotransformation of Selenium and Arsenic in Insects Environmental Implication, PhD. Thesis, University of Saskatchewan, SK, Canada, 2009.

200. Andrahennadi, R.; Fu, J.; Pushie, M. J.; Wiramanaden, C. I. E.; George, G.N.; Pickering, I. *J.* Insect Excretes Unusual Six-coordinate Pentavalent Arsenic Species *Environ. Chem.* **2009**, *6*(4), 298-304.

201. Smith, P.G.; Koch, I.; Gordon, R.A.; Mandoli, D.; Chapman, B.D.; Reimer, K. Absorption Near-Edge Structure Analysis of Arsenic Species for Application to Biological Environmental Samples *J. Environ. Sci. Technol*. **2005**, *39*, 248-254.

202. Hackett, M.J.; Smith, S.E.; Paterson, P.G.; Nichol, H.; Pickering, I.J.; George, G.N. X-ray Absorption Spectroscopy at the Sulfur K-edge: Anew Tool to Investigate the Biochemical Mechanism of Neurodegeneration, *ACS Chem. Neurosci*, **2012**, *3*, 178-185.

203. Bowers, G. M.; Kirkpatrick, R. J. High field ^{75}As NMR study of arsenic oxysalts *J. Magn. Reson.* **2007**, *188*, 311-321.

204. Luengo, C.; Mrigante, M.; Antelo, J.; Avena, M. Kinetics of phosphate adsorption on goethite: comparing batch adsorption and ATR-IR measurements *J. Colloid. Interf. Sci*. **2006**, *300*, 511-518.

205. Gao, Y.; Mucci, A. Acid base reactions, phosphate and arsenate complexation and their competitive adsorption at the surface of goethite in 0.7M NaCl solution phosphate *Geochim. Cosmochim. Acta*. **2001**, *65*(140), 2361-2378.